

Alma Mater Studiorum – Università di Bologna

DOTTORATO DI RICERCA IN
SCIENZE E TECNOLOGIE AGRARIE, AMBIENTALI E ALIMENTARI
Ciclo XXIX

Settore Concorsuale di afferenza: 07/D1
Settore Scientifico disciplinare: AGR/12

**A MOLECULAR STUDY OF THE *Botrytis cinerea* - *Vitis vinifera*
INTERACTION: FROM INFLORESCENCE TO RIPE BERRY**

presentata da

Zeraye Mehari Haile

Relatore:

Dr. ELENA BARALDI

Coordinatore:

Prof. GIOVANNI DINELLI

Correlatore:

Dr. CLAUDIO MOSER

Esame finale anno 2017

Declaration

I, Zeraye Mehari Haile, hereby declare that this thesis is my own work with due acknowledgement of other materials used. I further state that the thesis has not been submitted for any award at any other university than the Univeristy of Bologna.

Zeraye Mehari Haile

Contents

List of Abbreviations.....	1
ABSTRACT	2
1. GENERAL INTRODUCTION	3
1.1. Grapevine cultivation – production and uses	3
1.2. Grapevine diseases	5
1.3. <i>Botrytis cinerea</i>	6
1.4. Grapevine and <i>Botrytis cinerea</i>	8
1.4. OBJECTIVE.....	12
1.5. REFERENCES	13
2. GRAPEVINE FLOWER AND <i>Botrytis cinerea</i> INTERACTION	16
2.1. Abstract	16
2.2. Introduction	17
2.3. Materials and methods.....	18
2.3.1. Plant material and <i>Botrytis cinerea</i> inoculation.....	18
2.3.2. Microscopic observations and detection of quiescent <i>Botrytis cinerea</i>	19
2.3.3. Secondary metabolites and RNA extraction.....	20
2.3.4. RNA sequencing, data processing and data analysis.....	20
2.3.5. Quantitative polymerase chain reaction (qPCR)	21
2.3.6. DNA extraction, standard curve and DNA quantification.....	22
2.4. Results	22
2.4.1. <i>Botrytis cinerea</i> infection of grapevine flower	22
2.4.2. Transcriptome analysis of infected grapevine flowers	25
2.4.3. Defense related responses are largely induced in the flower upon <i>Botrytis cinerea</i> infection ..	27
2.4.4. Secondary metabolism, mainly related to polyphenols, is upregulated in infected flowers	32
2.4.5. Infection triggers cell wall reinforcement	36
2.4.6. <i>Botrytis cinerea</i> transcripts expressed <i>in planta</i> during grapevine flower infection	39
2.4.7. <i>Botrytis cinerea</i> genes required for pathogenesis are upregulated during flower infection	40
2.5. Discussion.....	44
2.6. Conclusions	49
2.7. References	50
2.8. Supplemental materials	58

2.8.1. Supplemental tables.....	58
2.8.2. Supplemental figures.....	67
3. INTERACTION BETWEEN GRAPE BERRY AND <i>B. cinerea</i> DURING QUIESCENT AND EGRESSED INFECTIONS.....	73
3.1. Abstract	73
3.2. Introduction	74
3.3. Materials and methods.....	75
3.3.1. Fungal isolate, plant material and inoculation.....	75
3.3.2. RNA extraction, qPCR and RNA-seq	76
3.3.3. Secondary metabolites extraction and analysis	77
3.3.4. Statistical analysis	77
3.3.5. Functional classification based on Gene Ontology, VitisNet, and MapMan.....	78
3.4. Results	79
3.4.1. <i>Botrytis cinerea</i> inoculation of grapevine	79
3.4.2. Transcriptional profiling of grapevine berry responses to <i>B. cinerea</i>	79
3.4.3. Transcriptional alterations of <i>B. cinerea</i> during quiescent infection, at 4 wpi.....	83
3.4.4. Response of hard-green berries to quiescent <i>B. cinerea</i> , at 4 wpi.....	86
3.4.5. <i>B. cinerea</i> transcriptome during pre-egression and egression stages, at ripening	90
3.4.6. Response of ripe berry for <i>B. cinerea</i> 's pre-egression and egression state	93
3.5. Discussion.....	99
3.6. Conclusions	105
3.7. References	106
3.8. Supplemental materials	113
3.8.1. Supplemental tables.....	113
3.8.2. Supplemental figures	118
4. CONCLUDING REMARKS	120
ACKNOWLEDGMENTS.....	122

List of Abbreviations

%	Per cent	GOX1	Galactose oxidase
<	Less than	GPX3	Glutathione peroxidase
>	Greater than	GST1	Glutathione S-transferase
°C	Degree Celsius	Gt	Germ tube
µm	Micrometer	hpi	Hour post inoculation
4CL	4-coumarate-CoA ligase	Hy	Hypha
ABA	Abscisic acid	IGS	Intergenic spacer region
ABC	ATP Binding Cassette	JA	Jasmonic acid
ACT	Actin	LCC	Laccase
ANOVA	Analysis of variance	LGA1	2-keto-3-deoxy-L-galactonate aldolase
AOX	Alcohol oxidase	LGD1	D-galactonate dehydrogenase
AP	Appressoria	Ma	Multicellular appressoria
AP8	Aspartic proteinase	NaClO	Sodium hypochlorite
BAK	Brassinosteroid insensitive 1- associated kinase	NW	Not washed
Bc	<i>Botrytis cinerea</i>	OAH	Oxaloacetate acetylhydrolase
BOA6	Botcinic acid	PAL	Phenylalanine ammonia lyase
BOT	Botrydial biosynthesis	PCA	principal component analysis
BR	Brassinosteroid	PDA	Potato dextrose agar
C4H	Cinnamate 4-hydroxylase	PDB	Potato dextrose broth
Ca	Calcium	PE	pectinesterases
CAD	cinnamyl alcohol dehydrogenase	PEL-like1	Pectate lyase
CCoAMT	Caffeoyl-CoA O-methyltransferase	PER	Peroxidase
CCR	Cinnamoyl CoA reductase	pg	picogram
cDNA	Complementary DNA	PG	Polygalacturonase
CHS	Chalcone synthase	PLR	Pinorexinol/lariciresinol reductase
Co	Conidium	PR	Pathogenesis related
COMT	caffeic acid o-methyltransferase	PRD1	Dyp-type peroxidase
Ct	Cycle threshold	qPCR	Quantitative polymerase chain reaction
Ctrl	Mock inoculated (Control)	REVIGO	Reduce + Visualize Gene Ontology
CUTA	Cutinase	RLK	Receptor-like kinases
CUT-like1	Cutinase	RNA	Ribonucleic acid
CWA	Cell wall apposition	RNA-seq	RNA sequence
CWDE	Cell wall degrading enzyme	ROS	Reactive oxygen species
DE	Differentially expressed	RS	Resveratrol synthase
DFR	Dihydroflavonol-4-reductase	SA	Salicylic acid
DNA	Deoxyribonucleic acid	SIRD	Secoisolariciresinol dehydrogenase
dpi	days post inoculation	SOD1	Superoxide dismutase1
EL	Eichorn and Lorenz	SS	Surface sterilized
ET	Ethylene	STS	Stilbene synthase
EXT	Proline-rich extensin-like protein	TF	Transcription factor
F3H	Flavanone 3-hydroxylase	Trt	<i>B. cinerea</i> inoculated (Treated)
F5H	Ferulate 5-hydroxylase	TUB	Tubulin
FDR	False discovery rate	Vv	<i>Vitis vinifera</i>
GA	Gibberellic acid	W	Washed
GAR2	D-galacturonic acid reductase2	WAK	Wall-associated kinase
GFP	Green fluorescent protein	wpi	weeks post inoculation
GLP	Germin-like protein	XYN11A	Endo-beta-1,4-xylanase
GO	Gene ontology	βGLUC	Beta-glucosidase 1 precursor
		µg	Microgram
FAOSTAT	Food and Agriculture Organization of the United Nations Statistics Division		
UHPLC-DAD-MS	Ultra High Performance Liquid Chromatography - Diode Array Detection - Mass Spectrometry		

ABSTRACT

Grapes quality and yield are affected by bunch rot disease caused by the necrotrophic fungus *Botrytis cinerea*. Primary infections are mostly initiated at blooming by airborne conidia from overwintered sources. The fungus often remains quiescent from bloom until maturity and egresses at ripe where it causes bunch rot. Here, it is reported molecular analyses of the interaction between *B. cinerea* and the flower/berry of the cultivated grapevine (*Vitis vinifera* L.), in a controlled infection system, using confocal microscopy and integrated transcriptomic and metabolic analysis of the host and the pathogen. Open flowers from fruiting cuttings of the cv. Pinot Noir were infected with GFP labeled *B. cinerea* and samples taken at 24 and 96 hours post inoculation (hpi) (infected flowers), at 4 weeks post inoculation (wpi) (asymptomatic hard-green berries), and at 12 wpi (pre-egression and egression of the fungus on ripe berries) were studied. The observed penetration of the flower epidermis by *B. cinerea* coincided with increased expression of fungal genes encoding virulence factors, representing the effort of the pathogen to invade the host. Grapevine flowers responded with a rapid defense reaction involving genes associated with the accumulation of PR proteins, phenylpropanoids including stilbenoids, reactive oxygen species and cell wall reinforcement. At 96 hpi the transcriptional reaction appeared largely diminished both in the host and in the pathogen and a new status of asymptomatic coexistence is established. Afterwards, infected berries continued their developmental program without any visible symptom, although the presence of *B. cinerea* could be ascertained by plating out on selective media. Nonetheless, at the transcriptional level, the expressed quiescent fungal transcriptome highlighted that the fungus was modifying its cell wall to evade plant chitinases, besides maintaining basal metabolic activities. Also hard-green berries maintained activated response based on the expression of several PR family genes and genes involved in monolignol, flavonoid and stilbenoid biosynthesis pathways, in order to keep the pathogen quiescent. At 12 wpi, the transcripts of *B. cinerea* in the pre-egressed samples showed that virulence-related genes were expressed again, suggesting pathogenesis was resumed. The egressed *B. cinerea* expressed almost all virulence and growth related genes to enable the pathogen to colonize the berries. In response to egression, ripe berries reprogram different defense responses, though futilely. In conclusion, this study showed that the defense responses occurring in the grapevine flower and hard-green berry were able to restrict invasive fungal growth at the epidermal tissues, thus forcing the fungus to enter quiescence. However the pathogen was able to perceive and exploit ripening associated modifications, such as fruit's cell wall self-disassembly, and favorable external conditions, such as high humidity induced by cluster bagging practice, to recover an active metabolism and pathogenic activity, and eventually caused bunch rot.

1. GENERAL INTRODUCTION

1.1. Grapevine cultivation – production and uses

Grapevines (*Vitis* spp.) have evolved in several areas of the world, leading to the development of many different species including *V. labrusca* (L.) and *V. vinifera* (L.) (Mullins *et al.*, 1992). The latter one being one of the most worldwide-grown perennial fruit crops whose origin of cultivation is probably in southern Caucasia, a region located on the border of Eastern Europe and Western Asia (Mullins *et al.*, 1992). The other well-known species, *V. labrusca*, which is widely used for juice production, is native to North America (Creasy and Creasy, 2009). This species as other American species such as *V. riparia*, *V. berlandieri*, is much more resistant to pests and diseases than *V. vinifera* (Creasy and Creasy, 2009). Actually, many of the non *V. vinifera* species, which are usually not used for grape production, including *V. labrusca*, are used in breeding to confer resistance to soil-related conditions and pests for commercial cultivars (Creasy and Creasy, 2009). *V. vinifera* (here synonymously referred as grapevine) is a highly adaptable species. Cultivation limitations imposed by climatic conditions that are different from its center of origin are usually compensated by agronomic practices. Currently grapevine is cultivated throughout the world in a wide range of climates (from temperate to tropical climates), countries of the Mediterranean basin being the world's main producers (Bouquet, 2011). According to FAOSTAT (2014), the total world grapes production was estimated about 77 million tons in 2013, where Italy was the second top producer next to China (Food and Agriculture Organization of the United Nations Statistics Division, FAOSTAT, 2014, <http://faostat3.fao.org/home/E>).

The economic benefits obtained from grapevine derive from its berry. The nature of grape berry development is represented by two successive sigmoidal growth cycles, each with distinctive characteristics separated by a lag phase (Figure 1.1) (Coombe, 1992; Coombe and McCarthy, 2000). In the first cycle, berry formation, cell division and enlargement occur in pericarp tissue which determines a berry's final size and shape. The cycle lasts about 60 days after bloom, while the berry is hard and green and accumulates organic acids. The second cycle lasts from véraison (color change) to ripening. This cycle begins with the onset of berry softening, sugar accumulation, acids degradation, and berry colouring. Phenols and anthocyanin (in black-skinned

grapes) are also accumulated in this growth phase. Toward the end of the second growth cycle, aroma and flavor compounds are also produced.

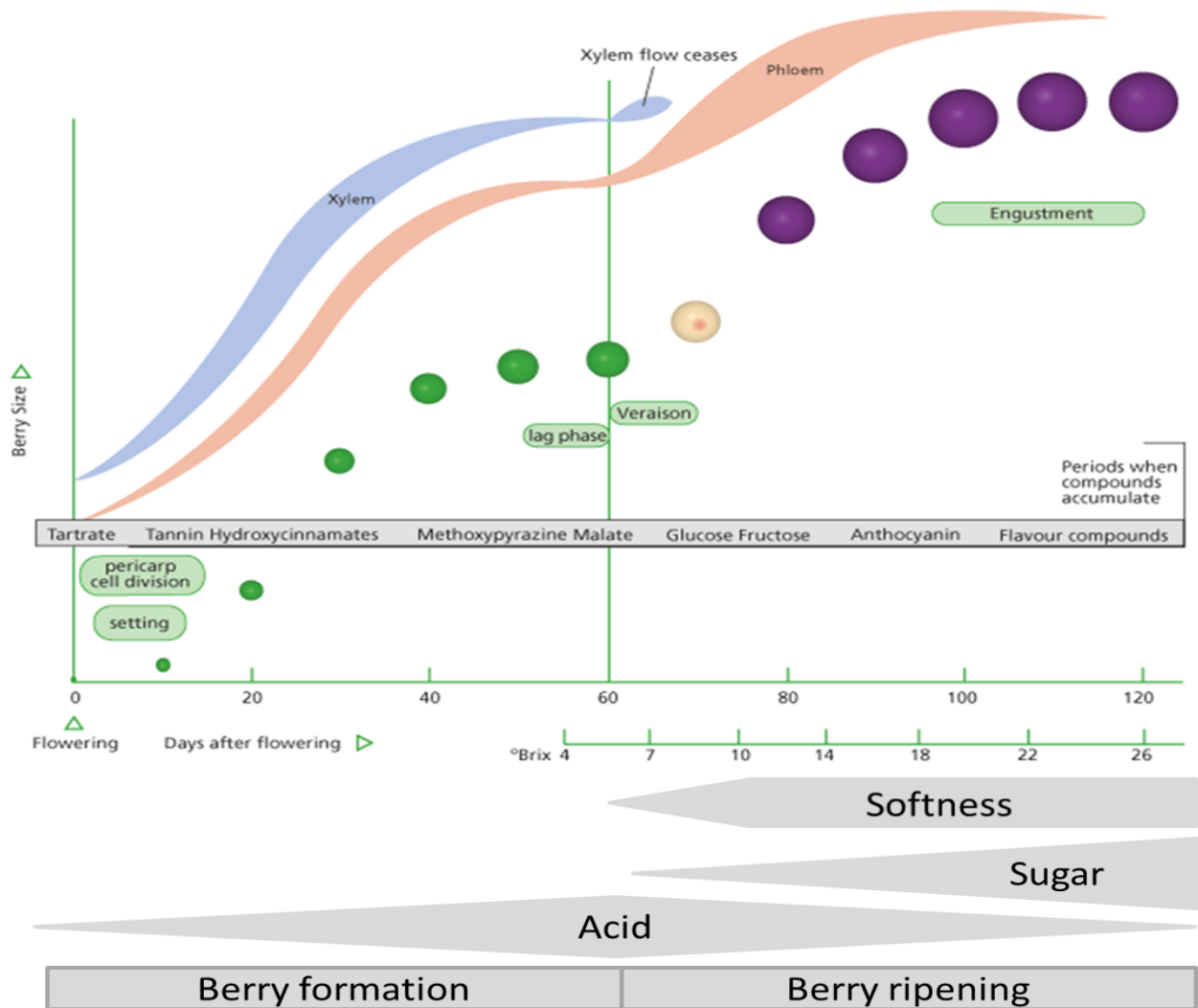


Figure 1.1. Diagram showing berry growth stages from flowering to ripening. Shown are: the relative size and color of berries at 10 days interval from flowering; periods when compounds accumulate; the level of juice brix; an indication of the rates of inflow of xylem and phloem vascular saps into the berry; and the rate of softness, sugar accumulation and acidity (Adopted from Kennedy, 2002)

The unique ability of grapevine berry to accumulate sugar, pectin (depending on cultivars), acids (particularly tartaric acid), and a wide range of aromatic compounds when ripe makes grapevine suitable for different uses (Creasy and Creasy, 2009). Major economic benefits come from wine and related fermented products, but also from fresh fruit, raisins, fruit juices and jams. To consumers, it has numerous nutritional and health benefits due to antioxidant polyphenols such as

flavonoids and resveratrol (Yadav et al., 2009). However, grapevine production can be jeopardized by adverse environmental conditions and biotic threats.

Disease and pest management consumes a large proportion of grapevine cultivation costs (Creasy and Creasy, 2009). Damage to grapevines can occur below and in the above-ground parts. Biotic stresses of grapes include diseases caused by bacteria, fungi, oomycetes, viruses, and pests from insects, arthropods, birds, and mammals. The major diseases caused by fungi and oomycetes are briefly reviewed in the next section.

1.2. Grapevine diseases

Fungi and oomycetes represent the major cause of damage and losses in grape cultivation. The biotrophic oomycete pathogen, *Plasmopara viticola*, causes downy mildew in grapevine provoking severe leaf, shoot, and cluster damage. When leaves are infected, the pathogen causes a characteristic yellowish oily spots on the upper surface and massive sporulation on the underside, which looks like downy white (Pearson and Goheen, 1988; Ash, 2000). Infected berries and shoots have also a similar downy white appearance. Downy mildew is primarily a disease of warm and humid growing regions, and the absence of rainfall and high humidity reduces the spread of the disease (Pearson and Goheen, 1988). However, should there be a need to use fungicide, mostly copper-containing formulates are used (Ash, 2000).

Grapevine powdery mildew, also called oidium, is a devastating disease caused by *Erysiphe necator* (syn. *Uncinula necator*), an obligate biotroph fungus that can infect all grapevine green tissues (Gubler et al., 1999; Gadoury et al., 2012). Infection compromises photosynthesis and often leads to premature senescence and abscission of leaves; on berries it causes crack, acidity increase, and decrease anthocyanin and sugar content at ripe, with an overall impact on yield and quality (Lakso et al., 1982; Gubler et al., 1999; Calonnet et al., 2004). Most cultivated varieties are susceptible to powdery mildew, and growers make use of synthetic fungicides to control the disease (Gubler et al., 1999; Gadoury et al., 2012).

The ubiquitous *Botrytis cinerea* is another important grapevine's fungal pathogen, which causes *Botrytis* bunch rot or gray mold. This pathogen is the focus of this study, and is discussed in detail in the next section. Other grapevine diseases caused by fungal pathogens include cane and

leaf spot (*Phomopsis viticola*), dieback (*Eutypa lata*), black rot (*Guignardia bidwellii*), anthracnose (*Elsinoë ampelina*), and blackfoot disease (*Cylindrocarpon spp.*).

1.3. *Botrytis cinerea*

The genus *Botrytis* comprises about 28 species (Beever and Weeds 2004). However, with the exception of *B. cinerea*, most *Botrytis* species have a limited host range (Beever and Weeds, 2004). *Botrytis cinerea* (Pers.:Fries) represents one of the first described ascomycetes and is an economically relevant plant pathogen worldwide (Hennebert, 1973). Taxonomically, it is classified under kingdom: Fungi, phylum: Ascomycota, subphylum: Pezizomycotina, class: Leotiomycetes, order: Helotiales, family: Sclerotiniaceae, genus: *Botrytis*; and species: *Botrytis cinerea* (Williamson et al., 2007; Elad et al., 2016). Other species of *Botrytis* that are known to cause significant losses in crops are listed in Table 1.1.

Table 1.1. Lists of important *Botrytis* species with their hosts (Adopted from Dewey and Grant-Downton, 2016)

Species	Date of description	Major plant host (genus/genera name)
<i>Botrytis aclada</i>	1850	<i>Allium</i>
<i>Botrytis allii</i>	1917	<i>Allium</i>
<i>Botrytis byssoidea</i>	1925	<i>Allium</i>
<i>Botrytis caroliniana</i>	2012	<i>Rubus, Fragaria</i>
<i>Botrytis cinerea</i>	1794	Multiple host
<i>Botrytis convoluta</i>	1932	<i>Iris</i>
<i>Botrytis deweyae</i>	2014	<i>Hemerocallis</i>
<i>Botrytis elliptica</i>	1881	<i>Lilium</i>
<i>Botrytis fabae</i>	1929	<i>Vicia</i>
<i>Botrytis fabiopsis</i>	2010	<i>Vicia</i>
<i>Botrytis gladiolorum</i>	1941	<i>Gladiolus</i>
<i>Botrytis globosa</i>	1938	<i>Allium</i>
<i>Botrytis hyacinthi</i>	1928	<i>Hyacinthus</i>
<i>Botrytis narcissicola</i>	1906	<i>Narcissus</i>
<i>Botrytis paeoniae</i>	1897	<i>Paeonia</i>
<i>Botrytis pelargonii</i>	1949	<i>Pelargonium</i>
<i>Botrytis polyblastis</i>	1926	<i>Narcissus</i>
<i>Botrytis porri</i>	1949	<i>Allium</i>
<i>Botrytis sinoallii</i>	2010	<i>Allium</i>
<i>Botrytis sinoviticola</i>	2014	<i>Vitis</i>
<i>Botrytis sphaerosperma</i>	1949	<i>Allium</i>
<i>Botrytis squamosa</i>	1925	<i>Allium</i>
<i>Botrytis tulipae</i>	1913	<i>Tulipa</i>
<i>Botrytis sp. Group S</i>	2013	<i>Fragaria, Vitis, likely multiple others</i>

B. cinerea can undergo both sexual and asexual lifecycle. In the asexual cycle, the fungus produces numerous asexual conidia (macroconidia) that are borne at the tips of branching conidiophores, specialized hyphae (Figure 1.2). Conidia are short-lived propagules and their survival depends on temperature, moisture availability, sunlight exposure and microbial activity (Holz et al., 2004). They are metabolically dormant fungal structures and are considered as survival structures (Holz et al., 2004). *B. cinerea* can also produce temporary resting structures having thickened (hyaline) walls, called chlamydospores (Urbasch, 1983). Chlamydospores are often found in ageing cultures and suited to survive short drought periods (Urbasch 1983; Beaver and Weeds, 2004). Another survival structures used for overwintering are sclerotia. These are structures resistant to adverse environmental condition, and are produced by melanized resting bodies (Holz et al., 2004).

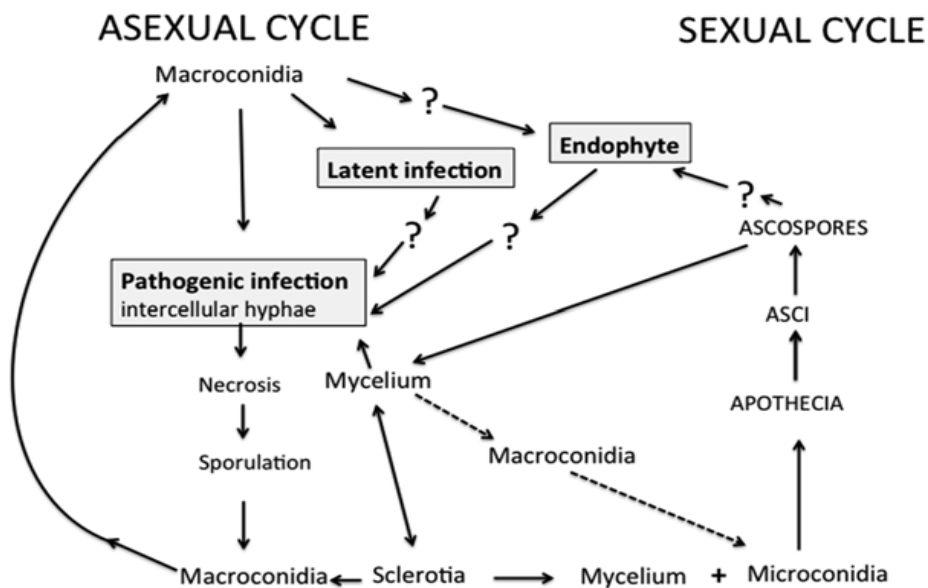


Figure 1.2. Diagram showing life cycle of *Botrytis cinerea* and interactions of different developmental stages in the life cycle (Adopted from Dewey and Grant-Downton, 2016). Macroconidia refer to conidia.

On the other hand, the fruiting structures in the sexual life cycle of *Botrytis* spp. are not commonly seen in nature (Lorbeer, 1980). Microconidia, are uninucleate and act as spermatia (Fukumori et al., 2004), are produced by macroconidia, old hyphae, and sclerotia (Lorenz and

Eichhorn, 1983; Fukumori et al., 2004) (Figure 1.2). The structure provides an alternative microscopic propagule when the fungus is under stress, in ageing culture or in cultures contaminated by other organisms (Holz et al., 2004). The fertilization of spermatia with receptive sclerotia give rise to apothecia from which asci, containing ascospores, are produced (Urbasch, 1983). Since most isolates of *B. cinerea* are naturally heterothallic, i.e. self-sterile, they can produce ascospore only when crossed with the opposite mating type, with the allele MAT-1 and MAT-2 being single mating type locus controlling sexual compatibility (Faretra et al., 1988).

B. cinerea is an intriguing pathogen because of its unique characteristics: it can live as a pathogen (as necrotroph) but also as saprophyte or endophyte; it can be very devastating in some crops but it can also be of some benefit under certain conditions; it can cause early latent infection which damages the fruits mostly not before ripening (Rosslbroich and Stuebler, 2000; Elad et al., 2004; Shaw et al., 2016). Upon conidial contact with plant tissues, germination and appressoria formation could possibly follow but without further invasion of the inner tissues (Williamson et al., 1987; Coertze and Holz, 2002). Such infections are described as quiescent or latent, where the fungus is arrested until favorable conditions are met, mostly when the tissue gets senescent (Shaw et al., 2016). There are also reports of *B. cinerea* colonizing host plants endophytically (Barnes and Shaw 2003; Sowley et al. 2010; Shaw et al., 2016). Endophytic *B. cinerea* can become infectious at a later stage of plant growth (maturity) or in storage or, can remain asymptomatic until the next cropping season, with a possibility to be transferred through clone or seed of the host (Barnes and Shaw 2003).

Undoubtedly, *B. cinerea* is an important pre- and post-harvest pathogen, damaging plant products in field, storage, transport/transit, and on markets (Elad et al., 2004). The pathogen can attack more than 200 plant species (Jarvis, 1977). As many plant pathogenic fungi, short generation cycles and high amounts of progeny allow *B. cinerea* to colonize host plants rapidly and abundantly. The fungus causes blossom and leaf blights, bunch rot disease, and post-harvest fruit rots (Jarvis, 1977; Elad et al., 2004).

1.4. Grapevine and *Botrytis cinerea*

With regard to grapevine-*Botrytis* interaction, *B. cinerea* is part of most vineyards' natural microflora. The proposed life and disease cycles of the pathogen in vineyards is shown in Figure 1.3 (Elmer and Michailides, 2004). The fungus overwinters as sclerotia and/or mycelia in organic

debris in the vineyard. When the environmental conditions become suitable, the overwintered sclerotia/mycelia produce conidia, which are usually a source of primary inoculum for pre-bloom and bloom infection (Elmer and Michailides, 2004). Grapevine cultivars greatly differ in their susceptibility to the *Botrytis* bunch rot disease (Creasy and Creasy, 2009). Cluster architecture, microclimate around the berry, and the content of preformed and inducible antifungal compounds (Langcake and McCarthy, 1979; Hill et al., 1981; Creasy and Coffee, 1988) are responsible for the varietal differences in *Botrytis* susceptibility.

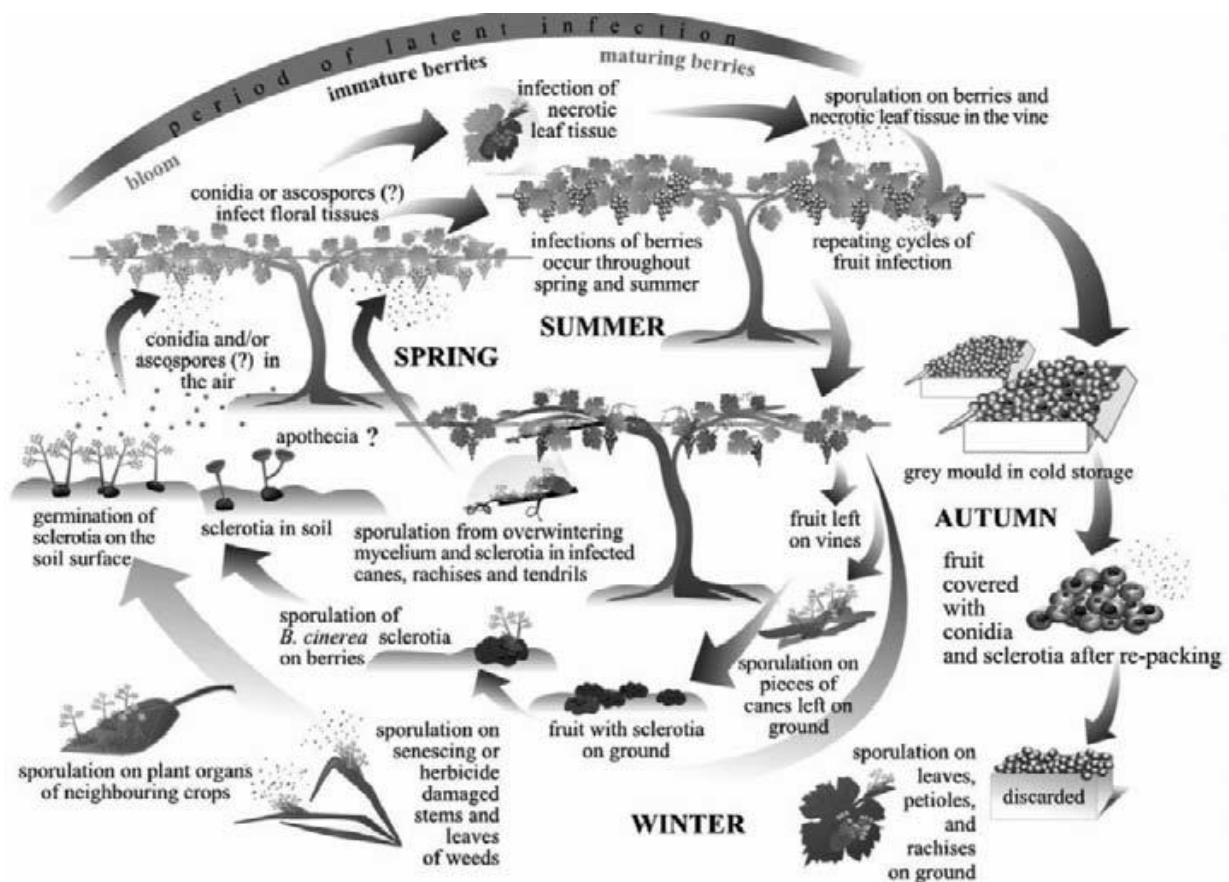


Figure 1.3. Life cycle of *Botrytis cinerea* and disease cycle of gray mold, as proposed by Elmer and Michailides (2004).

When infection happens at bloom, it generally remains quiescent until fruit ripening, and at ripening the pathogen resumes active growth to cause bunch rot. (McClellan and Hewitt, 1973; Nair et al., 1995; Keller et al., 2003; Pezet et al., 2003). Rainfall or long period of high humidity, cuticle cracking from pressure within the berry/cluster, and physical damages from insects, hail, and wind are environmental factors that dispose the outgrowth of the fungus causing ripe berries

bunch rot. Although *B. cinerea* is generally detrimental to grape quality by causing rotten berries in table grapes and off-flavors in wine (Loinger et al., 1977), for certain white-skinned cultivars, such as Sémillon, Riesling, Sauvignon Blanc, Muscadel, and Chenin Blanc under specific climatic conditions, it can be beneficial, as it happens in Tokaj (Hungary), Rheingau (Germany), and Sauternais (France) regions where enologists produce ‘Botrytised’ wine out of the rotten bunches, for this renamed ‘noble rot’ (Creasy and Creasy, 2009).

B. cinerea infection can possibly occur at any stage of fruit development, though primary infection often occurs at bloom time where symptoms are not apparent until berry ripening (McClellan and Hewitt, 1973; Nair et al., 1995; Keller et al., 2003). This delayed asymptomatic infection, whereby the infected tissue is not infectious, is known as quiescent or latent infection. Host factors that drive plant pathogens into quiescent stage are not fully known but limiting nutritional conditions, presence of preformed and inducible antifungal compounds, firm/thick cell wall, high production of reactive oxygen species, and inactivation of fungal pathogenicity factors are among the possible reasons (Prusky, 1996; Prusky et al., 2013). Besides these host factors, failure to produce adequate virulence factors by the pathogens drives them into quiescence. On the other hand, the physicochemical changes and gradual decline in antifungal compounds during ripening can lead to egression of quiescent pathogens (Prusky, 1996; Lattanzio et al., 2001).

In grapevine flowers inoculated with *B. cinerea* conidia, germ tubes were observed growing inside the narrow gap between calyx and ovary, that forms the receptacle area, and passing its quiescence there (Keller et al., 2003; Viret et al., 2004). According to Keller et al. (2003), higher disease severity at harvest was observed on bunches that received *B. cinerea* inoculation at flowering than controls, implying the importance of quiescent *B. cinerea* in determining the incidence of berry rot at ripe. In the epidemiology of *B. cinerea* in grape, flowering is an important stage as infection at this time is normally followed by quiescence. The asymptomatic presence of *B. cinerea* and its egression during ripening and/or post-harvest storage, when synthetic fungicides are not allowed, poses challenge in controlling the pathogen.

Knowledge of the molecular mechanisms involved during flower/berry-*Botrytis* interaction paves the way for devising appropriate control measure. Taking advantage of the availability of the genome sequences of *Vitis vinifera* (Jaillon et al., 2007; Velasco et al., 2007) and *B. cinerea* (Amselem et al., 2011; van Kan et al, 2016), a transcriptomic approach has been possible in this

study, allowing to unravel crosstalk between the pathogen and the plant at some key interaction stages of the infection process, i.e. at infection initiation, entry to quiescence, quiescence, and egression. All the infections have been conducted in controlled conditions in the greenhouse, using flowers raised from fruiting cuttings (as shown in Figure 1.4). In this way, it has been possible to overcome the seasonal requirements thus performing several experiments during the year, instead of one. Then, the use of the *Botrytis* strain expressing the fluorescent probe GFP would not have been allowed in the open field, due to law restrictions on the use of genetically modified organisms. Finally, *Botrytis* is naturally present in the field, so only using sterilized material grown in a protected environment would allow avoiding contamination during the experiment, which actually lasted from blooming to ripeness, i.e. more than 10 weeks.

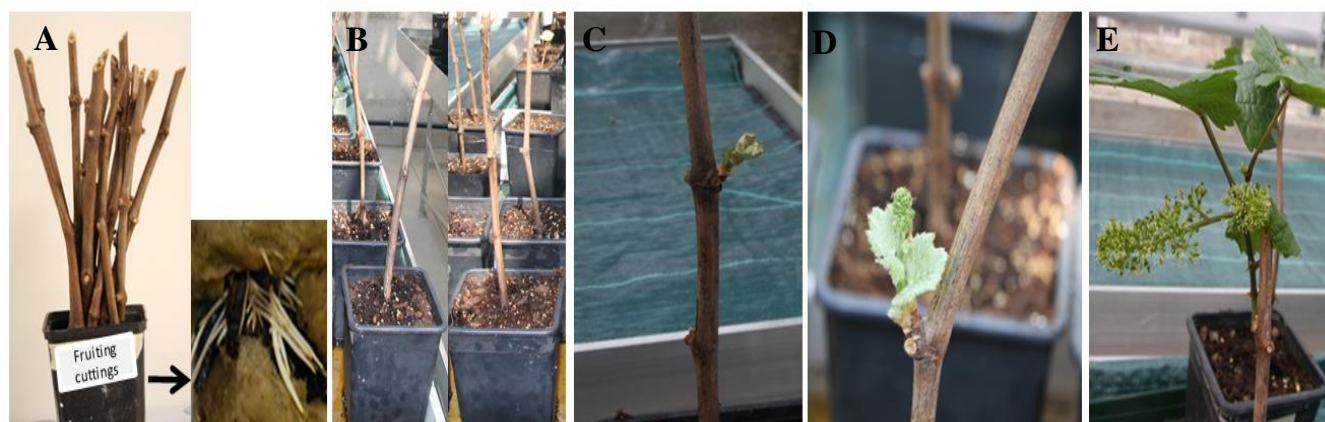


Figure 1.4. Grapevine flowers raised from fruiting cuttings. A, Fruiting cuttings in rooting pot with moistened rock wool in cold room (4 °C) on heat mat, to stimulate rooting while keeping the above buds dormant; adventitious roots after 6 weeks. B, Fruiting cuttings, with adventitious roots, transferred into pots with growing mix to greenhouse. C, Budburst, 1-2 week after being transferred to greenhouse. D, Emerging inflorescence after apical meristem was removed, 2-3 weeks after being transferred to greenhouse. E, Inflorescence with single flowers separated, 3-4 weeks after being transferred to greenhouse.

1.4. OBJECTIVE

The aim of this research was to understand the interaction between *B. cinerea* and grapevine inflorescences at molecular level using integrated approaches (confocal microscopy, transcriptome and metabolome approaches). The first objective was to understand the crosstalk between grapevine inflorescence and *B. cinerea* at the initiation of infection and entry to quiescence state. The second one was to understand the interaction between quiescent *B. cinerea* and hard-green berry and between egressed *B. cinerea* and ripe berry.

The results obtained will be described in two main chapters, responding to the two above mentioned objectives: i) Grapevine flower and *Botrytis cinerea* interaction and ii) Interaction between grape berry and *B. cinerea* during quiescent and egression infection stages. These two chapters correspond to two paper works, the first is already submitted to Plant Cell & Environment Journal and the second is under preparation

1.5. REFERENCES

- Amselem J, Cuomo CA, van Kan JA, Viaud M, Benito EP, Couloux A, Coutinho PM, de Vries RP, Dyer PS, Fillinger S, et al** (2011) Genomic analysis of the necrotrophic fungal pathogens *Sclerotinia sclerotiorum* and *Botrytis cinerea*. *PLoS Genet* **7**: e1002230
- Ash G** (2000) Downy mildew of grape. The Plant Health Instructor. DOI: 10.1094/PHI-I-2000-1112-01 Updated 2005.
- Barnes SE, Shaw ME** (2003) Infection of commercial hybrid *Primula* seed by *Botrytis cinerea* and latent disease spread through the plants. *Phytopathology* **93**:573–578
- Bouquet A** (2011) Grapevines and Viticulture. In: Adam-Blondon AF, Martínez –Zapater JM, Kole C, eds. Genetics, Genomics and Breeding of Grapes. Enfield, New Hampshire: Science Publishers, 1-29
- Beever RE, Weeds PL** (2004) Taxonomy and genetic variation of *Botrytis* and *Botryotinia* . In: Elad Y, Williamson B, Tudzynski P, Delen N, eds. *Botrytis* : biology, pathology and control. Dordrecht, The Netherlands: Kluwer Academic, 30–31
- Calonnec A, Cartolaro P, Poupot C, Dubourdiou D, Darriet P** (2004) Effects of *Uncinula necator* on the yield and quality of grapes (*Vitis vinifera*) and wine. *Plant Pathol* **53(4)**:434–445
- Creasy LL, Coffee M** (1988) Phytoalexin production potential of grape berries. *J Am Soc Hortic Sci* **113**: 230–234
- Creasy LG, Creasy LL** (2009) Grapes. Crop production science in horticulture series; 16. Wallingford: CABI.
- Coombe BG** (1992) Research on development and ripening of the grape berry. *Am J Enol Vitic* **43**: 101–110
- Coombe BG, McCarthy MG** (2000) Dynamics of grape berry growth and physiology of ripening. *Aust J Grape Wine Res* **6**: 131-135
- Coertze S, Holz G** (2002) Epidemiology of *Botrytis cinerea* on grape: wound infection by dry, airborne conidia. *S Afr J Enol Vitic* **23**: 72–77
- Dewey FM, Grant-Downton R** (2016) *Botrytis* -biology, detection and quantification. In: Fillinger S, Elad Y eds. *Botrytis – the Fungus, the Pathogen and its Management in Agricultural Systems*. Springer international publishing, 1-16
- Elad Y, Vivier M, Fillinger S** (2016) *Botrytis* , the Good, the Bad and the Ugly. In: Fillinger S, Elad Y eds. *Botrytis – the Fungus, the Pathogen and its Management in Agricultural Systems*. Springer international publishing, 17-14
- Elad Y, Williamson B, Tudzynski P, Delen N** (2004) *Botrytis* spp. and diseases they cause in agricultural systems. In: Elad Y, Williamson B, Tudzynski P, Delan N, eds. *Botrytis: Biology, Pathology and Control*. Dordrecht, The Netherlands: Kluwer Academic, 1-8
- Elmer PAG, Michailides TJ** (2004) Epidemiology of *Botrytis cinerea* in orchard and vine crops. In: Elad Y, Williamson B, Tudzynski P, Delan N, eds. *Botrytis: Biology, Pathology and Control*. Dordrecht, The Netherlands: Kluwer Academic, 243-272
- Fukumori Y, Nakajima M, Akuts K** (2004) Microconidia act the role as spermatia in the sexual reproduction of *Botrytis cinerea* . *J Gen Plant Pathol* **70**:256–260

Gadoury DM, Cadle-Davidson L, Wilcox WF, Dry IB, Seem RC, Milgroom MG (2012) Grapevine powdery mildew (*Erysiphe necator*): a fascinating system for the study of the biology, ecology and epidemiology of an obligate biotroph. *Mol Plant Pathol* **13**(1):1–16

Gubler WD, Rademacher MR, Vasquez SJ (1999) Control of Powdery Mildew Using the UC Davis Powdery Mildew Risk Index. *APSnet Features*. Online. doi: 10.1094/APSnetFeature-1999-0199

Hennebert GL (1973) *Botrytis* and *Botrytis*-like genera. *Persoonia* **7**: 183-204

Hill GK, Stellwaag-Kittler F, Huth G, Schlösser E (1981) Resistance of grapes in different development stages to *Botrytis cinerea*. *Phytopathology Zeitschrift* **102**: 329–338

Holtz G, Coertze S, Williamson B (2004) The ecology of *Botrytis* on plant surfaces. In: Elad Y, Williamson B, Tudzynski P, Delen N eds. *Botrytis* : biology, pathology and control. The Netherlands: Kluwer Academic, 9–24

Jaillon O, Aury JM, Noel B, Policriti A, Clepet C, Casagrande A, Choisne N, Aubourg S, Vitulo N, Jubin C, et al., French-Italian Public Consortium for Grapevine Genome Characterization (2007) The grapevine genome sequence suggests ancestral hexaploidization in major angiosperm phyla. *Nature* **449**: 463-467

Jarvis WR (1977) *Botryotinia* and *Botrytis* Species: Taxonomy, Physiology, and Pathogenicity. Research Branch, Canada Department of Agriculture, Ottawa, Canada

Keller M, Viret O, Cole M (2003) *Botrytis cinerea* infection in grape flowers: defense reaction, latency and disease expression. *Phytopathology* **93**: 316–322

Kennedy J (2002) Understanding grape berry development. *Practical wineray and vineyard journal*

Lakso AN, Pratt C, Pearson RC, Pool RM, Seem RC, Welser MJ (1982) Photosynthesis, transpiration, and water use efficiency of mature grape leaves infected with *Uncinula necator* (powdery mildew). *Phytopathology* **72**: 232–236

Langcake P, McCarthy WV (1979) The relationship of resveratrol production to infection of grapevine leaves by *Botrytis cinerea*. *Vitis* **18**: 244–253

Lattanzio V, Di Venere D, Linsalata V, Bertolini P, Ippolito A, Salerno M (2001) Low temperature metabolism of apple phenolics and quiescence of *Phlyctaena vagabunda*. *J Agric Food Chem* **49**:5817–21

Loinger C, Cohen S, Dror N, Berlinger MJ (1977) Effect of grape cluster rot on wine quality. *Am J Enol Vitic* **28**(4): 196–199

Lorbeer JW (1980) Variation in *Botrytis* and *Botryotinia*. In: Coley-Smith JR, Verhoeff K and Jarvis WR, eds. *The Biology of Botrytis*. London: Academic Press, 19-40

Lorenz DK, Eichhorn KW (1983) Investigations on *Botryotinia fuckeliana* Whetz., the perfect stage of *Botrytis cinerea* Pers. *Zeitschrift für Pflanzenkrankheiten und Pflanzenschutz* **90**: 1-11

McClellan WD, Hewitt WB (1973) Early *Botrytis* rot of grapes: Time of infection and latency of *Botrytis cinerea* Pers. in L. *Phytopathology* **63**: 1151-1157

Mullins MG, Bouquet A, Williams LE (1992) *Biology of the Grapevine*. Cambridge Univ Press, Cambridge, UK.

Nair NG, Guilbaud-Oulton S, Barchia I, Emmett R (1995) Significance of carry over inoculum, flower infection and latency on the incidence of *Botrytis cinerea* in berries of grapevines at harvest *Vitis vinifera* in New South Wales. *Aust J Exp Agric* **35**: 1177-1180

Pearson RC, Goheen AC (1988) *Compendium of Grape Diseases*. American Phytopathological Society, St. Paul, Minnesota

Pezet R, Viret O, Perret C, Tabacchi R (2003) Latency of *Botrytis cinerea* Pers.: Fr. and biochemical studies during growth and ripening of two grape berry cultivars, respectively susceptible and resistant to grey mould. *J Phytopathol* **151**: 208-214

Prusky D (1996) Pathogen quiescence in postharvest diseases. *Annu Rev Phytopathol* **34**: 413–434

Prusky D, Alkan N, Mengiste T, Fluhr R (2013) Quiescent and necrotrophic lifestyle choice during postharvest disease development. *Annu Rev Phytopathol* **51**: 155–176

Rosslenbroich HJ, Stuebler D (2000) *Botrytis cinerea* - History of chemical control and novel fungicides for its management. *Crop Protection*, **19 (8-10)**: 557-561

Shaw MW, Emmanuel CJ, Emilda D, Terhem RB, Shafia A, Tsamaidi D, Emblow M, van Kan JAL (2016) Analysis of cryptic, systemic *Botrytis* infections in symptomless hosts. *Front Plant Sci* **7**:625

Sowley ENK, Dewey FM, Shaw MW (2010) Persistent, symptomless, systemic and seed-borne infection of lettuce by *Botrytis cinerea*. *Eur J Plant Pathol* **126**:61–71

Urbasch I (1983) On the genesis and germination of chlamydospores of *Botrytis cinerea*. *J Phytopathol* **108**:54–60

van Kan JAL, Stassen JHM, Mosbach A, van Der Lee TAJ, Faino L, Farmer AD, Papasotiriou DG, Zhou S, Seidl MF, Cottam E, et al. (2016). A gapless genome sequence of the fungus *Botrytis cinerea*. *Mol. Plant. Pathol.* DOI: 10.1111/mpp.12384.

Velasco R, Zharkikh A, Troggio M, Cartwright DA, Cestaro A, Pruss D, Pindo M, Fitzgerald LM, Vezzulli S, Reid J, et al (2007) A high quality draft consensus sequence of the genome of a heterozygous grapevine variety. *PLoS ONE* **2**: e1326

Viret O, Keller M, Jaudzems VG, Cole FM (2004) *Botrytis cinerea* infection of grape flowers: Light and Electron Microscopical Studies of Infection Sites. *Phytopathology* **94**: 850–7

Williamson B, McNicol RJ, Dolan A (1987) The effect of inoculating flowers and developing fruits with *Botrytis cinerea* on post-harvest grey mould of red raspberry. *Ann Appl Biol* **111**: 285-294

Williamson B, Tudzynski P, van Kan JLA (2007) Pathogen profile *Botrytis cinerea*: the cause of grey mould disease. *Mol Plant Pathol* **8**:561-580

Yadav M, Jain S, Bhardwaj A, Nagpal R, Puniya M, Tomar R, Singh V, Parkash O, Prasad G, Marotta F, Yadav H (2009) Biological and medicinal properties of grapes and their bioactive constituents: an update. *Journal of Medicinal Food* **12**: 473–484

2. GRAPEVINE FLOWER AND *Botrytis cinerea* INTERACTION

2.1. Abstract

Grapes quality and yield can be severely impaired by bunch rot, caused by the necrotrophic fungus *Botrytis cinerea*. Infection often occurs at flowering and the pathogen stays quiescent until fruit maturity, when symptoms become evident. Here, we report a molecular analysis of the early interaction between *B. cinerea* and the flower of the cultivated grapevine (*Vitis vinifera* L.), using a controlled infection system, confocal microscopy and integrated transcriptomic and metabolic analysis of the host and the pathogen. Flowers from fruiting cuttings of the cv. Pinot Noir were infected with GFP labeled *B. cinerea* and studied at 24 and 96 hours post inoculation (hpi). We observed that penetration of the epidermis by *B. cinerea* coincided with increased expression of genes encoding cell wall degrading enzymes, phytotoxic secondary metabolites, and proteases. Grapevine responds with a rapid defense reaction involving 1193 genes associated with the accumulation of antimicrobial proteins, phenylpropanoids including stilbenoids, reactive oxygen species and cell wall reinforcement. At 96 hpi the reaction appears largely diminished both in the host and in the pathogen. Afterwards, berries continue their developmental program up to véraison without any visible symptom, whereas the presence of *B. cinerea* can be ascertained by plating out on selective media. Our data indicate that the defense responses occurring in the grapevine flower within 24 hours after *B. cinerea* inoculation collectively are able to restrict invasive fungal growth into the underlying tissues, thereby forcing the fungus to enter quiescence until the conditions become more favorable to resume pathogenic development.

2.2. Introduction

Grapevine yield and quality faces challenges worldwide from biotic stresses, mainly caused by fungi and oomycetes like *Botrytis cinerea*, *Plasmopara viticola*, and *Erysiphe necator*. *B. cinerea*, a necrotroph responsible for pre- and post-harvest disease in a wide range of crops, causes bunch rot in grapevine. In vineyards, *B. cinerea* is part of the natural microflora where primary infections of berries are usually initiated by airborne conidia from overwintering sources (Nair et al., 1995; Elmer and Michailides, 2004). Bunch rot frequently occurs on ripe berries close to harvest. Wet conditions together with damage to ripe berries, due to cuticle cracking from pressure within the berry/cluster and physical damage from biotic and abiotic sources occurring during ripening, the expression of bunch rot even though the primary infection could have occurred at earlier stages of berry development (McClellan and Hewitt, 1973; Nair et al., 1995). Bunches inoculated at flowering with *B. cinerea* were reported to have higher disease severity at maturity (Keller et al., 2003; Pezet et al., 2003b), implying that bunch rot disease observed during ripening may not only be due to *de novo* infection, but also due to latent infections that occurred at earlier stages of berry development. A similar infection strategy of the pathogen was also observed in strawberries and raspberries (Jarvis, 1962; Williamson et al., 1987; Jersch et al., 1989). This delayed asymptomatic infection is known as quiescent infection.

Usually the cosmopolitan *B. cinerea*, upon contact with the host, incites cell death by producing phytotoxins and cell wall degrading enzymes and manipulates hosts metabolisms to facilitate colonization (van Kan, 2006; Choquer et al., 2007; Williamson et al., 2007). A deviation from this common necrotrophic lifestyle, where *B. cinerea* behaves as a facultative endophyte has also been observed (Williamson et al., 1987; McNicol and Williamson, 1989; Coertze and Holz, 2002; Shaw et al., 2016). This symptomless colonization, caused by a long-lived physiological switch (van Kan et al., 2014), which can shift to active and symptomatic behavior under favorable conditions, differentiates the endophytic lifestyle from the relentless necrotrophic infection behavior.

In grapevine, *B. cinerea* infection often occurs at blooming and then remains quiescent until ripening (McClellan and Hewitt, 1973; Nair et al., 1995; Keller et al., 2003; Pezet et al., 2003b). Berry developmental stages between bloom and véraison are mostly resistant to *B. cinerea* infection. Such development related resistance could be linked to preformed and inducible

antifungal compounds, as well as skin features of immature berries. Phenylpropanoid and flavonoid extracts of young berries, as well as resveratrol, can inhibit *B. cinerea* growth *in vitro* (Goetz et al., 1999; Schouten et al., 2002b; Pezet et al., 2003b). Furthermore, polyphenols in the berry skin cell wall and the thickness of epidermal cell layer complex were reported among the resistance factors (Mlikota-Gabler et al. 2003; Deytieux-Belleau et al., 2009). More recently, Agudelo-Romero et al. (2015) reported a large transcriptional activation of genes related to secondary metabolism and hormonal signaling (jasmonic acid [JA], ethylene [ET], and auxins) upon *B. cinerea* infection of immature berries of cv. Trincadeira. Another study on grapes infected at véraison reported the accumulation of reactive oxygen species (ROS), the activation of the salicylic acid (SA) dependent pathway and the induction of stilbene and lignin biosynthesis as defense mechanisms to arrest *B. cinerea* progression (Kelloniemi et al., 2015).

In disease management, quiescent infection has important implications for proper timing of prophylactic measures, to reduce stresses factors that may trigger egression of the quiescent pathogen, and to prolong quiescence to the point where the produce is not affected even after harvest (Jarvis, 1994). Concerning grapevine, flowering is an important stage in the epidemiology of *B. cinerea* as infection at this stage is followed by quiescence. Therefore, understanding the interaction between *B. cinerea* and grapevine inflorescence is vital to implement proper management in order to limit consequent yield losses. Despite this, knowledge about the molecular mechanisms of the interplay between *B. cinerea* and grapevine inflorescences at bloom is lacking. Taking advantage of the availability of the genome sequences of *Vitis vinifera* (Jaillon et al., 2007; Velasco et al., 2007) and *B. cinerea* (Amselem et al., 2011; van Kan et al, 2016), we analyzed the transcriptional alterations of both organisms during flower infection to understand the molecular mechanisms associated with the early stage of this interaction. Microscopic observation and metabolic profiles were combined with the transcriptomic analyses to further our understanding of the infection process at infection initiation and initial fungal quiescent stages.

2.3. Materials and methods

2.3.1. Plant material and *Botrytis cinerea* inoculation

Winter woody cuttings were collected from an experimental vineyard (*Vitis vinifera* cv. Pinot Noir) of the Fondazione Edmund Mach, Trentino-Alto Adige, Italy and stored at 4 °C until use. Flowers were raised from the cuttings following the technique of Mullins and Rajaskekaren

(1981). At the stage when single flowers of an inflorescence separate (EL17, according to Eichorn and Lorenz [1977]), they were thinned in order to have a manageable number of flowers per inflorescence to ensure that each flower could receive *B. cinerea* conidia. Cuttings were grown in a growth chamber at 24°C, with a 16 h light cycle.

Transgenic grapevine plants (*Vitis vinifera*, Microvine mutant) harboring the H₂O₂-specific HyPer probe, targeted to the cytosol, were generated using the DNA construct described in Costa et al. (2010).

Botrytis cinerea (isolate B05.10) was cultured on potato dextrose agar (PDA) in Petri dishes and incubated at 25 °C. After 10 days, conidia were harvested in distilled water and conidia concentration was determined under light microscope using a hemacytometer. At full cap-fall stage (EL25/26), each flower was inoculated by positioning 1.5 µl of a 2 * 10⁵ ml⁻¹ conidia solution close to receptacle area. After inoculation, the whole cutting was immediately bagged in water sprayed, clear plastic bag for 24 h in order to ensure high humidity, an essential factor for conidial germination. For microscopic observation and post-inoculation evaluation (plating out test), a genetically transformed strain of B05.10 expressing a green fluorescent protein (GFP) was used due to its fluorescent signal and ability to grow on selective medium (PDA with 70 µg/ml Hygromycin B).

2.3.2. Microscopic observations and detection of quiescent *Botrytis cinerea*

Confocal laser scanning microscopy analyses were performed using a Leica SP5 imaging system (Leica Microsystems, D-68165 Mannheim, Germany) and a Zeiss LSM700 (Carl Zeiss Microscopy, Germany). GFP and chlorophyll were excited at 488 nm and the emission was collected at 515-560 nm and 650-750 nm, respectively. For HyPer detection confocal microscopy analyses were performed according to Costa et al. (2010). Thin slices of fertilized gynoecia, which were manually cut from inoculated flowers, were subjected to microscopic observation.

For quiescent *B. cinerea* detection, the plating out method on selective medium was used. Eight fruitlets from each of 6 biological replicates were sampled daily from 1 to 7 and at 14 days post inoculation. Fruitlets were incubated on PDA with hygromycin at room temperature for a week before or after washing, or after surface sterilization. Washing was with sterile water, three rinses of 1 minute each with gentle shaking; whereas surface sterilization was carried out with 70% ethanol (1 min) followed by 1% (vol/vol) NaClO (3 min) and three rinses in sterile water (Keller

et al., 2003). Appearance of mycelial growth from healthy-looking fruitlets was scored as confirmation of quiescent *B. cinerea* on the fruitlets. Fruitlets > 4 mm in diameter (approximately) were cut into half before plating. Statistical significance among the treatments was calculated by Tukey's Honestly Significant Difference test on square root transformed data.

2.3.3. Secondary metabolites and RNA extraction

Inflorescences from fruiting cuttings that were either mock (control) or B05.10-conidia inoculated at cap-off stage, were collected at 12, 24, 48, 72 and 96 hpi, in three biological replicates, immediately frozen in liquid nitrogen, and kept at -80 °C until use. A biological replicate, throughout this study, is an inflorescence from a fruiting cutting. The samples used for polyphenol and RNA extraction were independent. Prior to polyphenol and RNA extraction, the samples were ground in liquid nitrogen. RNA was extracted using Plant Total RNA Kit (Sigma-Aldrich) following the manufacturer's protocol. For targeted secondary metabolite analysis, sample preparation and Ultra High Performance Liquid Chromatography - Diode Array Detection - Mass Spectrometry (UHPLC-DAD-MS) analysis were conducted as described in Vrhovsek et al. (2012).

For *B. cinerea* RNA extraction, B05.10 conidia were incubated in flask with potato dextrose broth (PDB) for 12 hours (Supplemental Figure S2.1) with 30 rpm shake in three biological replicates. Conidia obtained from a Petri dish were considered as a biological replicate.

2.3.4. RNA sequencing, data processing and data analysis

Three biological replicates harvested at 24 and 96 hpi were used for RNA-Seq analysis. Approximately 20 million strand-specific, 100 bp long sequences were obtained for each sample using a Next Generation Sequencing Platform HiSeq 1500 (Illumina, San Diego, CA). The quality of the the Illumina single-end reads was checked using FastQC (version 0.11.2) software (<http://www.bioinformatics.babraham.ac.uk/projects/fastqc/>) and pre-processed for adapter with cutadapt (version 1.8.1) (Martin, 2011). The resulting reads were aligned separately to the *B.cinerea* (strain B05.10) (<http://fungi.ensembl.org>) and grapevine (12Xv1, <http://genomes.cribi.unipd.it/>) genomes using the Subread aligner (Liao et al., 2013). Raw read counts were extracted from the Subread alignments using the featureCount read summarization program (Liao et al., 2014).

For grapevine, differential expression analysis of genes was performed taking advantage of the voom method (Law et al., 2014) which estimates the mean-variance relationship of the log-counts, generating a precision weight for each observation that is fed into the limma empirical Bayes analysis pipeline (Smyth, 2004). Genes were considered differentially expressed if they fulfill a p -value <0.05 and an absolute fold change of ≥ 1.5 . Gene ontology enrichment was computed using customized annotation and annotated reference of GO terms into the AgriGO analysis tool (<http://bioinfo.cau.edu.cn/agriGO/analysis.php>; Du Z et al., 2010). Enriched GO terms (FDR <0.05) were visualized using the ‘Reduce + Visualize Gene Ontology’ (REViGO) webserver (<http://revigo.irb.hr>; Supek et al., 2011). Furthermore, the grapevine molecular network gene annotation, VitisNet, (Grimplet et al., 2012) was also used to identify enriched molecular networks ($P < 0.05$) using VESPUCCI (<http://vespucci.colombos.fmach.it>) (Moretto et al., 2016). MapMan tool (Thimm et al., 2004) was used to visualize differentially expressed genes in the context of biotic stress pathway using the GrapeGen 12Xv1 annotations version (Lijavetzky et al., 2012) as MapMan Bins. For *B. cinerea*, gene set enrichment analysis was performed using Fisher’s exact test.

2.3.5. Quantitative polymerase chain reaction (qPCR)

For qPCR assays, cDNA was synthesized from 3 μg of the same RNA used for RNA-Seq analysis, treated with DNase I (Ambion), using the SuperScript™ VILO™ cDNA Synthesis Kit (Invitrogen). qPCR was performed in a Viiia7 thermocycler (Applied Biosystems) using 0.31 μl of cDNA and 2.5 μM of primers in a total volume of 12.5 μl where half of the total volume was Fast SYBR Green Master Mix (Kapa Biosystems) using the standard fast protocol. Each amplification reaction was run in triplicate. For normalization, *VvACT* and *VvTUB*, and *BcRPL5* and *BcTUBA* genes were selected using GeNORM (Vandesompele et al., 2002) as reference for grapevine and *B. cinerea*, respectively. Amplification efficiencies of each primer pair were calculated with LinReg software (Ruijter et al., 2009). The obtained amplification efficiency was used to calculate the relative quantity (RQ) and normalized relative quantity (NRQ) according to Hellemans et al. (2007). Statistical analyses of the qPCR results were made after $\log_2(\text{NRQ})$ transformation (Rieu and Powers, 2009). All primers and corresponding gene identifiers can be found in Supplemental Table S2.1. Statistical significance was calculated by Tukey's Honestly Significant Difference test or an unpaired heteroscedastic Student's t test, considering each technical replicate as an individual sample.

2.3.6. DNA extraction, standard curve and DNA quantification

DNA was isolated from grapevine flowers and *B. cinerea* (strain B05.10) mycelium using the Dneasy Plant Minikit (Qiagen) following the manufacturer's protocol. DNA from mycelium, obtained from conidia incubated for 48 h as mentioned above, and uninoculated grapevine flower were used to generate calibration curves to estimate the amount of fungal DNA in inoculated samples, 12, 24, 48, and 96 hpi, and 1 wpi. The inoculated samples were replicated three times. From 1 wpi samples, RNA was also extracted following the technique mentioned above. The samples used were independent from those used for RNA-Seq and secondary metabolite studies.

Genomic DNA was used as a template for qPCR with similar amplification procedure described above using primers Bc3, ribosomal IGS spacer, and VvRS I, resveratrol synthase gene I. For the standard curve, qPCR reaction were carried out in triplicate from known fungal or plant DNA extracts which were serially diluted 5 times. The standard curves were generated by plotting the log of DNA (pg) against the Ct value (Supplemental Figure S2.2). The Ct values obtained from inoculated samples were used to extrapolate the amount of genomic DNA from the standard curves. Genomic DNA of *B. cinerea* in a sample was normalized to the amount of grapevine genomic DNA in that sample.

2.4. Results

2.4.1. *Botrytis cinerea* infection of grapevine flower

Artificial infection of grapevine flowers with GFP-labeled B05.10 strain was conducted at full cap-off stage (EL25/26) (Figure 2.1A). The infection was monitored for two weeks post inoculation (wpi) and during this period there were no visible symptoms of infection or fungal growth (Figure 2.1B-E). Although fungal conidia germination, formation of appressoria and penetration into the flower cuticle on the gynoecium above the floral disc were observed 24 hours post inoculation (hpi) by confocal microscopy following the GFP signal of *B. cinerea* (Figure 2.1 F and Supplemental Figure S2.3), no substantial progress in fungal growth was appreciated at 96 hpi (Figure 2.1G). The presence of viable fungus during 2 wpi was confirmed by plating out experiments. Inoculated but healthy-looking fruitlets were incubated on selective media to allow the growth of the GFP-labeled *Botrytis* strain only. Before plating, fruitlets were either washed with distilled water or surface sterilized, to discriminate respectively either non germinated conidia or germinated conidia laying on the external layer of the flower tissue, from those bearing

penetration structures and grown in the inner layers. Germinated *B. cinerea* conidia were present on the skin of 90 % of the inoculated fruitlets, whereas about 30 % of the samples showed the presence of *B. cinerea* below the external cell layers of the fruitlet (Figure 2.1H). A preliminary test confirmed that washing within 6 hpi was able to remove ungerminated conidia from flowers and that surface sterilization abolished *B. cinerea* viability (Supplemental Figure S2.4).

To check if a similar load of *B. cinerea* was present at different post inoculation times, the amount of fungal DNA was estimated by quantifying the ribosomal IGS DNA (Supplemental Figure S2.2A), while the amount of grapevine DNA was also estimated by amplification of the resveratrol synthase gene I (Supplemental Figure S2.2B). As shown in Figure 2.2A, the relative amount of fungal DNA compared to plant DNA ranged from 4 to 6%, with a slight increase within two dpi, indicating initial pathogen growth, followed by a slight decrease possibly associated to a quiescent state. Furthermore, the expression profile of *B. cinerea* actin, *BcACTA*, an indicator of active growth, confirmed that the growth of the fungus *in planta* was relatively high up to two dpi, and then decreased slightly but significantly, supporting pathogen quiescence (Figure 2.2B).

Inoculated inflorescences were inspected until fruit ripening. At full coloring (approximately 10 wpi), bunches were either bagged with plastic bags, to create favorable humidity for *B. cinerea*, or left as such. About two weeks after bagging, egression of *B. cinerea* was observed on about 40 % (39 ± 9 %) of the inoculated berries (Supplemental Figure S2.5A). Cross checking of the strain using fluorescence microscope on mass of mycelia taken from the rotting bunch confirmed that the strain was the GFP-labeled B05.10 inoculated at cap-off stage (Supplemental Figure S2.5B). On the other hand, no egression was observed from unbagged bunches. In addition, to see if bagging can also trigger egression before maturity, bunches at pepper-corn satge, which were infected at cap-off stage, were bagged for two weeks, but no *B. cinerea* egression was observed (Supplemental Figure S2.6).

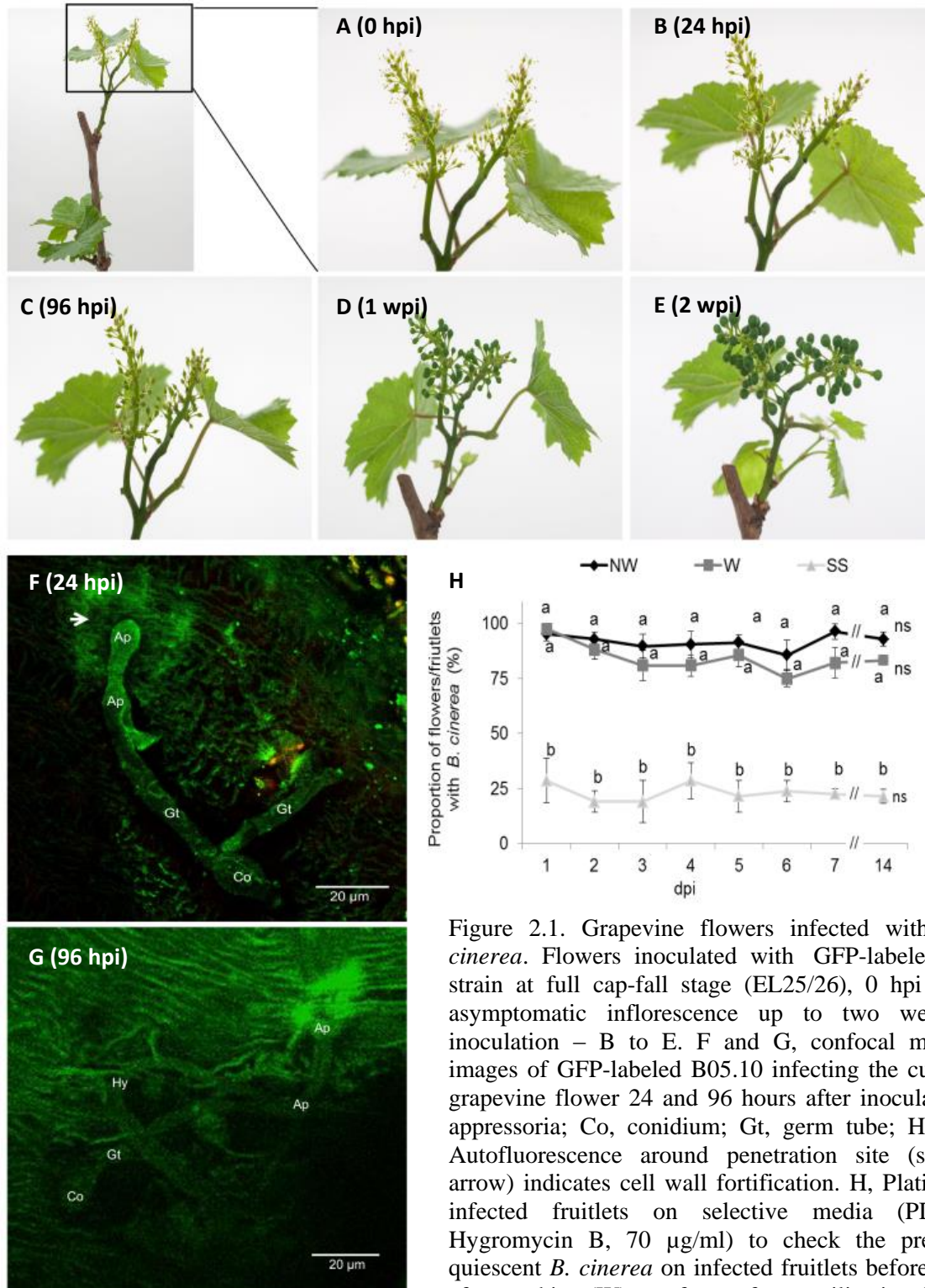


Figure 2.1. Grapevine flowers infected with *Botrytis cinerea*. Flowers inoculated with GFP-labeled B05.10 strain at full cap-fall stage (EL25/26), 0 hpi (A), and asymptomatic inflorescence up to two weeks post inoculation – B to E. F and G, confocal microscope images of GFP-labeled B05.10 infecting the cuticle of a grapevine flower 24 and 96 hours after inoculation. Ap, appressoria; Co, conidium; Gt, germ tube; Hy, hypha. Autofluorescence around penetration site (shown by arrow) indicates cell wall fortification. H, Plating out of infected fruitlets on selective media (PDA with Hygromycin B, 70 $\mu\text{g/ml}$) to check the presence of quiescent *B. cinerea* on infected fruitlets before (NW) or after washing (W), or after surface sterilization (SS). dpi, days post inoculation. Values at each day represent mean proportion of fruitlets (eight fruitlets from each of 6 biological replicate considered) showing GFP-labeled B05.10 growth on the selective media. Error bars indicate standard error. Mean proportions followed by a common letter within a dpi are significantly not different among NW, W and SS, according to Tukey's Honestly Significant Difference test ($P \leq 0.05$), using one way ANOVA. The mean proportions throughout the two weeks

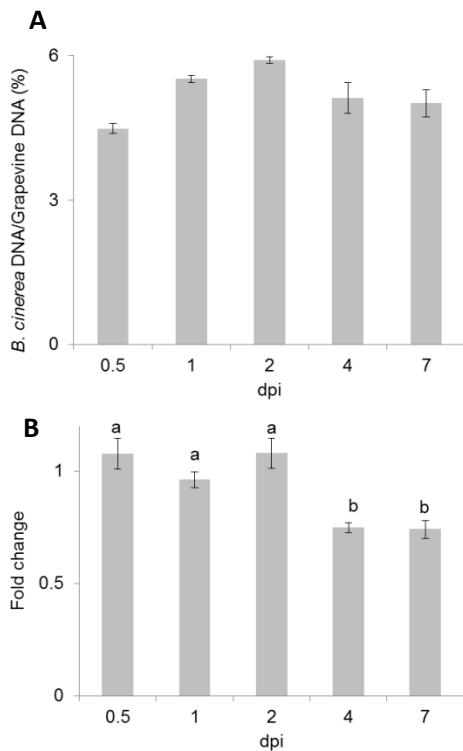


Figure 2.3. Relative quantification of genomic DNA (A) and expression profile of actin gene (B) from *B. cinerea* at different days post inoculation (dpi). A, Amount of *B. cinerea* gDNA relative to grapevine gDNA, measured by amplification of the *B. cinerea* gene *Bc3* (ribosomal IGS spacer) and the grapevine gene *VvRS 1* (resveratrol synthase gene I) on gDNA from *Botrytis*-inoculated flowers. The Kruskal-Wallis one way ANOVA test revealed that the amount of *B. cinerea* gDNA at different days post inoculation (dpi) is not significantly different, $P = 0.123$. Error bar represents standard error of mean of three biological replicates. B, Relative expression of a *B. cinerea* actin gene, *BcACTA*, to monitor the growth of the pathogen *in planta*. Bars represent fold change of inoculated samples relative to PDB cultured *B. cinerea* (control). Normalization based on the expression levels of ribosomal protein L5, *BcRPL5*, and α tubulin, *BcTUBA*, was carried out before calculating fold changes. Expression values followed by the same letter are significantly not different between samples, according to Tukey's Honestly Significant Difference test ($P \leq 0.05$), using one way ANOVA on $\log_2(\text{NRQ})$.

2.4.2. Transcriptome analysis of infected grapevine flowers

Three biological replicates of mock or B05.10 inoculated flowers were harvested at 24 and 96 hpi for dual (plant and fungus) transcriptome analysis using RNA-seq. These time points were chosen to understand the process of infection initiation (24 hpi) and progress (96 hpi), if any. As a control sample for *Botrytis*, an *in vitro* grown culture was used. The high quality trimmed reads obtained from the RNA-seq experiment were aligned against the 12Xv1 gene prediction of *V. vinifera* genome (<http://genomes.cribi.unipd.it/grape/>) and the *B. cinerea* strain B05.10 genome (<http://fungi.ensembl.org>). The fraction of reads from *Botrytis*- and mock-inoculated flowers mapped to the *V. vinifera* reference genome was between 65 and 82 %, whereas only up to 4.6 % could be mapped to the *B. cinerea* genome (Supplemental Table S2.2). In the case of *B. cinerea*, cultured in PDB, a much larger proportion of reads was mapped to the fungal genome (about 90%), suggesting that the scarce number of fungus reads derived from the infected flowers is likely caused by low number of conidia used for the infection (around 300) and of the limited fungal growth after inoculation.

As for grapevine, the biological variability within replicates and among experimental conditions was analyzed by principal component analysis (PCA). As shown in Figure 2.3A, the first principal component, which explains 38.4% of the variance, separates the two time-points (24

and 96 hpi) and also the 24-hours' *Botrytis* treated vs. untreated samples. In contrast, all samples collected at 96 hpi seem very similar at a whole transcriptome level, as indicated by the large overlap in the PCA.

Differential expression of grapevine genes was calculated between *Botrytis*- vs. mock-inoculated flowers within each time point after *t*-test, imposing an absolute minimum fold-change of 1.5 and a *p*-value < 0.05. At 24 hpi, 1193 genes were differentially expressed (upregulated or downregulated), whereas at 96 hpi only 265 genes were differentially expressed (Figure 2.3B, Supplemental Figure S2.7 and Supplemental Table S2.3). The overlap between the two sets was limited to 49 upregulated and 4 downregulated genes (Figure 2.3C). Interestingly, at 24 hpi the plant seems to respond to the presence of the pathogen with a prevalent induction of genes, which appeared to be no longer modulated at 96 hpi.

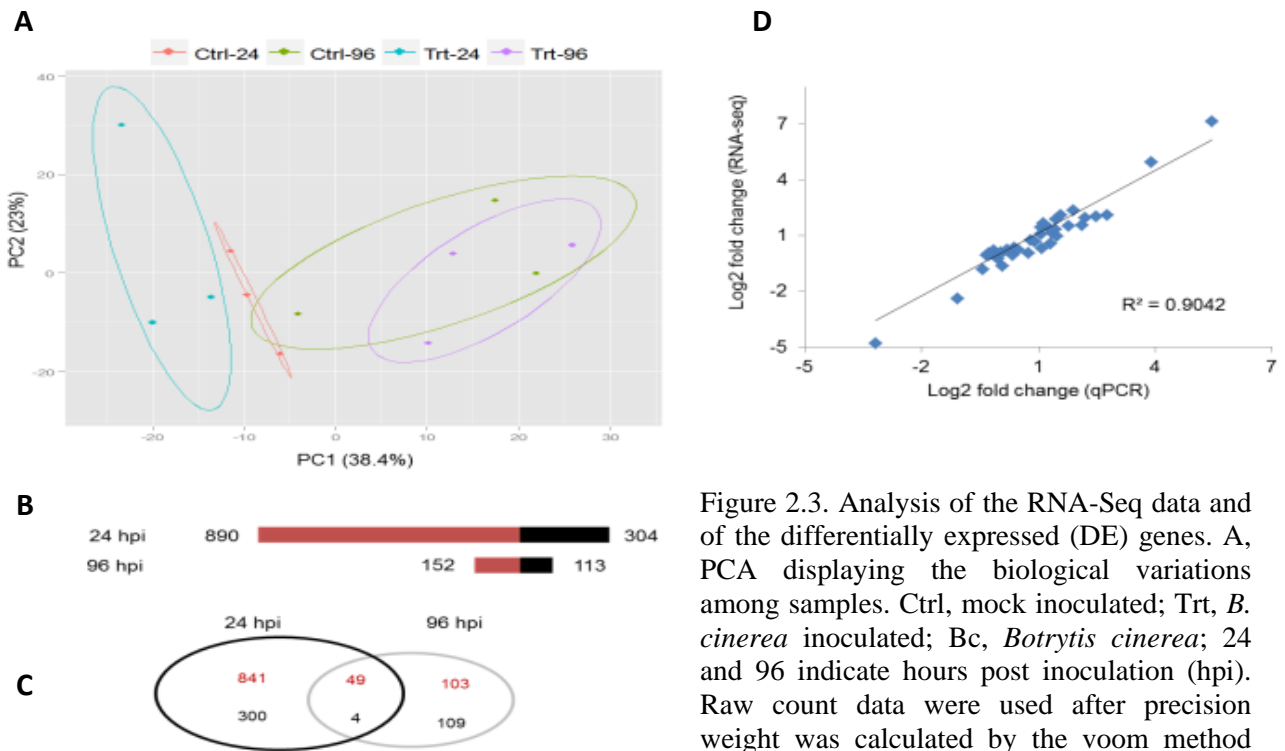


Figure 2.3. Analysis of the RNA-Seq data and of the differentially expressed (DE) genes. A, PCA displaying the biological variations among samples. Ctrl, mock inoculated; Trt, *B. cinerea* inoculated; Bc, *Botrytis cinerea*; 24 and 96 indicate hours post inoculation (hpi). Raw count data were used after precision weight was calculated by the voom method (Law et al., 2014). B, Number of DE genes

($P < 0.05$, absolute fold change > 1.5) upon *B. cinerea* infection at 24 and 96 hpi; upregulated genes (red) and downregulated genes (black). C, Venn diagram showing the number of DE genes unique or common to 24 and 96 hpi. D, Validation of RNA-Seq data by qPCR assay: correlation of fold change values for 20 *Vitis* genes obtained by RNA-Seq and qPCR.

Gene expression values from RNA-Seq analysis were validated using qPCR assay. The expression measurement of 20 grapevine genes (Supplemental Table S2.2) by qPCR was in very good agreement ($R^2 > 0.90$) with the results obtained by RNA-Seq (Figure 2.3D).

2.4.3. Defense related responses are largely induced in the flower upon *Botrytis cinerea* infection

Differentially expressed (DE) genes were annotated according to two different publicly available databases for grapevine, namely Gene Ontology (GO) (<http://genomes.cribi.unipd.it/grape/>) and VitisNet (<https://www.sdstate.edu/ps/research/vitis/pathways.cfm>), in order to characterize them in a comprehensive manner. Functional class enrichment analyses performed on the GO and VitisNet databases provided consistent and complementary results (Table 2.1 and Supplemental Table S2.5). A clear regulation of those classes typically modulated during biotic stress responses was found, they are represented in the MapMan pathway depicted in Figure 2.4 and significantly enriched in *Botrytis*-infected flowers (Supplemental Table S2.6). In the following text, these classes will be presented in detail.

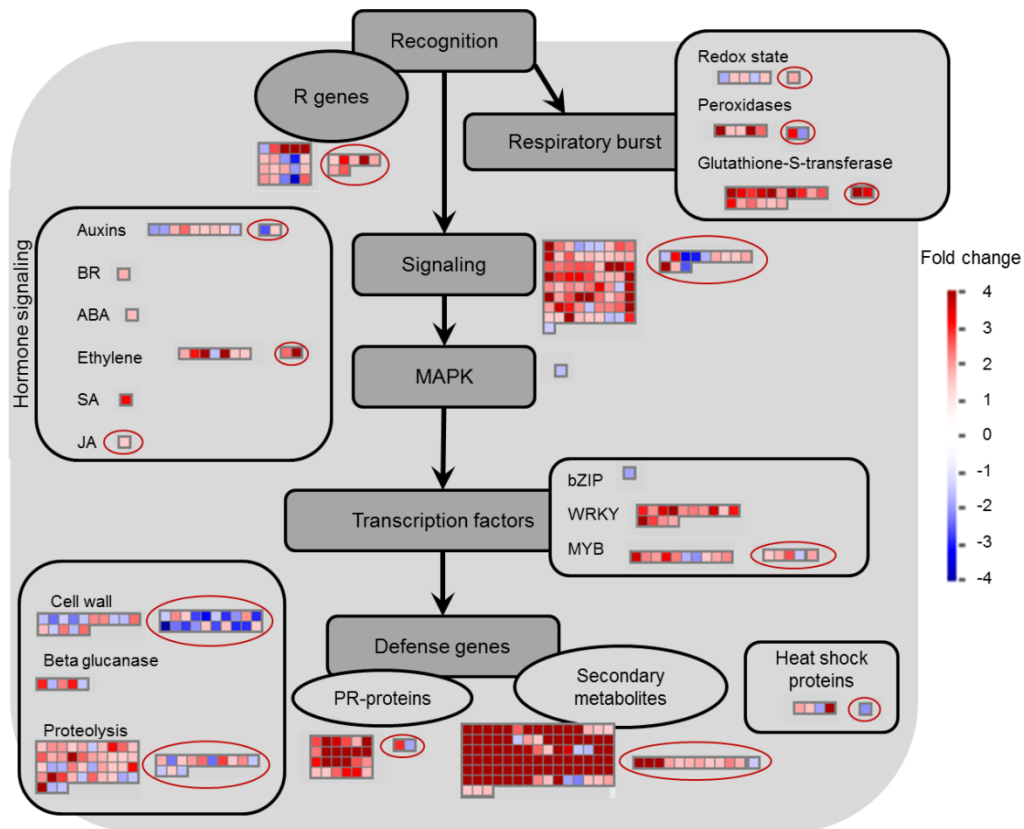


Figure 2.4. MapMan overview of biotic stress in inoculated flower at 24 and 96 hpi (red circled). Upregulated and downregulated genes are shown in red and blue, respectively. The scale bar displays fold change values. ABA, abscisic acid; BR, brassinosteroid; JA, jasmonic acid; MAPK, mitogen-activated protein kinase; SA, salicylic acid. The list of MapMan enriched pathways within DE genes is provided in Supplemental Table S2.6.

Table 2.1. Enriched Grapevine Molecular Networks according to VitisNet annotation

VVID	Network Name	Description	Number in input list	Number in reference list	<i>p</i> -value
<u>Upregulated genes (24 hpi)</u>					
10530	Aminosugars metabolism	carbohydrate metabolism	9	76	1.15E-03
10910	Nitrogen metabolism	energy metabolism	8	83	2.04E-03
10350	Tyrosine metabolism	amino acid metabolism	10	130	3.23E-03
10460	Cyanoamino acid metabolism	other amino acids metabolism	4	31	9.99E-03
10480	Glutathione metabolism	other amino acids metabolism	16	127	4.14E-07
10770	Pantothenate and CoA biosynthesis	cofactors and vitamin metabolism	5	39	4.16E-03
10940	Phenylpropanoid biosynthesis	biosynthesis of secondary metabolites	40	187	2.00E-12
11000	Single reactions	other	11	154	3.65E-03
34020	Calcium signaling pathway	signal transduction	9	128	9.05E-03
30008	Ethylene signaling	hormone signaling	15	232	2.00E-03
34626	Plant-pathogen interaction	plant specific signaling	25	311	1.75E-06
60003	AP2/EREBP	transcription factor	10	131	3.41E-03
60066	WRKY	transcription factor	19	62	1.93E-11
60069	ZIM	transcription factor	4	13	3.36E-04
<u>Downregulated genes (24 hpi)</u>					
10500	Starch and sucrose metabolism	carbohydrate metabolism	12	324	2.71E-04
44110	Cell cycle	cell growth and death	21	316	3.85E-11
44810	Regulation of actin cytoskeleton	cell motility	27	340	5.85E-16
60076	Other GTF		2	6	1.79E-03
<u>Upregulated genes (96 hpi)</u>					
10640	Propanoate metabolism	carbohydrate metabolism	4	63	6.66E-04
50121	Porters cat 1 to 6	transporter catalogue	6	160	5.20E-04
<u>Downregulated genes (96 hpi)</u>					
40006	cell wall	cell growth and death	12	445	1.31E-07

One of the earliest cellular responses following plant-pathogen interaction is the production of reactive oxygen species (ROS). Upon *B. cinerea* infection, genes putatively encoding enzymes involved in oxidative stress such as GST, ascorbate oxidase, 2OG-Fe(II) oxygenase, and cytochrome P450 monooxygenases were strongly upregulated (Table 2.2 and Supplemental Table S2.7). ROS accumulation at 24 hpi was proven by a localized green fluorescence emitted at the site of penetration in flowers obtained from a cytoplasmic HyPer (cHyPer) grapevine transgenic line expressing a cytosolic hydrogen peroxide molecular sensor (Figure 2.5).

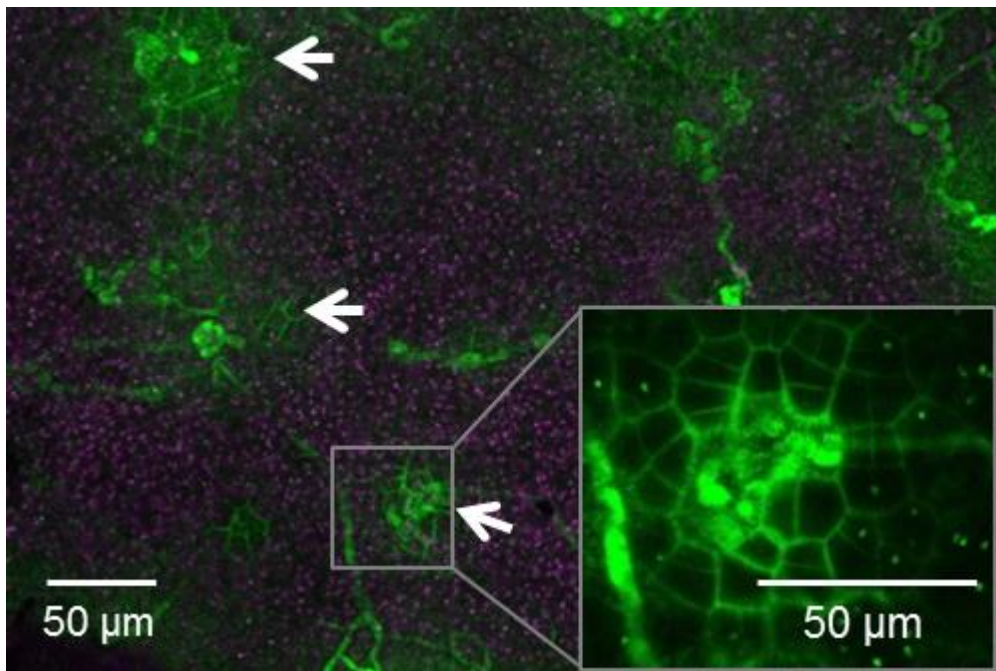


Figure 2.5. Confocal image of cytoplasmic HyPer grapevine transgenic flowers infected with *B. cinerea*. A higher intensity of HyPer fluorescence is evident 24 hpi at the penetration site of *B. cinerea*, compared with the rest of the plant tissue, indicating a localized and specific H_2O_2 accumulation (shown by arrows). The inset at higher magnification clearly shows that the bright signal comes from the cytosol of proximal cells to the site of infection.

Several genes encoding membrane-localized receptor-like kinases (*RLK*), such as, *Clavata1 receptor kinase*, *Wall-associated kinase 1*, and *Brassinosteroid insensitive 1– associated kinase 1 (BAK1)*, which have been characterized in connection with immune responses to necrotrophic pathogens (Kemmerling et al., 2007; Brutus et al., 2010), were also upregulated at 24 hpi (Supplemental Table S2.7). Genes associated with phytohormones, known to be involved in pathogen response signaling, were also differentially expressed (Figure 2.4 and Table 2.1).

Table 2.2. Selected differentially expressed grapevine genes due to *B. cinerea* inoculation (at 24 and 96 hpi)

	Fold change (log2)		Functional annotation	Id	Fold change (log2)		Functional annotation
	24 hpi	96 hpi			24 hpi	96 hpi	
Recognition and signaling				Response to stress and secondary metabolism			
VIT_15s0046g02220	2.67		ACC synthase	VIT_18s0001g04280	5.07		(-)-germacrene D synthase
VIT_07s0031g01070	2.21		Ascorbate oxidase	VIT_11s0052g01110	1.96		4-coumarate-CoA ligase 1
VIT_14s0030g02150	2.04	2.33	Calmodulin	VIT_04s0008g07250	2.04		Aspartyl protease
VIT_11s0016g03080	1.42		Clavata1 receptor kinase (CLV1)	VIT_05s0077g01540	5.43		Bet v I allergen
VIT_12s0035g00610	6.01		CYP82M1v3	VIT_16s0098g00850	0.68		Caffeic acid O-methyltransferase
VIT_18s0001g00030	1.01	2.79	CYP87A2	VIT_16s0100g00860	4.99		Chalcone synthase
VIT_17s0000g07400	1.01		Disease resistance protein (EDS1)	VIT_11s0149g00280	2.13		Chitinase A
VIT_17s0000g07420	1.38		Enhanced disease susceptibility 1 (EDS1)	VIT_03s0180g00250	4.41		Cinnamyl alcohol dehydrogenase
VIT_02s0234g00130	1.60		Ethylene responsive element binding factor 1	VIT_16s0039g02350	1.07		Dihydroflavonol 4-reductase
VIT_15s0048g01350	2.22		Gibberellin receptor GID1L3	VIT_18s0122g01150	6.57	2.61	Diphenol oxidase
VIT_08s0040g00920	2.94	1.71	Glutathione S-transferase 25 GSTU7	VIT_06s0004g01020	5.62	2.10	Dirigent protein
VIT_11s0016g00710	0.83		Jasmonate ZIM-domain protein 1	VIT_07s0031g01380	2.04	0.96	ferulate 5-hydroxylase
VIT_01s0011g03650	2.21		Map kinase substrate 1 MKS1				Inhibitor of trypsin and hageman factor (CMTI-V)
VIT_00s0250g00090	4.42	2.72	Oxidoreductase, 2OG-Fe(II) oxygenase	VIT_05s0020g05000	1.70		
VIT_03s0063g02440		-1.71	Proline extensin-like receptor kinase 1	VIT_18s0001g00850	6.48	2.84	Laccase
VIT_13s0064g01790	-1.62		R protein MLA10	VIT_16s0098g00460	3.29		Lipase class 3
VIT_00s0748g00020	4.14		Receptor kinase RK20-1	VIT_14s0083g00850		-1.67	Lipase GDSL 7
VIT_17s0000g04400	1.38		Wall-associated kinase 1 (WAK1)	VIT_13s0067g00050	3.32		Myrcene synthase
Trascription factors				VIT_15s0048g02430	1.65		Naringenin,2-oxoglutarate 3-dioxygenase
VIT_07s0005g03220		3.53		VIT_05s0077g01530	4.94	1.56	Pathogenesis protein 10
VIT_11s0016g02070	3.09	1.43	Basic helix-loop-helix (bHLH) family	VIT_05s0077g01550	4.62		Pathogenesis protein 10.3
VIT_07s0005g03340	1.87		Myb domain protein 14	VIT_03s0088g00750	1.45		Pathogenesis related protein 1 precursor
VIT_19s0027g00860	3.64		NAC domain-containing protein 42	VIT_01s0010g02020	7.12	2.09	Peroxidase
VIT_08s0058g00690	1.65		WRKY DNA-binding protein 33	VIT_16s0039g01280	5.40		Phenylalanin ammonia-lyase
VIT_14s0068g01770	3.29		WRKY DNA-binding protein 75	VIT_00s2849g00010	5.83		Phenylalanine ammonia-lyase
Cell wall				VIT_02s0025g02920	1.67		Quercetin 3-O-methyltransferase 1
VIT_14s0128g00970	2.75	1.40	Germin-like protein 3	VIT_08s0058g00790	1.51		Secoisolariciresinol dehydrogenase
VIT_05s0077g01280	-1.72	-2.40	Glycosyl hydrolase family 3 beta xylosidase	VIT_16s0100g01010	4.64		Stilbene synthase (VvSTS29)
VIT_06s0009g02560	3.21		Pectinesterase family	VIT_16s0100g01130	4.34		Stilbene synthase (VvSTS41)
VIT_08s0007g08330	-4.80		Polygalacturonase PG1	VIT_16s0100g01160	4.39		Stilbene synthase (VvSTS45)
VIT_09s0054g01080	3.10		Polygalacturonase QRT3	VIT_16s0100g00990	4.60		Stilbene synthase 2 (VvSTS27)
VIT_06s0004g01990	4.87	3.15	Proline-rich extensin-like family protein	VIT_16s0100g00950	4.63		Stilbene synthase 3 (VvSTS25)
VIT_03s0017g01990	1.79		UDP-glucose glucosyltransferase	VIT_02s0025g04230	2.21		Thaumatococin
				VIT_11s0065g00350	3.54		Trans-cinnamate 4-monooxygenase

According to the number of DE genes related to ET biosynthesis or signaling, this hormone seems to be important in the interaction between grapevine flower and *B. cinerea*. Two ACC synthase and one ACC oxidase genes in addition to seven ET responsive TFs were differentially expressed (Supplemental Table S2.7). Also genes encoding an SA marker *PR1* and the plant defense regulator involving SA signaling *Enhanced disease susceptibility 1* (Wiermer et al., 2005) were upregulated in the infected sample at 24 hpi (Table 2.2). Jasmonate ZIM-domain protein, a marker for JA, was slightly but significantly upregulated. Other genes involved in the synthesis of and signalling by phytohormones (apart from ET, JA and SA pathways) showed changes in transcript levels following inoculation with *B. cinerea*, suggesting a complex hormonal interplay. For example, five genes encoding nitrilase and nitrile hydratases, putatively involve in indole 3-acetic acid synthesis, were differentially regulated, as well as receptor genes for gibberellic acid (GA) and abscisic acid (ABA) (Supplemental Data S2). The global hormonal alterations related to infection were evaluated by Hormonometer software (Volodarsky et al., 2009) and presented in Supplemental Figure S2.8. The results of this analysis also suggested the involvement of several hormones.

Following the *Botrytis*-induced signaling cascades, about 100 TFs were differentially expressed in infected flowers. Most prominent were genes encoding WRKY TFs, Myb domain proteins, ethylene-responsive element-binding proteins, and NAC TFs (Supplemental Table S2.7). Among the transcriptional regulators previously associated to the defense reaction were *WRKY33*, a key transcriptional regulator involved in defense against *B. cinerea* and *Plasmopara viticola* in *Arabidopsis* and grapevine, respectively (Birkenbihl et al., 2012; Merz et al., 2015), and *Myb14*, which in grapevine regulates stilbene biosynthesis (Höll et al., 2013). This fast and strong induction of specific TFs leads to the activation of specific pathways, clearly related to plant defense. A number of genes encoding different classes of PR-proteins, such as chitinase, and Bet v I allergen, and Beta 1-3 glucanase were upregulated, up to 40 fold, following *Botrytis* inoculation. In this work, the transcription levels of *VvPR10.1* and *VvPR10.3*, and their putative regulator *WRKY33*, as indicated by previous studies for *VvPR10.1* (Dadakova et al., 2015; Merz et al., 2015), were analyzed in more detail. The transcription profiles measured by qPCR at five time points within the first 96hpi revealed that the transcript level of *VvWRKY33* was higher at 12 and 24 hpi (as compared to mock-treated samples) and dropped to the control level at later time points, 48 hpi and beyond, while the PR-proteins were always higher than control, except

VvPR10.1 at 48 hpi (Figure 2.6). *VvPR10.1* reached its peak level at 24 hpi, dropped at 48 hpi and then slowly increased at 72 and 96 hpi; whereas *VvPR10.3* showed a double peak of expression, the first at 24 hpi and a second one at 96 hpi. Proteases including those involved in defense such as subtilisin-like protease, aspartic protease, and serine protease inhibitor were also more expressed in *Botrytis*-inoculated than in mock-treated flowers (Supplemental Table S2.7).

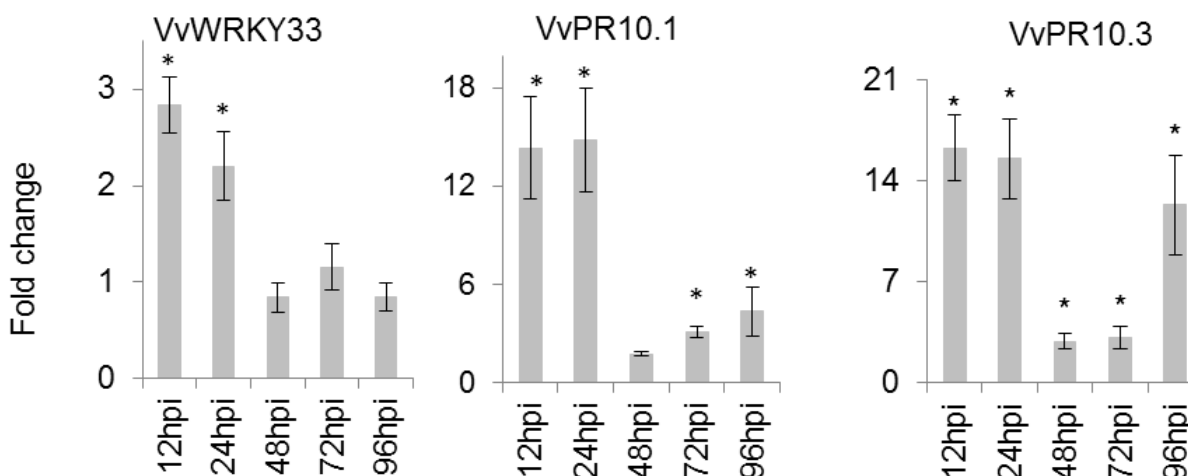


Figure 2.6. Expression profiles of *VvWRKY33*, *VvPR10.1*, and *VvPR10.3* following *B. cinerea* inoculation. Gene expression levels were determined by qPCR. Bars represent fold change of inoculated sample relative to mock-inoculated sample at each post-inoculation time. Normalization based on the expression levels of actin, *VvACT* and tubulin, *VvTUB* was carried out before calculating fold changes. Error bar represents standard error of the mean of three biological replicates. Asterisks (*) indicate statistically significant difference ($P < 0.05$) between mock- and *B. cinerea*-inoculated samples within a post-inoculation time using unpaired heteroscedastic Student's t test. hpi, hours post inoculation.

2.4.4. Secondary metabolism, mainly related to polyphenols, is upregulated in infected flowers

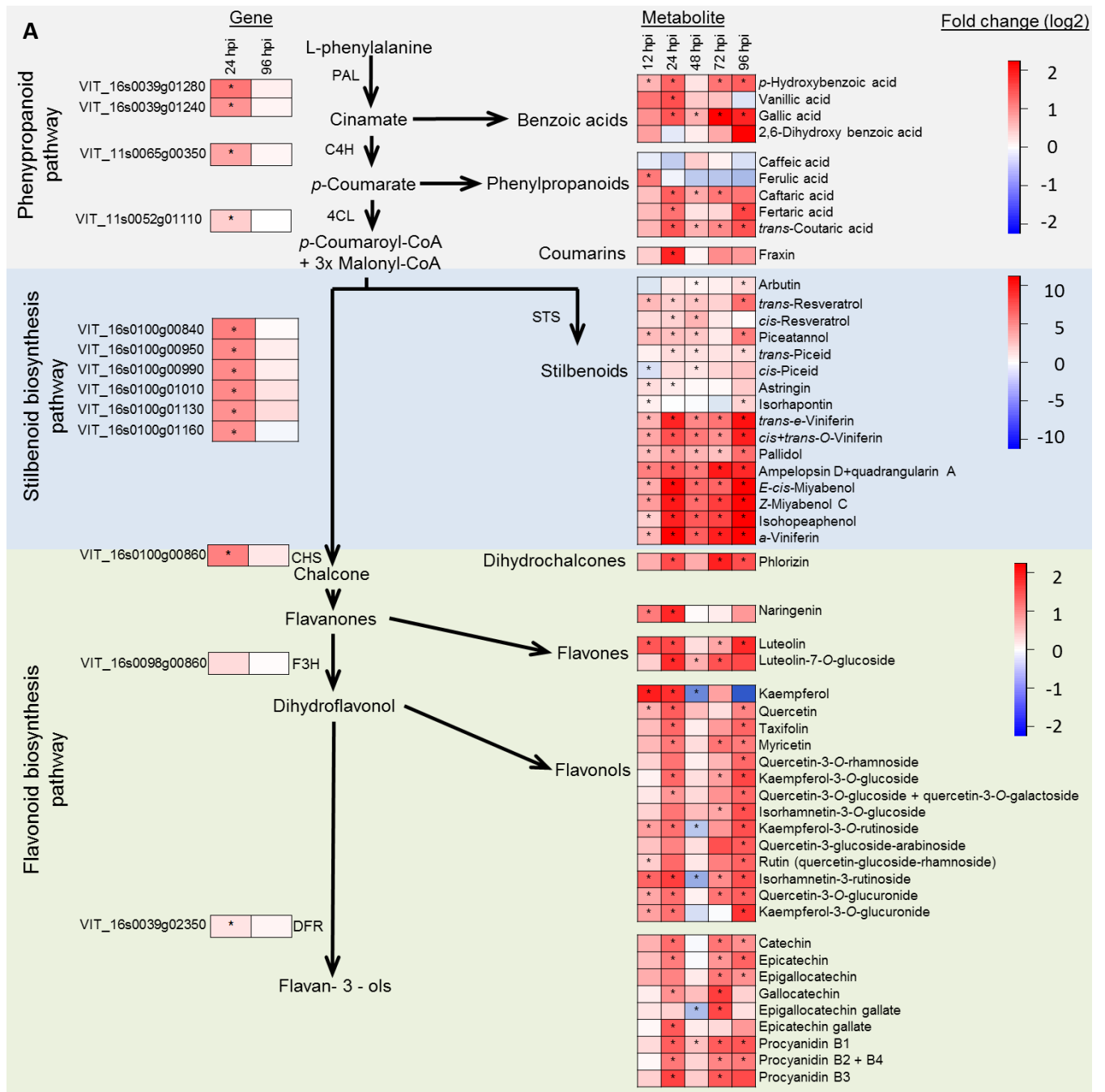
The RNA-Seq results underlined a reprogramming in the host transcriptome towards secondary metabolism, especially at 24 hpi (Figure 2.4 and Supplemental Table S2.7). Several genes related to terpenoid, benzoic acids, monolignol precursors, stilbenoid and flavonoid biosynthesis were strongly upregulated at the initial stage of *B. cinerea* infection. From the enrichment analysis, secondary metabolic process, protein modification process and phenylpropanoid biosynthesis were among the enriched functional categories at 24 hpi (Table 2.1 and Supplemental Table S2.5). To confirm these RNA-Seq observations, targeted secondary metabolites, mainly polyphenols, were quantified by UHPLC-DAD-MS at five time points between 12 and 96 hpi. The analysis revealed that a number of benzoic acid, monolignol precursors, stilbenoid

compounds and flavonoids, and their derivatives, many of which are associated with plant defense, were detected at higher concentrations in *Botrytis*-infected flowers as compared to mock-treated flowers (Supplemental Table S2.8), suggesting a huge defense-oriented metabolome reprogramming following *B. cinerea* inoculation. Figure 2.7 shows a heat map of the concentrations of metabolites in correlation with gene expression profiles, taken from the RNA-Seq result. In the phenylpropanoid pathway, ten genes encoding PAL were upregulated, between 13 and 55 fold at 24 hpi (Supplemental Table S2.7). Furthermore, genes encoding key enzymes in the pathway cinnamate 4-hydroxylase (C4H) and 4-coumarate-CoA ligase (4CL) had a fold change of about 12 and 4 times, respectively, also at 24 hpi (Table 2.2). The concentrations of benzoic acids (*p*-hydroxybenzoic acid, vanillic acid, and gallic acid) and monolignol precursors (ferulic acid, caftaric acid, fertaric acid, and *trans*-couteric acid) were higher in infected flowers, at least in one of the post inoculation time points considered (Figure 2.7A).

Regarding stilbenoids biosynthesis, an overwhelming number of STS genes were highly upregulated at 24 hpi (Supplemental Table S2.7). Of the 46 *V. vinifera* genes functionally annotated as STS, more than 80% of them were expressed in the infected flowers with a relative induction between 15 and 90 fold. Two genes which encode VvMYB14, an R2R3-MYB-type TF regulating stilbene biosynthesis (Höll et al., 2013), were also upregulated at 24 hpi (Table 2.2), suggesting that this regulatory circuit is activated at 24 hpi. The expression profiles of VvMYB14 and two STS genes, VvSTS29 and VvSTS41 (Vannozzi et al., 2012) were further monitored using qPCR (Figure 2.7B). Because of high sequence similarity among STS genes (Vannozzi et al., 2012), the primers used for VvSTS29 also detect the isoforms VvSTS25 and VvSTS27, while the primers used for VvSTS41 detect the isoform VvSTS45 too (Table 2.2) (Höll et al., 2013). These results showed a strong coinduction between the STS genes and VvMYB14 in grapevine flowers/fruitlets in response to *B. cinerea* infection, confirming the results of the RNA-Seq analysis (Figure 2.7B). The expression patterns observed in the qPCR assay also fitted with the quantification of stilbenoids. The phytoalexin resveratrol and its monomeric-derivatives piceatannol and *trans*-piceid were detected at higher concentrations in the infected flowers/fruitlets than control, in most of the post inoculation time points examined (Figure 2.7A). The other monomers astringin and isorhapontin, both tetrahydroxystilbenes with antifungal activity (Hammerbacher et al., 2011), were also induced. All of the quantified oligomeric resveratrols (dimers: *trans*- ϵ -viniferin, *cis*+*trans*-*o*-viniferin, pallidol, ampelopsin D and

quadrangularin A, and E-*cis*-miyabenol; trimers: Z-miyabenol C and α -viniferin; and the tetramer isohopeaphenol) were found highly concentrated in the infected flowers/fruitlets as compared to the control throughout the post inoculation time points examined (Figure 2.7A). The quantities of the stress related *trans*- ϵ - and α -viniferins, which are also involved in grapevine – *B. cinerea* interaction (Langcake, 1981), ranged from 0.9 to 13.4 $\mu\text{g/g}$ fresh weight (fw) and 2.8 to 151.8 $\mu\text{g/g}$ fw, respectively, in the inoculated fruitlets as compared to basal levels in mock inoculated controls. A similar increase in concentration was also observed in Z-miyabenol C and isohopeaphenol: 1.2 to 46.4 $\mu\text{g/g}$ fw and 0.2 to 20.9 $\mu\text{g/g}$ fw, respectively (Supplemental Table S2.8). Such an increase in the concentration of these monomeric and oligomeric stilbenoids suggests that they contribute to inhibiting the pathogen's advancement in colonizing the fruitlet.

In addition to STS genes, chalcone synthase (CHS), and dihydroflavonol-4-reductase (DFR), key flavonoid biosynthetic genes, were differentially expressed at 24 hpi (Table 2.2). The quantification of flavonoids revealed that flavanones, flavones, flavonols, and flavan-3-ols were detected at higher concentrations following *Botrytis* inoculation, most pronouncedly at 24, 72 and 96 hpi (Figure 2.7A). A number of flavonoids known to restrict fungal growth and in some cases also inhibit stilbene oxidases (Goetz et al., 1999; Guestsky et al., 2005; Puhl and Treutter, 2008; Nagpala et al., 2016), such as naringenin, kaempferol, quercetin, taxifolin, quercetin-3-glucuronide, catechin, epicatechin, epicatechin gallate, and procyanidin B1, B2, B3 and B4, were elevated within 24 hpi and often after 72hpi compared to control samples (Figure 2.7A).



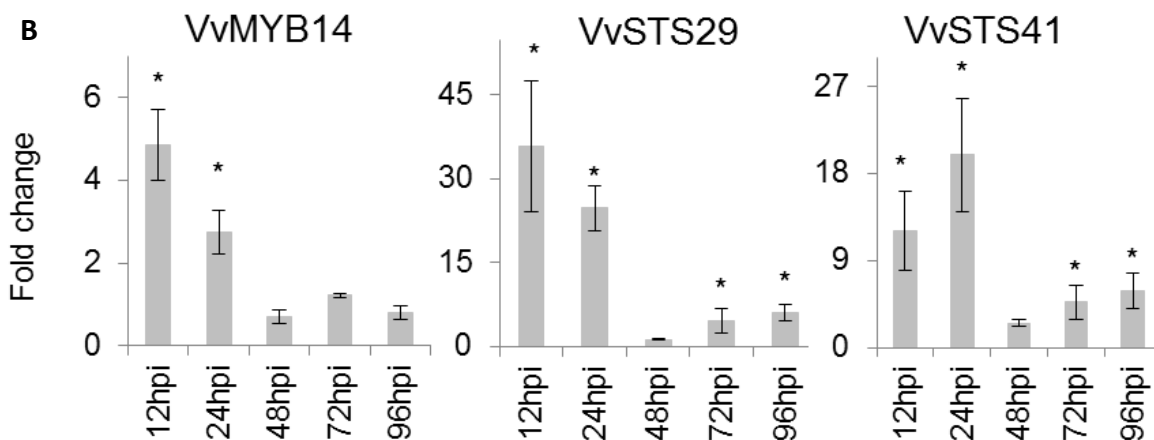


Figure 2.7. Transcript and metabolite analyses of the grapevine phenylpropanoid pathway upon *B. cinerea* inoculation. A, Heatmaps of gene expression (from RNA-Seq result) and secondary metabolite concentration ($\mu\text{g/g}$ fw, from HPLC-DAAD-MS) expressed as fold change. Fold changes were computed based on the ratio of average values in *B. cinerea*- and mock-inoculated flowers, for each time point. CHS, chalcone synthase; C4H, cinnamate 4-hydroxylase; 4CL, 4-coumarate-CoA ligase; DFR, dihydroflavonol-4-reductase; F3H, flavanone 3-hydroxylase; PAL, phenylalanine ammonia lyase; STS, stilbene synthase (out of 39, only 6 are depicted). B, Expression profile of *VvSTS29* (-27-25), *VvSTS41* (-45), and *VvMYB14*. Gene expression levels were determined by qPCR. Bars represent fold change of inoculated sample relative to mock-inoculated sample at each post-inoculation time. Normalization based on the expression levels of actin, *VvACT* and tubulin, *VvTUB* was carried out before calculating fold changes. Error bar represents standard error of the mean of three biological replicates. Asterisks (*) indicate statistically significant difference ($P < 0.05$) between mock- and *B. cinerea*-inoculated samples within a post-inoculation time using unpaired heteroscedastic Student's t test. hpi, hours post inoculation.

2.4.5. Infection triggers cell wall reinforcement

Reinforcing the cell wall to combat pathogen intrusion is a well-established mechanism in plants. A sign of cell wall apposition (CWA) at the site of penetration was observed by the autofluorescence of CWA regions (Figure 2.8A). The GO enrichment analyses also proposed that the L-phenylalanine catabolic process, cell wall, and extracellular region were among the enriched functional classes (Supplemental Table S2.5). This preliminary evidence was strengthened by modulation of genes encoding cell wall modifying enzymes such as pectinesterases (PEs), catalyzing the hydrolysis of methylester groups from polygalacturonans, polygalacturonases (PGs) and pectate lyases, degrading the pectic homogalacturonans (Supplemental Table S2.7). PE is involved both in cell wall loosening, by making polygalacturonans accessible to degradation by PG, and cell wall strengthening, by increasing the availability of polygalacturonan to Ca^{2+} binding (Micheli, 2001). The induction and suppression

of PEs and PGs observed in the RNA-Seq result may suggest that the flower is fine tuning between cell wall stiffening, as a barrier against the pathogen, and cell expansion and separation, as the flower itself is also in its active growth phase. Complementary to this, we observed that genes encoding germin-like protein 3 (GLP3) and proline-rich extensin-like protein (EXT), proteins involved in H₂O₂-mediated oxidative cross-linking to toughen cell walls during pathogen attack (Bradley et al., 1992; Godfrey et al., 2007; Kelloniemi et al., 2015), were highly upregulated both at 24 and 96 hpi (Table 2.2). Grapevine genes which encode enzymes involved in monolignol biosynthesis, cinnamyl alcohol dehydrogenase and *trans*-cinnamate 4-monooxygenase, were also highly upregulated (Table 2.2). These all suggest that cell wall fortification process might have been activated due to the infection.

Cell wall reinforcement is one of the possible mechanisms by which the grapevine flower arrests the advancement of *Botrytis*. Therefore, ten genes encoding enzymes in the monolignol biosynthesis pathway (based on the VitisNet annotations of phenylpropanoid biosynthesis), from the differentially expressed genes of RNA-Seq analysis, were selected for further investigation with a qPCR assay. The quantities of L-phenylalanine and other seven intermediate metabolites in this pathway were also measured by HPLC-DAD-MS (Supplemental Table S2.8). Transcripts of cinnamate 4-hydroxylase (*VvC4H*) and 4-coumarate-CoA ligase (*Vv4CL*), enzymes in the upstream of the pathway, were upregulated at the onset of *B. cinerea* infection, between 12 and 24 hpi, with *VvC4H* showing a peak at 12 hpi (Figure 2.8B). A similar trend was observed for cinnamoyl CoA reductase (*VvCCR*), the first enzyme specific to monolignol synthesis (Naoumkina et al., 2010). Caffeic acid o-methyltransferase (*VvCOMT*) and caffeoyl-CoA O-methyltransferase (*VvCCoAMT*) were slightly, but significantly, upregulated at 24 hpi only; however, ferulate 5-hydroxylase (*VvF5H*) was upregulated throughout the post inoculation time points examined. Cinnamyl alcohol dehydrogenase (*VvCAD*) was significantly upregulated up to 48 hpi. *VvCAD* is the final enzyme in the sequential actions of *Vv4CL*, *VvCCR*, and *VvCAD* to reduce aldehyde derivatives into the corresponding alcohols before monolignols synthesis. In the cell wall, monolignols undergo oxidative polymerization, catalyzed by peroxidases/laccases (Naoumkina et al., 2010). A strong upregulation of a lignin-forming anionic peroxidase-like (*VvPER*) was observed throughout the post inoculation time points examined, with the highest induction being within 24 hpi. With regard to laccase, about 10 putative grapevine laccase genes, having the same KEGG enzyme code of *Arabidopsis thaliana* lignin laccase (Zhao et al., 2013),

were also found extremely upregulated, up to 90 fold (Supplemental Table S2.7).

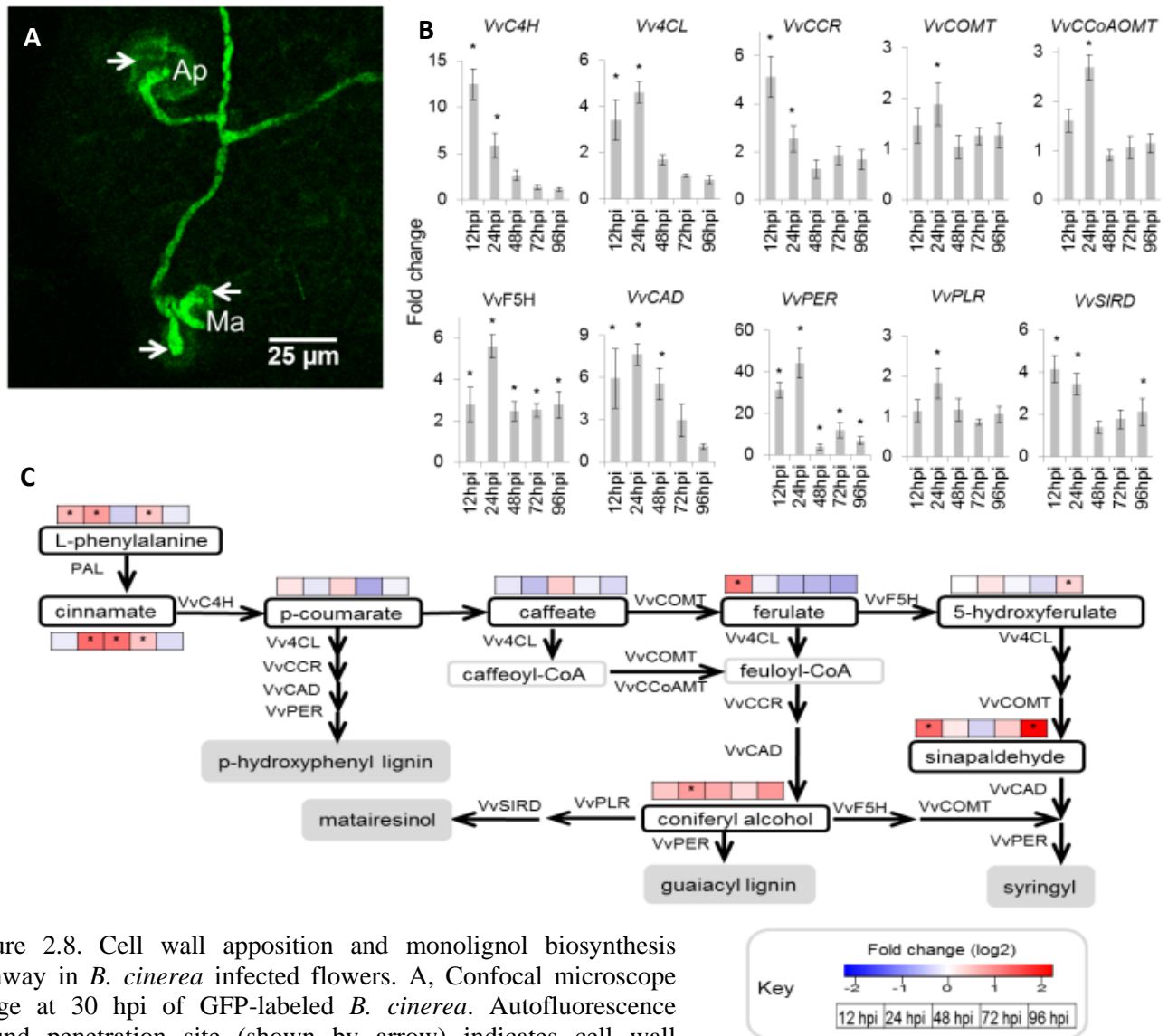


Figure 2.8. Cell wall apposition and monolignol biosynthesis pathway in *B. cinerea* infected flowers. A, Confocal microscope image at 30 hpi of GFP-labeled *B. cinerea*. Autofluorescence around penetration site (shown by arrow) indicates cell wall apposition. Ap, appressoria; and Ma, multicellular appressoria (infection cushions). B, Expression profile of genes encoding key enzymes of the grapevine monolignol biosynthetic pathway. *VvCAD*, cinnamyl alcohol dehydrogenase; *VvCOMT*, caffeic acid o-methyltransferase; *VvCCoAMT*, caffeoyl-CoA O-methyltransferase; *VvC4H*, cinnamate 4-hydroxylase; *VvCCR*, cinnamoyl CoA reductase; *Vv4CL*, 4-coumarate-CoA ligase; *VvF5H*, ferulate 5-hydroxylase; *PAL*, phenylalanine ammonia lyase; *VvPER*, peroxidase (lignin-forming anionic peroxidase-like); *VvPLR*, pinoresinol/lariciresinol reductase; *VvSIRD*, secoisolariciresinol dehydrogenase. Gene expression levels were determined by qPCR. Bars represent fold change of *B. cinerea*-inoculated sample relative to mock-inoculated sample at each post-inoculation time. Normalization based on the expression levels of actin, *VvACT* and tubulin, *VvTUB* was carried out before calculating fold changes. Error bar represents standard error of the mean of three biological replicates. C, Heatmap of monolignol precursors superimposed to the biosynthetic pathway. The amounts of monolignol precursors ($\mu\text{g/g}$ fw) were quantified by HPLC-DAAD-MS. Fold changes were computed based on the ratio of average values of *B. cinerea*- and mock-inoculated flowers, for each time point. Monolignol and lignan compounds are highlighted in gray background. Asterisks (*) indicate statistically significant difference ($P < 0.05$) between mock- and *B. cinerea*-inoculated samples within a post-inoculation time using unpaired heteroscedastic Student's t test.

Pinoresinol/lariciresinol reductase (*VvPLR*) and secoisolariciresinol dehydrogenase (*VvSIRD*), which catalyze subsequent metabolic steps to give rise to matairesinol, a lignan, as well as most of the DE genes which putatively encode dirigent-like proteins, a disease resistance-responsive family protein involved in lignan biosynthesis, were also upregulated in response to *B. cinerea*.

The quantification of metabolites also revealed that the concentrations of L-phenylalanine and cinnamate, which represent the two key entry substrates in the monolignol biosynthesis pathway, were significantly higher in *Botrytis*-inoculated flowers (Figure 2.8C). In contrast, the concentration of p-coumarate, caffeate, ferulate, and 5-hydroxyferulate were not different between *Botrytis*-inoculated flowers and control samples, probably due to their rapid conversion into the next metabolite of the pathway. Exceptions were the two intermediates, sinapaldehyde and coniferyl alcohol, metabolites found towards the end of the pathway, which were generally higher in the *Botrytis*-inoculated flowers than in the control samples.

These results indicate that upon *B. cinerea* infection, cell wall fortification was among the defense mechanisms employed by the flowers/fruitlets to contain the pathogen in its quiescent state.

2.4.6. *Botrytis cinerea* transcripts expressed *in planta* during grapevine flower infection

The signal of *B. cinerea* transcripts detected in inoculated flowers was very low (Supplemental Table S2.2). As mentioned above, the reasons could be the limited amount of conidia used for inoculation, about 300 conidia per flower, and/or the arrest in fungal growth after penetration resulting in a very low abundance of fungal RNA in the samples. Therefore, it was not possible to perform a statistical comparison between the transcriptome of the infecting pathogen vs. the PDB-grown fungus in order to identify the pathogenicity genes of *Botrytis* and an alternative approach was applied. Genes from *B. cinerea* were considered expressed if they were represented by an average of at least 10 reads in the three biological replicates of inoculated flower samples. 1325 genes met these conditions and will be herein referred to as “*in planta* expressed genes”. Of these, 751 and 59 were expressed only at 24 and 96 hpi, respectively; and 515 genes were expressed at both 24 and 96 hpi (Supplemental Table S2.9).

The set of *in planta* expressed genes were functionally annotated using Blast2GO (Conesa et al., 2005) and Amselem et al. (2011) (Supplemental Table S2.9). The joined biological meaning of the genes was visualized using the Combined Graph Function of Blast2GO based on their GO

slim terms, and primary metabolic process, nitrogen compound metabolic process, ion binding, oxidoreductase activity, and cytoplasmic component were among the most represented GO terms (Supplemental Table S2.10). This automatic annotation was manually curated to improve gene description and the most important functional categories are reported in Table 2.3. *In planta* expressed genes encompassed genes involved in pathogenesis, such as Carbohydrate-Active enZymes (CAZymes) devoted to plant cell wall degradation, in ROS production and detoxification, in toxins biosynthesis, as well as in transcriptional regulation; all these genes were more abundant at 24 hpi. Besides, many ribosomal and histone genes were equally abundant at 24 and 96 hpi indicating the maintenance of a basal metabolism during quiescence.

Table 2.3. Specific functions of *in planta* detected *B. cinerea* transcripts

Functions of of <i>Botrytis cinerea</i> genes	No.of genes involved	
	24hpi	96hpi
Proteins identified as early secretome, within 16 h of germination (Espino et al., 2010)	39	9
Carbohydrate-Active Enzymes (CAZymes) (Amselem et al., 2011; Blanco-Ulate et al., 2014)	203	64
CAZymes acting on fungal cell wall	36	16
CAZymes acting on Plant Cell Wall	56	11
CAZymes acting on cellulose	5	2
CAZymes acting on hemicellulose	20	3
CAZymes acting on hemicellulose and pectin side chains	9	0
CAZymes acting on pectin	23	1
Proteins generating Reactive Oxygen Species (ROS) (Schumacher et al., 2014)	10	2
Proteins involved in the detoxification of ROS (Schumacher et al., 2014)	23	8
Protease (Amselem et al., 2011)	38	8
secondary metabolism key enzymes (Amselem et al., 2011)	3	0
60S & 40S ribosomal protein (Amselem et al., 2011)	78	78
Appressorium-associated genes (orthologs in <i>Magnaporthe oryzae</i>) (Amselem et al., 2011)	7	2
Transporters	64	22
Transcription factors	29	13
Histone	8	7
Actin	11	6

2.4.7. *Botrytis cinerea* genes required for pathogenesis are upregulated during flower infection

A group of 23 *in planta* expressed genes known to be related or possibly associated to *Botrytis* growth or pathogenesis were further characterized by qPCR to study their expression profiles during the early interaction with the grapevine flower, in comparison to their expression during

Botrytis growth in PDB medium. In addition, other two genes, glutathione S-transferase (*BcGST1*) and polygalacturonase2 (*BcPG2*), reported to be induced during pathogenesis were analyzed. qPCR expression profiles are shown in Figure 2.9, while gene names together with the expression level from the RNA-seq analysis are reported in Table 2.4.

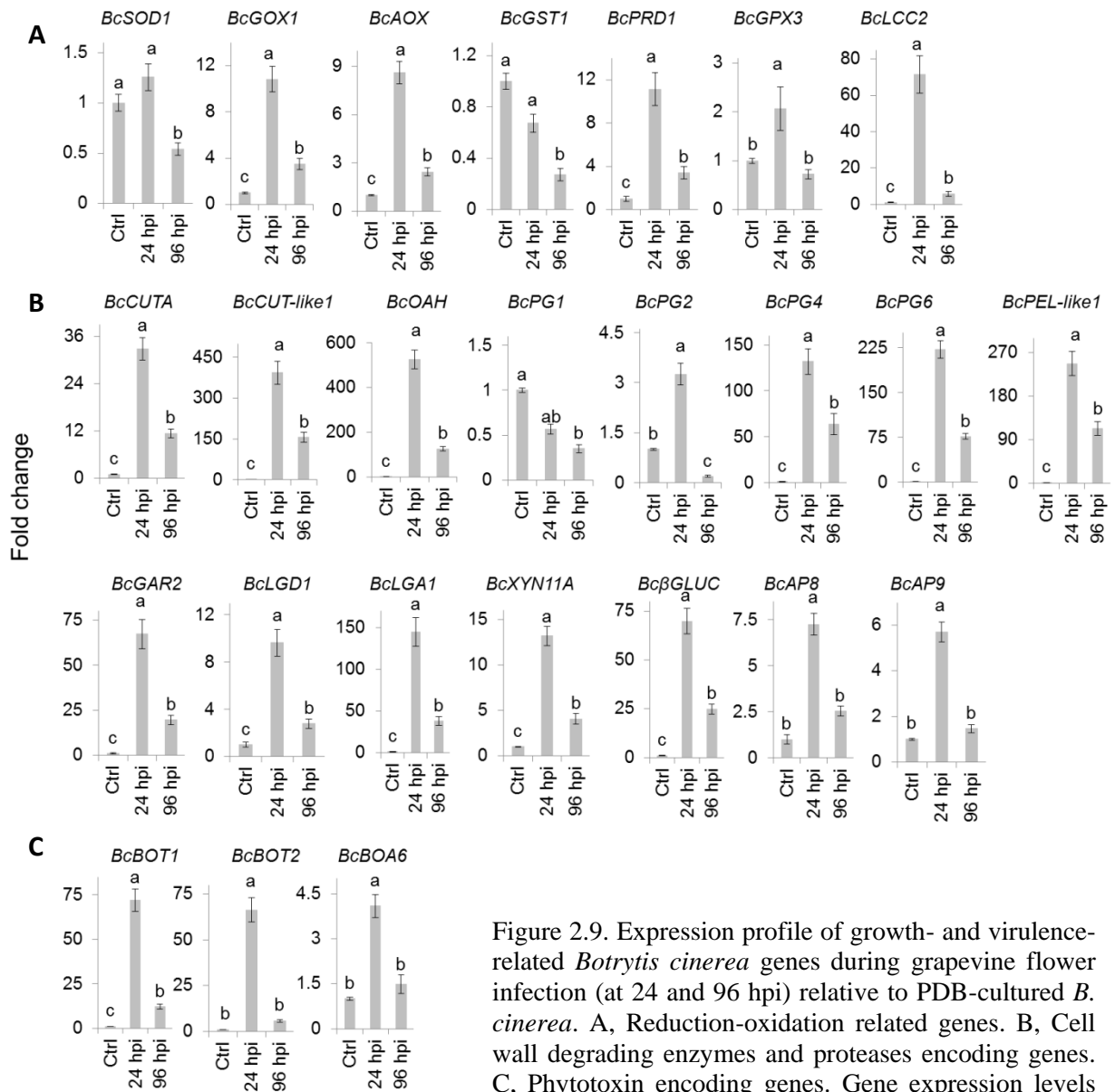


Figure 2.9. Expression profile of growth- and virulence-related *Botrytis cinerea* genes during grapevine flower infection (at 24 and 96 hpi) relative to PDB-cultured *B. cinerea*. A, Reduction-oxidation related genes. B, Cell wall degrading enzymes and proteases encoding genes. C, Phytotoxin encoding genes. Gene expression levels were determined by qPCR. Bars represent fold change

of sample at 24 or 96 hpi relative to the PDB-cultured *B. cinerea* (Ctrl). Normalization based on the expression levels of ribosomal protein L5, *BcRPL5*, and α tubulin, *BcTUBA*, was carried out before calculating fold changes. Error bar represents standard error of the mean of three biological replicates. Expression values followed by a common letter are significantly not different between samples, according to Tukey's Honestly Significant Difference test ($P \leq 0.05$), using one way ANOVA of $\log_2(\text{NRQ})$.

Table 4. RNA-seq reads of *B. cinerea* transcripts checked by qPCR assay

Abbreviation	Transcript description	Gene ID	Average no. of raw reads from RNA-seq analysis		
			In planta expressed		PDB culture
			24hpi	96hpi	
<i>BcSOD1</i>	Superoxide dismutase1	Bcin03g03390	76	26	9,411 ^a
<i>BcGOX1</i>	Galactose oxidase	Bcin13g05710	21		609
<i>BcAOX</i>	Alcohol oxidase	Bcin07g03040	24		490
<i>BcGST1</i>	Glutathione S-transferase	Bcin10g00740			2,655 ^a
<i>BcPRD1</i>	Dyp-type peroxidase	Bcin13g05720	19		312
<i>BcGPX3</i>	Glutathione peroxidase	Bcin03g01480	23		2,871 ^a
<i>BcLCC2</i>	Laccase2	Bcin14g02510	15		32 ^b
<i>BcCUTA</i>	Cutinase	Bcin15g03080	15		54 ^b
<i>BcCUT-like1</i>	Cutinase	Bcin01g09430	68	11	9 ^b
<i>BcOAH</i>	Oxaloacetate acetylhydrolase	Bcin12g01020	386		38 ^b
<i>BcPG1</i>	Polygalacturonase1	Bcin14g00850	209	175	147,821 ^a
<i>BcPG2</i>	Polygalacturonase2	Bcin14g00610			362
<i>BcPG4</i>	Polygalacturonase4	Bcin03g01680	44		47 ^b
<i>BcPG6</i>	Polygalacturonase6	Bcin02g05860	75		62
<i>BcPEL-like1</i>	Pectate lyase	Bcin03g05820	87	24	40 ^b
<i>BcGAR2</i>	D-galacturonic acid reductase2	Bcin03g01500	37		104
<i>BcLGD1</i>	D-galactonate dehydrogenase	Bcin01g09450	61	10	804
<i>BcLGA1</i>	2-keto-3-deoxy-L-galactonate aldolase	Bcin03g01490	70	13	66
<i>BcXYN11A</i>	Endo-beta-1,4-xylanase	Bcin03g00480	18		129
<i>BcβGLUC</i>	Beta-glucosidase 1 precursor	Bcin10g05590	32		75
<i>BcAP8</i>	Aspartic proteinase8	Bcin12g02040	30	12	1,064 ^a
<i>BcAP9</i>	Aspartic proteinase9	Bcin12g00180	16		569
<i>BcBOT1</i>	Botrydial biosynthesis1	Bcin12g06380	58		86
<i>BcBOT2</i>	Botrydial biosynthesis2	Bcin12g06390	41		55
<i>BcBOA6</i>	Botcinic acid6	Bcin01g00060	13		1,048 ^a

(a) transcripts whose average raw reads is in the top 25 %, most expressed, while (b) are those transcripts whose average reads is in the bottom 25 %, least expressed, in PDB culture.

All genes showed a sharp peak of expression at 24 hpi, except superoxide dismutase1 (*BcSOD1*), *BcGST1*, and the constitutively expressed *BcPG1*. Interestingly, the expression level at 24 hpi of some genes was extremely high, due to their very low level of expression in PDB culture, which was taken as a reference. These genes, which included oxaloacetate acetyl hydrolase (*BcOAH*), cutinase (*BcCUT-like1*), and pectate lyase (*BcPEL-like1*), appeared to be expressed exclusively during *Botrytis* attack, while other genes were also expressed in the absence of the host, but relatively much more during the host-pathogen interaction.

B. cinerea cutinases *BcCUTA* and *BcCUT-like1* are involved in the breaching of the cuticle layer by appressoria. This invasive step normally causes oxidative burst in the host (Schouten et al., 2002a) which is counteracted by the activation of scavenging mechanisms in the pathogen. The transcription levels of several *B. cinerea* genes taking part in the ROS-mediated fungus-plant

interaction were quantified (Figure 2.9A). *BcSOD1*, which plays role in oxidative stress response during cuticle penetration (Rolke et al., 2004); H₂O₂ generators galactose oxidase (*BcGOX1*) and alcohol oxidase (*BcAOX*); ROS scavengers *BcGST*, peroxidase1 (*BcPRD1*), and glutathione peroxidase (*BcGPX3*) (Schumacher et al., 2014); and *BcLCC2*, a gene involved in the oxidation of resveratrol and tannins (Schouten et al., 2002b), were all involved in the *Botrytis*-grapevine interaction. Necrotrophic fungi seem to stimulate the oxidative burst response of the plant and even contribute to it to favor the colonization process (review Heller and Tudzinsky, 2011).

A similar expression profile, albeit quantitatively different, was shown by cell wall degrading enzymes (CWDEs) (Figure 2.9B). *PG*, pectate lyase (*BcPEL-like1*), and oxaloacetate acetyl hydrolase (*BcOAH*), a gene with numerous functions including enhancing the activity of PG, are involved in pectin degradation. Galacturonate reductase (*BcGAR2*), galactonate dehydratase (*BcLGD1*), and 2-keto-3-deoxy-L- galactonate aldolase (*BcLGAI*), genes which play a role in the catabolic pathway of D-galacturonic acid (Zhang et al., 2011), a major component of pectin polysaccharides (Mohnen, 2008; Caffall and Mohnen, 2009), also had similar trends of expression. D-galacturonic acid may serve as an energy source when *B. cinerea* grows in and through plant cell walls (Zhang et al., 2011). The strong and similar expression pattern in pectin and D-galacturonic acid degrading enzymes suggested that the degradation of the pectin backbone was initiated at 24 hpi. The involvement of other CWDEs, such as the endo-beta-1,4-xylanase precursor (*BcXYN1IA*), which degrades hemicellulose and also induces necrosis (Noda et al., 2010), beta-glucosidase (*BcβGLUC*), which degrades both cellulose and hemicellulose (Gilbert, 2010; Blanco-Ulate et al., 2014), and secreted aspartic proteinases (AP) was also highlighted from the qPCR assay (Figure 2.9B). The RNA-Seq data further suggested the involvement of pectin lyases (Bcin03g00280 and Bcin03g07360), enzyme acting preferentially on highly methyl esterified pectin, in the infection process (Supplemental Table S2.9).

The strong upregulation of botcinic acid (*BcBOA*) and botrydial phytotoxins (*BcBOT*) genes, involved in phytotoxins synthesis, pointed towards their participation in the fungal infection program (Figure 2.9C). *BcBOA6* gene encodes a polyketide synthase (PKS), a key enzyme for botcinic acid synthesis (Dalmais et al., 2011), and the *BcBOT1* and *BcBOT2* genes encode P450 monooxygenase and sesquiterpene cyclase, respectively (Siewers et al., 2005).

Taken together, these results indicate the readiness of the fungus to colonize the flowers within 24 hpi. However, the transcript levels of all of the tested infection-related *B. cinerea* genes were much lower at 96 hpi, suggesting that the pathogenesis program initiated at 24 hpi is halted at a later time point. The transcriptional profile of *BcACTA* also suggested that the activity of the fungus decreased towards the later hours of infection. From the post-inoculation inspection of the infected flowers, no visible disease progress was detected until ripening (Figure 2.1). This strengthens the hypothesis that the fungus reduced its biological activity and entered into a quiescent phase.

2.5. Discussion

In grapevine, gray mold disease caused by *B. cinerea* occurs mainly on ripe berries close to harvest. The epidemiology of the fungus on grapevine, especially the infection process of the pathogen during flowering, is largely unknown. *B. cinerea* infection of grapevine inflorescence at blooming followed by a “latency period” as a possible source of early bunch rot at véraison was first reported by McClellan and Hewitt (1973). This observation was further confirmed by Keller and colleagues who demonstrated that inoculation at full bloom leads to high disease severity at harvest (Keller et al., 2003). Using the advantage of a GFP-labeled B05.10 strain, we could show for the first time that *B. cinerea* inoculated at flower cap-off stage remained in a quiescent state until berry full coloration (for about two and half months) and then it resumed active growth and invaded the berries when the microclimate was conducive (high humidity). This study provides a detailed description of the infection processes from infection initiation (24 hpi) to initial fungal quiescent (96 hpi) stages by means of transcriptomic and metabolic analyses and microscopic observations, laying the foundation for understanding the mechanism of the plant-fungus interaction during flowering which leads to pathogen quiescence.

Confocal microscopy and transcriptomic studies showed that the fungus, upon contact with the grapevine flowers, attempted to establish infection before becoming quiescent as observed from the germinated appressoria in the flower gynoecium (Figure 2.1B & G) and a prevalent modulation of defense related genes within 24 hpi. The main functional categories of the *in planta* expressed genes of the fungus were those related to pathogenesis, such as CAZymes, oxidative stress, proteases, and transporters (Table 2.3). Interestingly, much of these *in planta* expressed genes were also differentially regulated during successful infection of ripe grapevine

berries (16, 24 and 48 hpi) (Kelloniemi et al., 2015), *Lactuca sativa* (12, 24, and 48 hpi) (De Cremer et al., 2013), and *Solanum lycopersicoides* (24 and 48 hpi) (Smith et al., 2014). This suggests that the *in planta* expressed genes were part of the pathogenesis mechanisms deployed in grapevine flowers that would help to establish infection.

One of the key processes in establishing infection by *B. cinerea* is the depolymerization of cell wall components (van Kan, 2006; Williamson et al., 2007; Zhang et al., 2011). Generally, after breaching the cuticular layer of host tissues, *B. cinerea* often grows into the pectin-rich anticlinal wall of the underlying epidermal cell (van Kan, 2006; Williamson et al., 2007), by the activation of pectinases. In our study, almost all of the assayed CAZymes, including pectinases, were expressed at a higher level at 24 hpi (Figure 2.9). Besides increased levels of CWDEs, the upregulation of genes encoding the biosynthesis of phytotoxic secondary metabolites and secreted proteases, which assist the infection process (Dalmais et al., 2011; Rossi et al., 2011), further confirmed that the fungus put in place several strategies to invade the grapevine flowers. Nonetheless, there was no visible disease symptoms observed in the post-inoculation observations despite the presence of *B. cinerea* was confirmed by the plating out experiment (Figure 2.1H); implying that the pathogen could not grow actively and switched into quiescent phase. The much lower number of *Botrytis* genes expressed *in planta* at 96 hpi as compared to 24 hpi (65% less), as well as the estimated ratio of *B. cinerea* to grapevine RNA (1:500, Supplemental Table S2.2) compared to the much smaller ratio for genomic DNA (about 1:20, Figure 2.1I) in the same tissue, is also a confirmation that the fungus entered the quiescent phase.

Quiescence of a pathogen can happen before conidia germination, at initial hyphal development stage, before or after appressorium formation, after appressorium germination and/or at subcuticular hyphae stage (Prusky, 1996). In unripe tomato, *Colletotrichum gloeosporioides* becomes quiescent as a swollen hyphae after appressorium germination (Alkan et al., 2015), whereas *Alternaria alternata* enters into quiescence after its hypha penetrates the cuticular layer of young apricot, persimmon, and mango fruits (Prusky, 1996). For *B. cinerea*, cell wall penetrated hypha was proposed as a quiescent stage of infection in immature grape berries (Keller et al., 2003). Although the quiescence of ungerminated conidia cannot be completely ruled out in our case, the microscopic observation of conidia germination and appressoria formation (Figure 2.1G and Supplemental Figure S2.3), together with the results of the plating out experiment,

which showed a non-significant effect of washing the inoculated berries (Figure 2.1H), indicate that the pathogen entered into a quiescent state after penetrating the cell wall. The burst of defense related reactions from the plant is also an indirect support for this claim.

In our study the attempted infection by *B. cinerea* instigated a multilayered defense response in the grapevine flower tissues. Following inoculation, more than 70 RLKs were differentially expressed within 24 hpi (Supplemental Table S2.7). Several of these RLKs have been described to be involved in immune response to pathogens. The perception of cell wall fragments, such as oligogalacturonides (OGs) due to CWDE, induces basal resistance to the pathogen (Boller and Felix, 2009). In *A. thaliana*, over-expressing the OG receptor *Wall-associated kinase 1* enhanced resistance to *B. cinerea* (Brutus et al. 2010), but on the other hand increased susceptibility to *Sclerotinia sclerotiorum* and *B. cinerea* was observed in BAK1 mutant *Arabidopsis* (Kemmerling et al., 2007; Zhang et al., 2013). The RLK BAK1 constitutes a negative control element of microbial infection-induced cell death in plants (Kemmerling et al. 2007). These two RLKs exhibited increased expression levels in powdery mildew resistant *V. pseudoreticulata* in response to *E. necator* (Weng et al., 2014) and in *B. cinerea* challenged lettuce (De Cremer et al., 2013). We also saw upregulation of genes coding for these membrane receptor proteins at 24 hpi, indicating that the plant recognizes the pathogen and triggers an immunity response: quick and strong induction of PR-proteins and accumulation of stress related secondary metabolites, as well as cell wall lignification are deployed as major defense responses to halt the infection. The oxidative stress caused during the interaction seemed mainly managed by GSTs and ascorbate oxidases (Marrs, 1996) as more than 20 genes coding for them were upregulated at 24 hpi. The pathogen responsive *PR10*, *PR5* (thaumatococin-like protein), and chitinases also had a marked upregulation (between 5 and 40-fold upregulation within 24 hpi) compared to the rest of differentially expressed PR-proteins. Chitinases and thaumatococin-like proteins are known for their inhibition of fungal growth including *B. cinerea* (Giannakis et al., 1998; Monteiro et al., 2003). From our qPCR result, a very quick induction, as early as 12 hpi, of *VvPR10.1* and *VvPR10.3* was observed. *VvPR10.1* was recently associated to *P. viticola* resistance, under the regulation of *VvWRKY33* (Merz et al., 2015). We demonstrated a coordinated expression of *VvWRKY33* and *VvPR10.1* during *B. cinerea* infection, too. Even though the two pathogens are biologically different and may not necessarily activate similar response from their hosts, *VvPR10.1* and *VvPR10.3*, a PR belonging to the same group of *VvPR10.1* (Lebel et al., 2010), had the highest

upregulation among the expressed PRs, making them strong candidates for the resistance of grapevine flower to *B. cinerea*. In *Arabidopsis WRKY33*, the functional homologue of *VvWRKY33* (Merz et al., 2015), plays a key role in the plant defense process, regulating redox homeostasis, SA signaling, ET-JA-mediated cross-communication, and phytoalexin biosynthesis conferring resistance to *B. cinerea* (Birkenbihl et al., 2012).

Upon *B. cinerea* infection, grapevine berries activate stilbenoid biosynthesis (Langcake, 1981; Jeandet et al., 1995; Keller et al., 2003; Agudelo-Romero et al., 2015; Kelloniemi et al., 2015). Our results were in line with previous evidence: many genes involved in stilbenoid and flavonoid biosyntheses were upregulated, STS and laccase coding genes were the ones with the highest upregulation. From the RNA-Seq results, it seemed that the genes coding for STS and laccase proteins were switched on following the infection, since most of them were below the detection limit in the mock-inoculated flowers. The activation of the polyphenol biosynthetic pathway was further investigated by a more fine-grained expression profile of the transcription factor regulating stilbene biosynthesis (*VvMYB14*, Höll et al., 2013) together with *VvSTS29* and *VvSTS41*, and by measuring the concentration of several classes of polyphenols (phenylpropanoids, stilbenoids, and flavonoids). The phytoalexin resveratrol, which inhibits *B. cinerea* growth (Schouten et al., 2002b; Favaron et al., 2009) and its monomeric and oligomeric derivatives, some with documented antifungal activity (Hammerbacher et al., 2011), were all upregulated starting from 12 hpi. The concentrations of ϵ -viniferin and α -viniferin, dimer and trimer resveratrol respectively, were higher in *Botrytis*-infected flowers than control throughout the measured period. These compounds represent the predominant stress metabolites in *Vitaceae* - *B. cinerea* interactions reported previously (Langcake, 1981). We also observed a marked oligomerization of resveratrol to ampelopsin D and quadrangularin, E-cis-miyabenol, Z-miyabenol C, and isohopeaphenol upon infection, which agrees with the hypothesis that oligomerization of resveratrol leads to more toxic compounds (Pezet et al., 2003a). On the other hand, overexpressing the glycosylated form of resveratrol, trans-piceid, in *Arabidopsis* that overexpresses a resveratrol gene *PcRS*, increased its resistance to *Colletotrichum higginsianum* (Liu et al., 2011). In line with this, over-expression of an *STS* gene in transgenic grapevine plants led to resistance to *B. cinerea* colonization (Coutos-Thévenot et al., 2001; Dabauza et al., 2014) and a strong correlation was also observed between the concentration of stilbenic phytoalexins

and resistance to *P. viticola* both in a *V. riparia* and *Merzling* × *Teroldego* cross population (Langcake, 1981; Malacarne et al., 2011).

The potent stilbene oxidase inhibitors caftaric and *trans*-coutaric acids (both phenylpropanoids), catechin, and quercetin-3-O-glucuronide (both flavonoids) (Goetz et al., 1999) were also detected at higher concentrations in the *Botrytis*-infected flowers than in the control, contributing to the defense reaction. These compounds possibly interfered with the fungal laccase activity by inactivating its oxidizing and insolubilizing effects on stilbenic phytoalexins and PR proteins (Goetz et al., 1999; Favaron et al., 2009). In addition, different classes of flavonoids including proanthocyanidins (procyanidins B1, B2, B3 and B4) were also detected at a higher concentration in the infected flowers; these compounds can act as inhibitors of enzymes such as polygalacturonases. Higher concentration of proanthocyanidins in the epidermal layer of immature strawberry, at the periphery of *B. cinerea* penetration, was reported to restrict further growth of *B. cinerea* and keep the pathogen under quiescence (Jersch et al., 1989). Taken together, our results indicated a dramatic and rapid accumulation of the polyphenolic metabolites, in particular stilbenoids, at the site of infection suggesting this is a mechanism of defense to induce *B. cinerea* quiescence in grapevine flower.

Reinforcing cell walls is another strategy of plant resistance against pathogens. From our microscopic observations, cell wall apposition occurred at the appressorium penetration site (Figure 2.1F and Figure 2.8A). Gene expression and metabolite analysis also indicated that grapevine flowers, upon *B. cinerea* infection, activated the monolignol biosynthesis pathway within 24 hpi. A significant accumulation of the metabolites at the beginning of the pathway (L-phenylalanine and cinnamate) as well as at the end of the pathway (sinapaldehyde and coniferyl alcohol) was indeed observed. Instead, whereas, most of the intermediates were very low (such as p-coumarate and caffeate) or not detectable, possibly due to their rapid conversion into products for the next steps in the pathway. A similar phenomenon occurs in wheat, where upregulation of monolignol genes within 24 hpi conferred resistance to *Blumeria graminis* f. sp. *Tritici*; and silencing a few key genes in the pathway (PAL, COMT, CCoAMT and CAD) compromised penetration resistance of the plant to the pathogen (Bhuiyan et al., 2009). The upregulation of *GLP3* and *EXT*, both at 24 and 96 hpi, and accumulation of H₂O₂ around the penetration site, as shown using the HyPer signal (Figure 2.5), suggests CWA was triggered as an early response to

the infection. H₂O₂-mediated oxidative cross-linking and lignin synthesis to reinforce CWA and halt *B. cinerea* infection was recently shown in grapevine by Kelloniemi et al. (2015). In their study, the upregulation of lignin forming enzymes (GLP3 and EXT) together with the accumulation of H₂O₂ at the site of *Botrytis* penetration, were part of the defense mechanisms used by the véraison berry to arrest the pathogen. However, no such queues of responses were seen in the mature berry where the pathogen readily managed to colonize the berry tissue (Kelloniemi et al., 2015). In green tomatoes, usually resistant to *B. cinerea*, the accumulation of H₂O₂ and lignin occurs at the site of inoculation (Cantu et al., 2009), and in a tomato *sitiens* mutant, primed H₂O₂ accumulation and cell wall reinforcement were among the resistant factors against *B. cinerea* (Asselbergh et al., 2007). These all show that the CWA-mediated resistance was also active in the *B. cinerea* infected flowers.

2.6. Conclusions

Flowering is a critical phenological stage in the epidemiology of *B. cinerea* in the vineyard leading to quiescent infection. Our work provides the first transcriptomic and targeted metabolites analyses of the interaction between the two organisms at this critical phenological stage. Our results showed that upon contact with the grapevine flower, within 24 hpi, *B. cinerea* induced genes encoding for CWDE, phytotoxic secondary metabolites, and proteases, indicating a readiness to establish a successful infection. There was no visible disease symptom in the post inoculation time however, despite the confirmed presence of the pathogen and an egression at the later ripening stage. Flowers reacted readily to the infection as their defense mechanisms were very in-line upon recognizing the intruder. There was a marked accumulation of antimicrobial proteins (mainly PR-proteins), monolignol precursors, stilbenoids, and reactive oxygen species accompanied by cell wall reinforcement. The conjugated actions of these induced defense responses seem to be responsible for forcing *B. cinerea* into quiescence until more favorable conditions occur in the berry.

2.7. References

- Agudelo-Romero P, Erban A, Rego C, Carbonell-Bejerano P, Nascimento T, Sousa L, Martínez-Zapater JM, Kopka J, Fortes AM** (2015) Transcriptome and metabolome reprogramming in *Vitis vinifera* cv. Trincadeira berries upon infection with *Botrytis cinerea*. *J Exp Bot* **66**: 1769–1785
- Alkan N, Friedlander G, Ment D, Prusky D, Fluhr R** (2015) Simultaneous transcriptome analysis of *Colletotrichum gloeosporioides* and tomato fruit pathosystem reveals novel fungal pathogenicity and fruit defense strategies. *New Phytol* **205**: 801–815
- Amselem J, Cuomo CA, van Kan JA, Viaud M, Benito EP, Couloux A, Coutinho PM, de Vries RP, Dyer PS, Fillinger S, et al** (2011) Genomic analysis of the necrotrophic fungal pathogens *Sclerotinia sclerotiorum* and *Botrytis cinerea*. *PLoS Genet* **7**: e1002230
- Asselbergh B, Curvers K, Franca SC, Audenaert K, Vuylsteke M, Van Breusegem F, Höfte M** (2007) Resistance to *Botrytis cinerea* in sitiens, an abscisic acid-deficient tomato mutant, involves timely production of hydrogen peroxide and cell wall modifications in the epidermis. *Plant Physiol* **144**: 1863–1877
- Audenaert K, De Meyer GB, Hofte MM** (2002) Abscisic acid determines basal susceptibility of tomato to *Botrytis cinerea* and suppresses salicylic acid-dependent signaling mechanisms. *Plant Physiol* **128**: 491–501
- Bèzier A, Lambert B, Baillieul F** (2002) Study of defense-related gene expression in grapevine leaves and berries infected with *Botrytis cinerea*. *Eur J Plant Pathol* **108**: 111–120
- Bari R, Jones J** (2009) Role of plant hormones in plant defence responses. *Plant Mol Biol* **69**: 473–488
- Bhuiyan NH, Selvaraj G, Wei Y, King J** (2009) Role of lignification in plant defense. *Plant Signal Behav* **4**: 158–159
- Birkenbihl RP, Diezel C, Somssich IE** (2012) Arabidopsis WRKY33 is a key transcriptional regulator of hormonal and metabolic responses toward *Botrytis cinerea* infection. *Plant Physiol* **159**: 266–285
- Blanco-Ulate B, Morales-Cruz A, Amrine KC, Labavitch JM, Powell AL, Cantu D** (2014) Genome-wide transcriptional profiling of *Botrytis cinerea* genes targeting plant cell walls during infections of different hosts. *Front Plant Sci* **5**: 435
- Blanco-Ulate B, Vincenti E, Powell AL, Cantu D** (2013) Tomato transcriptome and mutant analyses suggest a role for plant stress hormones in the interaction between fruit and *Botrytis cinerea*. *Frontiers in Plant Science* **4**: 142. doi: 10.3389/fpls.2013.00142
- Boller T, Felix G** (2009) A renaissance of elicitors: perception of microbe-associated molecular patterns and danger signals by pattern-recognition receptors. *Annu Rev Plant Biol* **60**: 379–406
- Bradley DJ, Kjellbom P, Lamb CJ** (1992) Elicitor- and wound- induced oxidative cross-linking of a proline-rich plant cell wall protein: A novel, rapid defense response. *Cell* **70**: 21–30
- Brutus A, Sicilia F, Macone A, Cervone F, De Lorenzo G** (2010) A domain swap approach reveals a role of the plant wall-associated kinase 1 (WAK1) as a receptor of oligogalacturonides. *Proc Natl Acad Sci USA* **107**: 9452–57
- Caffall KH, Mohnen DB** (2009) The structure, function, and biosynthesis of plant cell wall pectic polysaccharides. *Carbohydr Res* **344**: 1879–1900

- Cantu D, Blanco-Ulate B, Yang L, Labavitch JM, Bennett AB, Powell AL** (2009) Ripening-regulated susceptibility of tomato fruit to *Botrytis cinerea* requires NOR but not RIN or ethylene. *Plant Physiol* **150**: 1434-1449
- Cantu D, Vicente AR, Greve LC, Dewey FM, Bennett AB, Labavitch JM, Powell ALT** (2008) The intersection between cell wall disassembly, ripening, and fruit susceptibility to *Botrytis cinerea*. *Proc Natl Acad Sci USA* **105**:859–64
- Choquer M, Fournier E, Kunz C, Levis C, Pradier JM, Simon A, Viaud M** (2007) *Botrytis cinerea* virulence factors: new insights into a necrotrophic and polyphagous pathogen. *FEMS Microbiol Lett* **277**: 1–10
- Coertze S, Holz G** (2002) Epidemiology of *Botrytis cinerea* on grape: wound infection by dry, airborne conidia. *S Afr J Enol Vitic* **23**: 72–77
- Comménil P, Brunet L, Audran JC** (1997) The development of the grape berry cuticle in relation to susceptibility to bunch rot disease. *J Exp Bot* **48**:1599–1607
- Conesa A, Götz S, García-Gómez JM, Terol J, Talón M, Robles M** (2005) Blast2GO: a universal tool for annotation, visualization and analysis in functional genomics research. *Bioinformatics* **21(18)**: 3674–3676
- Conn S, Curtin C, Bézier A, Franco C, Zhang W** (2008) Purification, molecular cloning, and characterization of glutathione S-transferases (GSTs) from pigmented *Vitis vinifera* L. cell suspension cultures as putative anthocyanin transport proteins. *J Exp Bot* **59**: 3621-3634
- Costa A, Drago I, Behera S, Zottini M, Pizzo P, Schroeder JI, Pozzan T, Lo Schiavo F** (2010) H₂O₂ in plant peroxisomes: an in vivo analysis uncovers a Ca²⁺-dependent scavenging system. *Plant J* **62**: 760-772
- Coutos-Thévenot P, Poinssot B, Bonomelli A, Yean H, Breda C, Buffard D, Esnault R, Hain R, Boulay M** (2001) *In vitro* tolerance to *Botrytis cinerea* of grapevine 41B rootstock in transgenic plants expressing the stilbene synthase Vst1 gene under the control of a pathogen-inducible PR 10 promoter. *J Exp Bot* **52**: 901-910
- Dabauza M, Velasco L, Pazos-Navarro M, Pérez-Benito E, Hellín P, Flores P, Gómez-Garay A, Martínez M, Lacasa A** (2014) Enhanced resistance to *Botrytis cinerea* in genetically-modified *Vitis vinifera* L. plants over-expressing the grapevine stilbene synthase gene. *Plant Cell Tissue Org Cult* **120**: 229-238
- Dadakova K, Havelkova M, Kurkova B, Tlojkova I, Kasparovsky T, Zdrahal Z, Lochman J** (2015) Proteome and transcript analysis of *Vitis vinifera* cell cultures subjected to *Botrytis cinerea* infection. *J Proteomics* **119**: 143–153
- Dalmis B, Schumacher J, Moraga J, Le Pecheur P, Tudzynski B, Collado IG, Viaud M** (2011) The *Botrytis cinerea* phytotoxin botcinic acid requires two polyketide synthases for production and has a redundant role in virulence with botrydial. *Mol Plant Pathol* **12**: 564-579
- De Cremer K, Mathys J, Vos C, Froenicke L, Michelmore RW, Cammue BP, De Coninck B** (2013) RNAseq-based transcriptome analysis of *Lactuca sativa* infected by the fungal necrotroph *Botrytis cinerea*. *Plant Cell Environ* **36**: 1992-2007
- Deytieux-Belleau C, Geny L, Roudet J, Mayet V, Donèche B, Fermaud M** (2009) Grape berry skin features related to ontogenic resistance to *Botrytis cinerea*. *Eur J Plant Pathol* **125**: 551-563

- Du Z, Zhou X, Ling Y, Zhang Z, Su Z** (2010) agriGO: a GO analysis toolkit for the agricultural community. *Nucleic Acids Res* **38**: W64–W70
- Eichorn KW, Lorenz DH** (1977) Phänologische entwicklungsstadien der rebe. *Nachrichtenbl. Deut Pflanzenschutz* **29**: 119-120
- Elmer PAG, Michailides TM** (2004) Epidemiology of *Botrytis cinerea* in orchard and vine crops. In: Elad Y, Williamson B, Tudzynski P, Delan N, eds. *Botrytis: Biology, Pathology and Control*. Dordrecht, The Netherlands: Kluwer Academic, 243–72
- Espino JJ, Gutiérrez-Sánchez G, Brito N, Shah P, Orlando R, González C** (2010) The *Botrytis cinerea* early secretome. *Proteomics* **10**: 3020–3034
- Favaron F, Lucchetta M, Odorizzi S, da Cunha ATP, Sella L** (2009) The role of grape polyphenols on *trans*-resveratrol activity against *Botrytis cinerea* and of fungal laccase on the solubility of putative grape PR proteins. *J Plant Pathol* **91**: 579-588
- Giacomelli L, Nanni V, Lenzi L, Zuang J, Dalla Serra M, Banfield MJ, Town CD, Silverstein KAT, Baraldi E, Moser C** (2012) Identification and characterization of the defensin-like gene family of grapevine. *Mol Plant Microbe Interact* **25**: 1118–31
- Giannakis C, Bucheli CS, Skene KGM, Robinson SP, Scott NS** (1998) Chitinase and beta-1,3-glucanase in grapevine leaves: a possible defence against powdery mildew infection. *Aust J Grape Wine Res* **4**: 14–22
- Gilbert HJ** (2010) The biochemistry and structural biology of plant cell wall deconstruction. *Plant Physiol* **153**: 444–455
- Godfrey D, Able AJ, Dry IB** (2007) Induction of a grapevine germin-like protein (VvGLP3) gene is closely linked to the site of *Erysiphe necator* infection: A possible role in defense? *Mol Plant Microbe Interact* **20**: 1112-1125
- Goetz G, Fkyerat A, Metais N, Kunz M, Tabacchi R, Pezet R, Pont V** (1999) Resistance factors to grey mould in grape berries: Identification of some phenolics inhibitors of *Botrytis cinerea* stilbene oxidase. *Phytochemistry* **52**: 759-767
- Grimplet J, Van Hemert J, Carbonell-Bejerano P, Díaz-Riquelme J, Dickerson J, Fennell A, Pezzotti M, Martínez-Zapater, JM** (2012) Comparative analysis of grapevine whole-genome gene predictions, functional annotation, categorization and integration of the predicted gene sequences. *BMC Res Notes* **5**:213
- Guetsky R, Kobiler I, Wang X, Perlman N, Gollop N, Avila-Quezada G, Hadar I, Prusky D** (2005) Metabolism of the flavonoid epicatechin by laccase of *Colletotrichum gloeosporioides* and its effect on pathogenicity on avocado fruits. *Phytopathology* **95** (11): 1341– 1348
- Hammerbacher A, Ralph SG, Bohlmann J, Fenning TM, Gershenzon J, Schmidt A** (2011) Biosynthesis of the major tetrahydroxystilbenes in spruce, astringin and isorhapontin, proceeds viasveratrol and is enhanced by fungal infection. *Plant Physiol* **157**(2): 876–890
- Hellemans J, Mortier G, De Paepe A, Speleman F, Vandesompele J** (2007) qBase relative quantification framework and software for management and automated analysis of real-time quantitative PCR data. *Genome Biol* **8**: R19
- Heller J, Tudzynski P** (2011) Reactive oxygen species in phytopathogenic fungi: signaling, development, and disease. *Annu Rev Phytopathol* **49**: 369–390

- Höll J, Vannozzi A, Czemplin S, D'Onofrio C, Walker AR, Rausch T, Lucchin M, Boss PK, Dry IB, Bogs J** (2013) The R2R3-MYB transcription factors MYB14 and MYB15 regulate stilbene biosynthesis in *Vitis vinifera*. *Plant Cell* **25**: 4135–4149
- Jaillon O, Aury JM, Noel B, Policriti A, Clepet C, Casagrande A, Choisne N, Aubourg S, Vitulo N, Jubin C, et al.**, French-Italian Public Consortium for Grapevine Genome Characterization (2007) The grapevine genome sequence suggests ancestral hexaploidization in major angiosperm phyla. *Nature* **449**: 463-467
- Jarvis WR** (1962) The infection of strawberry and raspberry fruits by *Botrytis cinerea* Fr. *Ann Appl Biol* **50**: 569–575
- Jarvis WR** (1994) Latent infections in the pre- and post-harvest environment. *Hortscience* **29**: 749–51
- Jeandet P, Bessis R, Sbaghi M, Meunier P** (1995) Production of the phytoalexin resveratrol by grapes as a response to *Botrytis* attack under natural conditions. *J Phytopathol* **143**:135-139
- Jersch S, Scherer C, Huth G, Schlösser E** (1989) Proanthocyanidins as basis for quiescence of *Botrytis cinerea* in immature strawberry fruits *Z. Pflanzenkrankh Pflanzenschutz* **96**: 365–378
- Keller M, Viret O, Cole M** (2003) *Botrytis cinerea* infection in grape flowers: defense reaction, latency and disease expression. *Phytopathology* **93**: 316–322
- Kelloniemi J, Trouvelot S, Heloir MC, Simon A, Dalmais B, Frettinger P, Cimerman A, Fermaud M, Roudet J, Baulande S, et al** (2015) Analysis of the molecular dialogue between graymold (*Botrytis cinerea*) and grapevine (*Vitis vinifera*) reveals a clear shift in defense mechanisms during berry ripening. *Mol Plant Microbe Interact* **28**: 1167–1180
- Kemmerling B, Schwedt A, Rodriguez P, Mazzotta S, Frank M, Abu Qamar S, Mengiste T, Betsuyaku S, Parker JE, Mussig C, et al** (2007) The BR11- associated kinase 1, BAK1, has a Brassinoli-independent role in plant cell-death control. *Curr Biol* **17**: 1116–1122
- Kretschmer M, Kassemeyer HH, Hahn M** (2007) Age-dependent grey mould susceptibility and tissue-specific defence gene activation of grapevine berry skins after infection by *Botrytis cinerea*. *J Phytopathol* **155**:258-263
- Langcake P** (1981) Disease resistance of *Vitis* spp. and the production of the stress metabolites resveratrol, epsilon -viniferin, alpha - viniferin and pterostilbene. *Physiol Plant Pathol* **18**: 213-226
- Law CW, Chen Y, Shi W, Smyth GK** (2014) Voom: Precision weights unlock linear model analysis tools for RNA-Seq read counts. *Genome Biol* **15**(2):R29
- Lebel S, Schellenbaum P, Walter B, Maillot P** (2010) Characterisation of the *Vitis vinifera* PR10 multigene family. *BMC Plant Biol* **10**:184
- Li X, Zhang Y, Huang L, Ouyang Z, Hong Y, Zhang H, Li D, Song F** (2014) Tomato SIMKK2 and SIMKK4 contribute to disease resistance against *Botrytis cinerea*. *BMC Plant Biol* **14**: 166-10
- Liao Y, Smyth GK, Shi W** (2013) The Subread aligner: fast, accurate and scalable read mapping by seed-and-vote. *Nucleic Acids Res* **41**:e108
- Liao Y, Smyth GK, Shi W** (2014) featureCounts: an efficient general-purpose program for assigning sequence reads to genomic features. *Bioinformatics* **30**(7): 923-930

- Lijavetzky D, Carbonell-Bejerano P, Grimplet J, Bravo G, Flores P, Fenoll J, Hellín P, Oliveros JC, Martínez-Zapater JM** (2012) Berry flesh and skin ripening features in *Vitis vinifera* as assessed by transcriptional profiling. *PLoS ONE* **7**:e39547
- Liu ZY, Zhuang CX, Sheng SJ** (2011) Overexpression of a resveratrol synthase gene (PcRs) from *Polygonum cuspidatum* in transgenic *Arabidopsis* causes the accumulation of trans-piceid with antifungal activity. *Plant Cell Rep* **30**: 2027–2036
- Malacarne G, Vrhovsek U, Zulini L, Cestaro A, Stefanini M, Mattivi F, Delledonne M, Velasco R, Moser C** (2011) Resistance to *Plasmopara viticola* in a grapevine segregating population is associated with stilbenoid accumulation and with specific host transcriptional responses. *BMC Plant Biol* **11**:114
- Marrs KA** (1996) The functions and regulation of glutathione *S*-transferases in plants. *Annu Rev Plant Physiol Plant Mol Biol* **47**: 127–158
- Martin M** (2011) Cutadapt removes adapter sequences from high-throughput sequencing reads. *EMBnetjournal* **17**: 10–12
- McNicol RJ, Williamson B** (1989) Systemic infection of blackcurrant flowers by *Botrytis cinerea* and its possible involvement in premature abscission of fruits. *Ann Appl Biol* **114**: 243–254
- McClellan WD, Hewitt WB** (1973) Early *Botrytis* rot of grapes: Time of infection and latency of *Botrytis cinerea* Pers. in *L. Phytopathology* **63**: 1151-1157
- Mehli L, Kjellsen TD, Dewey FM, Hietala AM** (2005) A case study from the interaction of strawberry and *Botrytis cinerea* highlights the benefits of comonitoring both partners at genomic and mRNA level. *New Phytol* **168**:465-474
- Merz PR, Moser T, Höll J, Kortekamp A, Buchholza G, Zyprian E, Bogs J** (2015) The transcription factor VvWRKY33 is involved in the regulation of grapevine (*Vitis vinifera*) defense against the oomycete pathogen *Plasmopara viticola*. *Physiol Plant* **153**: 365–380
- Micheli F** (2001) Pectin methylesterases: cell wall enzymes with important roles in plant physiology. *Trends Plant Sci* **6**: 414–9
- Mlikota-Gabler F, Smilanick JL, Mansour M, Ramming DW, Mackey BE** (2003) Correlation of morphological, anatomical, and chemical features of grape berries with resistance to *Botrytis cinerea*. *Phytopathology* **93**: 1263–1273
- Mohnen D** (2008) Pectin structure and biosynthesis. *Curr Opin Plant Biol* **11**: 226–277
- Monteiro S, Barakat M, Picarra-Pereira MA, Teixeira AR, Ferreira RB** (2003) Osmotin and thaumatin from grape: a putative general defense mechanism against pathogenic fungi. *Phytopathology* **93**: 1505-1512
- Moretto M, Sonogo P, Dierckxsens N, Brilli M, Bianco L, Ledezma-Tejeida D, Gama-Castro S, Galardini M, Romualdi C, Laukens K, et al** (2016) COLOMBOS v3.0: leveraging gene expression compendia for cross-species analyses. *Nucleic Acids Res* **44(D1)**:D620-3
- Mullins M.G, Rajaskekaren K** (1981) Fruiting cuttings: Revised method for producing test plants of grapevine cultivars. *Am J Enol Vitic* **32**: 35-40
- Nagpala EG, Guidarelli M, Gasperotti M, Masuero D, Bertolini P, Vrhovsek U, Baraldi E** (2016) Polyphenols Variation in Fruits of the Susceptible Strawberry Cultivar Alba during Ripening and upon Fungal Pathogen Interaction and Possible Involvement in Unripe Fruit Tolerance. *J Agric Food Chem* **64(9)**: 1869-78

- Nair NG, Guilbaud-Oulton S, Barchia I, Emmett R** (1995) Significance of carry over inoculum, flower infection and latency on the incidence of *Botrytis cinerea* in berries of grapevines at harvest *Vitis vinifera* in New South Wales. *Aust J Exp Agric* **35**: 1177-1180
- Naoumkina MA, Zhao Q, Gallego-Giraldo L, Dai X, Zhao PX, Dixon RA** (2010) Genome-wide analysis of phenylpropanoid defence pathways. *Mol Plant Pathol* **11**: 829–846
- Noda J, Brito N, Gonzalez C** (2010) The *Botrytis cinerea* xylanase Xyn11A contributes to virulence with its necrotizing activity, not with its catalytic activity. *BMC Plant Biol* **10**:38
- Padgett M, Morrison JC** (1990). Changes in the grape berry exudates during fruit development and their effect on the mycelial growth of *Botrytis cinerea*. *J Am Soc Hortic Sci* **115**: 269–273
- Pezet R, Perret C, Jean-Denis JB, Tabacchi R, Gindro K., Viret O** (2003a) δ -Viniferin, a resveratrol dehydrodimer: one of the major stilbenes synthesized by stressed grapevine leaves. *J Agric Food Chem* **51**: 5488–5492
- Pezet R, Viret O, Perret C, Tabacchi R** (2003b) Latency of *Botrytis cinerea* Pers.: Fr. and biochemical studies during growth and ripening of two grape berry cultivars, respectively susceptible and resistant to grey mould. *J Phytopathol* **151**: 208-214
- Pinedo C, Wang CM, Pradier JM, Dalmais B, Choque M. Le Pêcheur P, Morgant G, Collado IG, Cane DE, Viaud M** (2008) Sesquiterpene synthase from the botrydial biosynthetic gene cluster of the phytopathogen *Botrytis cinerea*. *ACS Chem Biol* **3**: 791–801
- Prusky D** (1996) Pathogen quiescence in postharvest diseases. *Annu Rev Phytopathol* **34**: 413–434
- Prusky D, Alkan N, Mengiste T, Fluhr R** (2013) Quiescent and necrotrophic lifestyle choice during postharvest disease development. *Annu Rev Phytopathol* **51**: 155–176
- Puhl I, Treutter D** (2008) Ontogenetic variation of catechin biosynthesis as basis for infection and quiescence of *Botrytis cinerea* in developing strawberry fruits. *J Plant Dis Prot* **115**: 247–251
- Ramirez-Suero M, Benard-Gellon M, Chong J, Laloue H, Stempien E, Abou-Mansour E, Fontaine F, Larignon P, Mazet-Kieffer F, Farine S, Bertsch C** (2014) Extracellular compounds produced by fungi associated with *Botryosphaeria dieback* induce differential defence gene expression patterns and necrosis in *Vitis vinifera* cv. Chardonnay cells. *Protoplasma* **251**:1417–1426
- Rieu I, Powers SJ** (2009) Real-time quantitative RT-PCR: design, calculations, and statistics. *The Plant Cell* **2**: 1031–1033
- Rolke Y, Liu S, Quidde T, Williamson B, Schouten S, Weltring K.M, Siewers V, Tenberge K.B, Tudzynski B, Tudzynski, P** (2004) Functional analysis of H₂O₂-generating systems in *Botrytis cinerea*: the major Cu-Zn-superoxide dismutase (BCSOD1) contributes to virulence on French bean, whereas a glucose oxidase (BCGOD1) is dispensable. *Mol Plant Pathol* **5**: 17–27
- Rossi FR, Garriz A, Marina M, Romero FM, Gonzalez ME, Collad IG, Pieckenstain FL** (2011) The sesquiterpene botrydial produced by *Botrytis cinerea* induces the hypersensitive response on plant tissues and its action is modulated by salicylic acid and jasmonic acid signaling. *Mol Plant Microbe Interact* **24**: 888–896
- Ruijter JM, Ramakers C, Hoogaars WM, Karlen Y., Bakker O, van den Hoff M J, Moorman AF** (2009) Amplification efficiency: Linking baseline and bias in the analysis of quantitative PCR data. *Nucleic Acids Res.* **37**:e45

- Schouten A, Tenberge KB, Vermeer J, Stewart J, Wagemakers CAM, Williamson B, van Kan JAL** (2002a) Functional analysis of an extracellular catalase of *Botrytis cinerea*. *Mol Plant Pathol* **3**: 227–238
- Schouten A, Wagemakers L, Stefanato FL, van der Kaaij RM, van Kan JAL** (2002b) Resveratrol acts as a natural fungicide and induces self-intoxication by a specific laccase. *Mol Microbiol* **43**: 883–894
- Schumacher J, Simon A, Cohrs K C, Traeger S, Porquier A, Dalmais B, Viaud M, Tudzynski B** (2015) The VELVET complex in the gray mold fungus *Botrytis cinerea*: impact of BcLAE1 on differentiation, secondary metabolism and virulence. *Mol Plant Microbe Interact* **28(6)**:659–674
- Schumacher J, Simon A, Cohrs KC, Viaud M, Tudzynski P** (2014) The transcription factor BcLTF1 regulates virulence and light responses in the necrotrophic plant pathogen *Botrytis cinerea*. *PLoS Genet* **10**:e1004040
- Shaw MW, Emmanuel CJ, Emilda D, Terhem RB, Shafia A, Tsamaidi D, Emblow M, van Kan JAL** (2016) Analysis of cryptic, systemic *Botrytis* infections in symptomless hosts. *Front. Plant Sci.* **7**:625
- Siewers V, Viaud M, Jimenez-Teja D, Collado IG, Gronover CS, Pradier JM, Tudzynski B, Tudzynski P** (2005) Functional analysis of the cytochrome P450 monooxygenase gene *bcbot1* of *Botrytis cinerea* indicates that botrydial is a strain-specific virulence factor. *Mol Plant Microbe Interact* **18**:602–612
- Smith JE, Mengesha B, Tang H, Mengiste T, and Bluhm BH** (2014) Resistance to *Botrytis cinerea* in *Solanum lycopersicoides* involves widespread transcriptional reprogramming. *BMC Genomics* **15**:334
- Smyth GK** (2004) Linear models and empirical bayes methods for assessing differential expression in microarray experiments. *Stat Appl Genet Mol Biol* **3**:3
- Suarez BM, Walsh K, Boonham N, O'Neill T, Pearson S, Barker I** (2005) Development of real-time PCR (TaqMan) assays for the detection and quantification of *Botrytis cinerea* in planta. *Plant Physiol Bioch* **43**: 890–899
- Supek F, Bošnjak M, Škunca N, Šmuc T** (2011) REVIGO summarizes and visualizes long lists of gene ontology terms. *PloS one* **6**:e21800
- ten Have A, Espino JJ, Dekkers E, Van Sluyter SC, Brito N, Kay J, González C, van Kan JAL** (2010) The *Botrytis cinerea* aspartic proteinase family. *Fungal Genet Biol* **47**: 53–65
- Thimm O, Bläsing O, Gibon Y, Nagel A, Meyer S, Krüger P, Selbig J, Müller LA, Rhee SY, Stitt M** (2004) MAPMAN: a user-driven tool to display genomics data sets onto diagrams of metabolic pathways and other biological processes. *Plant J* **37**: 914–939
- Trdá L, Fernandez O, Boutrot F, Héloir MC, Kelloniemi J, Daire X, Adrian M, Clément C, Zipfel C, Dorey S, Poinssot B** (2014) The grapevine flagellin receptor VvFLS2 differentially recognizes flagellin-derived epitopes from the endophytic growth-promoting bacterium *Burkholderia phytofirmans* and plant pathogenic bacteria. *New Phytol.* **201(4)**:1371–1384
- Valsesia G, Gobbin D, Patocchi A, Vecchione A, Pertot I, Gessler C** (2005) Development of a high-throughput method for quantification of *Plasmopara viticola* DNA in grapevine leaves by means of quantitative real-time polymerase chain reaction. *Phytopathology* **95**: 672–678
- Vandesompele J, De Preter K, Pattyn F, Poppe B, Van Roy N, De Paepe A, Speleman F** (2002) Accurate normalization of real-time quantitative RT-PCR data by geometric averaging of multiple internal control genes. *Genome Biology* **3(7)**: RESEARCH0034
- van Kan JAL** (2006) Licensed to kill: the lifestyle of a necrotrophic plant pathogen. *Trends Plant Sci* **11**: 247–253

- van Kan JAL, Shaw MW, Grant-Downton RT** (2014) *Botrytis* species: relentless necrotrophic thugs or endophytes gone rogue? *Mol Plant Pathol* **15**(9): 957–961
- van Kan JAL, Stassen JHM, Mosbach A, van Der Lee TAJ, Faino L, Farmer AD, Papasotiriou DG, Zhou S, Seidl MF, Cottam E, et al.** (2016). A gapless genome sequence of the fungus *Botrytis cinerea*. *Mol. Plant. Pathol.* DOI: 10.1111/mpp.12384.
- Vannozzi A, Dry IB, Fasoli M, Zenoni S, Lucchin M** (2012) Genome-wide analysis of the grapevine stilbene synthase multigenic family: genomic organization and expression profiles upon biotic and abiotic stresses. *BMC Plant Biol* **12**: 130
- Velasco R, Zharkikh A, Troggio M, Cartwright DA, Cestaro A, Pruss D, Pindo M, Fitzgerald LM, Vezzulli S, Reid J, et al** (2007) A high quality draft consensus sequence of the genome of a heterozygous grapevine variety. *PLoS ONE* **2**: e1326
- Volodarsky D, Leviatan N, Otcheretianski A, Fluhr R** (2009) HORMONOMETER: a tool for discerning transcript signatures of hormone action in the Arabidopsis transcriptome. *Plant Physiol* **150**: 1796–1805
- Vrhovsek U, Masuero D, Gasperotti M, Franceschi P, Caputi L, Viola R, Mattivi F** (2012) A versatile targeted metabolomics method for the rapid quantification of multiple classes of phenolics in fruits and beverages. *J Agric Food Chem* **60**(36): 8831–8840
- Weng K, Li ZQ, Liu RQ, Wang L, Wang YJ, Xu Y** (2014) Transcriptome of *Erysiphe necator* infected *Vitis pseudoreticulata* leaves provides insight into grapevine resistance to powdery mildew. *Hort Res* **1**: 14049
- Wiermer M, Feys BJ, Parker JE** (2005) Plant immunity: the EDS1 regulatory node. *Curr Opin Plant Biol* **8**: 383–389
- Williamson B, McNicol RJ, Dolan A** (1987) The effect of inoculating flowers and developing fruits with *Botrytis cinerea* on post-harvest grey mould of red raspberry. *Ann Appl Biol* **111**: 285-294
- Williamson B, Tudzynski B, Tudzynski P, van Kan JAL** (2007) *Botrytis cinerea*: the cause of grey mould disease. *Mol Plant Pathol* **8**: 561–580
- Zhang L, Thiewes H, van Kan JAL** (2011) The D-galacturonic acid catabolic pathway in *Botrytis cinerea*. *Fungal Genet Biol* **48**: 990–997
- Zhang L, van Kan JAL** (2013) *Botrytis cinerea* mutants deficient in D-galacturonic acid catabolism have a perturbed virulence on *Nicotiana benthamiana* and *Arabidopsis*, but not on tomato. *Mol Plant Pathol* **14**:19–29
- Zhang W, Fraiture M, Kolb D, Löffelhardt B, Desaki Y, Boutrot FF, Tör M, Zipfel C, Gust AA, Brunner F** (2013) *Arabidopsis* RECEPTOR- LIKE PROTEIN30 and receptor-like kinase SUPPRESSOR OF BIR1-1/ EVERSHED mediate innate immunity to necrotrophic fungi. *Plant Cell* **25**: 4227–4241
- Zhao Q, Nakashima J, Chen F, Yin Y, Fu C, Yun J, Shao H, Wang X, Wang ZY, Dixon RA** (2013) Laccase is necessary and nonredundant with peroxidase for lignin polymerization during vascular development in *Arabidopsis*. *Plant Cell* **25**: 3976–3987

2.8. Supplemental materials

2.8.1. Supplemental tables

Supplemental Table S2.1. List of qPCR primers. Gene and/or accession identification, gene name, primer name, primer sequence, and source are listed.

	Gene/Accession ID	Gene name	Primer name	Primer sequence	Reference
<i>Botrytis cinerea</i>	AM233400.1	<i>Bc3</i>	Bc3-F	TGTAATTTCAATGTGCAGAATCC	Suarez et al. 2005
			Bc3-R	TTGAAATGCGATTAATTGTTGC	
	Bcin16g02020	<i>BcACTA</i>	BcactA-F	CGTCACTACCTTCAACTCCATC	Li et al. 2014
			BcactA-R	CGGAGATACCTGGGTACATAGT	
	Bcin07g03040	<i>BcAOX</i>	Bcaox-F	GTTCTCAAAGGGGTCTGCTG	This study
			Bcaox-R	GTTCTACCGAGTGCCATGT	
	Bcin12g02040	<i>BcAP8</i>	Bcap8-F	CATCGTGCATACTGGATCCTC	ten Have et al. 2010
			Bcap8-R	TGAACCACTTCCGTAGGAGAC	
	Bcin12g00180	<i>BcAP9</i>	Bcap9-F	AGCAAGGTTCAAGGTGCTGT	This study
			Bcap9-R	CACGGACGGTAGCCATGTAG	
	Bcin01g00060	<i>BcBOA6</i>	BcPks6q-F	CAGCAATCGTTGTCTGAAATC	Schumacher et al. 2015
			BcPks6q-R	GTTTATCGCGTTCTCACCTGTTA	
	Bcin12g06380	<i>BcBOT1</i>	Bcbot1-F	GGTCCCCTGCTTGCA	Pinedo et al. 2008
			Bcbot1-R	GCGAGGTGAAGAAGTTAGAGAAGGT	
	Bcin12g06390	<i>BcBOT2</i>	Bcbot2 F	CAGGTTATCCCTTTGCATGAGTAGT	Pinedo et al. 2008
			Bcbot2 R	TTACACTGGTGAATGATGTTTTGTCTT	
	Bcin15g03080	<i>BcCUTA</i>	BccutA-F	TGCTGGCAGTCAGACTATGG	This study
			BccutA-R	TTCCGGCTGGTAAAAGTTTGG	
	Bcin01g09430	<i>BcCUT-like1</i>	Bccut-like1-F	TCACCAACTACGCTTCCACC	This study
			Bccut-like1-R	GCAATCTTGGCCGTTACAGC	
	Bcin03g01500	<i>BcGAR2</i>	Begar2-F	CCCAGCTATCCGTGAACATC	Zhang et al. 2011
			Begar2-R	CACCTGGGGAAAGCGCATC	
	Bcin03g01490	<i>BcGLA1</i>	Begl1-F	CAAGGTTTGGGAATTGTACAGAG	Zhang et al. 2011
			Begl1-R	GTATCCTCCATATCCATAGTAGC	
	Bcin13g05710	<i>BcGOX1</i>	Begox1-F	AAGGGTTTGAATGCAGGTG	This study
			Begox1-R	AGCTTCCCTTCGTCTGTCAA	
	Bcin03g01480	<i>BcGPX3</i>	Begpx3-F	GGTGACAATGCTGCTCCTCT	This study
			Begpx3-R	TCTGGCTTGGTTGTGGATGC	
	Bcin10g00740	<i>BcGST1</i>	Begst1-F	GTTGAGAAGGGCCGTCATGT	Kolloniemi et al. 2015
			Begst1-R	CCTCACGTTCCAGGGTCTTTCTT	
Bcin14g02510	<i>BcLCC2</i>	Belcc2-F	TGCCCTCACTGCATTATTTG	This study	
		Belcc2-R	CTGGAAGTAGCCGAGTTTGC		
Bcin01g09450	<i>BcLGD1</i>	Belgd1-F	TGGTCATGGCATGACTTTCAC	Zhang et al. 2011	
		Belgd1-R	GTTGCGAATCGGAAACGAGATA		
Bcin12g01020	<i>BcOAH</i>	Bcoah-F	CGACGAGTGCATCAAGAGGT	This study	
		Bcoah-R	AACAGTCTTTGCGGCCATCT		
Bcin03g05820	<i>BcPEL-like1</i>	Bepri-like1-F	ACCACCACTGTCTCCACCTA	This study	
		Bepel-like1-R	CCTTGACTTGGGAAGCAGCT		
Bcin14g00850	<i>BcPG1</i>	Bepg1-F	CTGCCAACGGTGTCCGTATC	Zhang and vanKan 2013	
		Bepg1-R	GAACGACAACACCGTAGGATG		
Bcin14g00610	<i>BcPG2</i>	Bepg2-F	CGAGTTAAGACCGTCAGCGATA	This study	
		Bepg2-R	CGATGAGAGTGATGTCCTGGAA		
Bcin03g01680	<i>BcPG4</i>	Bepg4-F	CTTATTGAGTACGCCACTGTC	Zhang and vanKan 2013	
		Bepg4-R	AGTGTGACGGTGTGTTGTC		

Supplemental Table S2.1. Continued

	Gene/Accession ID	Gene name	Primer name	Primer sequence	Reference
<i>Botrytis cinerea</i>	Bcin02g05860	<i>BcPG6</i>	Bcpg6-F	ATTGATGTCAGCTCGTCCAG	Zhang and vanKan 2013
			Bcpg6-R	ACCTGAGCAATATAACCCGTC	
	Bcin13g05720	<i>BcPRD1</i>	Bcprd1-F	ACCCAGCAATTGAGTTCACC	This study
			Bcprd1-R	CCTGGGTGTCACCTCATCT	
	Bcin01g09620	<i>BcRPL5</i>	Bcrpl5-F	GATGAGACCGTCAAATGGTTC	Zhang and vanKan, 2013
			Bcrpl5-R	CAGAAGCCCACGTTACGACA	
	Bcin03g03390	<i>BcSOD1</i>	BcSod1-F	CCATCAATTCGGTGACAACACT	Kelloniemi et al. 2015
			BcSod1-R	TGGCCGTGTGGGTTGAA	
	Bcin01g08040	<i>BcTUBA</i>	BctubA-F	TTTGGAGCCAGGTACCATGG	Mehli et al. 2005
			BctubA-R	GTCGGGACGGAAGAGTTGAC	
Bcin03g00480	<i>BcXYN11A</i>	Bcxyn-F	CCTGGAAGAAGTTGGGATTG	This study	
		Bcxyn-R	AACAGTGATGGAAGCGGAAC		
Bcin10g05590	<i>BcβGLUC</i>	Bcβgluc-F	TGCAGCTACCTTTGATCGTG	This study	
		Bcβgluc-R	TCCTTCCCAGTTACGTCCAC		
<i>Vitis vinifera</i>	VIT_11s0052g01110	<i>Vv4CL</i>	Vv4CL-F	TTCCCAGCATCAACATCCCG	This study
			Vv4CL-R	TTACGTGCGGTGAGATGGAC	
	VIT_04s0044g00580	<i>VvACT</i>	VvACT-F	ATGTGCCTGCCATGTATGTTGCC	Bèzier et al. 2002
			VvACT-R	AGCTGCTCTTTCAGTTCCAGC	
	VIT_11s0065g00350	<i>VvC4H</i>	VvC4H-F	ATTGACGTGTCCGAAAAAGG	This study
			VvC4H-R	CTATGCGGTGATTGGAGTGA	
	VIT_03s0180g00250	<i>VvCAD</i>	VvCAD-F	GTGGAGGTGGGATCAGATGT	This study
			VvCAD-R	TCCATCTCTGATTTGCATGG	
	VIT_03s0063g00140	<i>VvCCoAOMT</i>	VvCCoAOMT-F	TCGATTTGGTGAAGGTGGGG	This study
			VvCCoAOMT-R	AGAGCCTTGTTTCAGCTCCAA	
	VIT_14s0066g01150	<i>VvCCR</i>	VvCCR-F	AGCAGAAACAGGGATGCCAT	This study
			VvCCR-R	AGAGAGCCTCCCATCTGACA	
	VIT_05s0094g00360	<i>VvCHIT4c</i>	VvCHIT4c-F	TCGAATGCGATGGTGGAAA	Ramírez-Suero et al. 2014
			VvCHIT4c-R	TCCCCTGTGAAACACCAAG	
	VIT_16s0098g00850	<i>VvCOMT</i>	VvCOMT-F	GCCTTCTTGCCACCTATGCT	This study
			VvCOMT-R	TCATGAGGAGAAGAGGGGCT	
	VIT_07s0031g01380	<i>VvF5H</i>	VvF5H-F	CTTTGTGCCCGCCATTGTTG	This study
			VvF5H-R	TTGAACACTCATGGGGTGGC	
	VIT_14s0060g00120	<i>VvGLP2</i>	VvGLP2-F	CGAGTTGGATGTGGGGTTCA	Godfrey et al. 2007
			VvGLP2-R	GACTTCGCCGTTGTTCTTCT	
	VIT_19s0093g00320	<i>VvGST1</i>	VvGST1-F	CCAAAGAGCAAAAAGCCAAGT	Conn et al. 2008
			VvGST1-R	TGTCCAGAAAACCCAAAGTC	
	VIT_01s0146g00480	<i>VvJAZ10</i>	VvJAZ10-F	TCCGAAGAATAATCCGCCGT	This study
			VvJAZ10-R	CAGGACTGTAAACCCGGCAAC	
	VIT_07s0005g03340	<i>VvMYB14</i>	VvMYB14-F	TCTGAGGCCGGATATCAAAC	Höll et al. 2013
			VvMYB14-R	GGGACGCATCAAGAGAGTGT	
	VIT_01s0010g02020	<i>VvPER</i>	VvPER-F	AGGGCAAGCAAGATGTGTGA	This study
			VvPER-R	TCCAGGGGTGCAAGATTGTC	
	VIT_08s0007g08330	<i>VvPG1</i>	VvPG1-F	CAAGCGAGCCCACCTTATGA	This study
			VvPG1-R	CTACGGCTTTGAATGGTGC	
VIT_08s0040g00550	<i>VvPLR</i>	VvPLR-F	AAAGGCCGGATATGGGTGTG	This study	
		VvPLR-R	TCTACCAACTTCACGGCGTC		
VIT_03s0088g00750	<i>VvPRI</i>	Vv_PRIi-F	CTCCCCTTCATTGACAGGCA	This study	
		Vv_PRIi-R	ATAGTGCCTGCATTCCCAC		
VIT_03s0088g00710	<i>VvPRI</i>	Vv_PRIii-F	GCGTGGGTGGGAATGCCGA	Trdá et al. 2014	
		Vv_PRIii-R	GATGTTGCCCTGATAGTTGCC		

Supplemental Table S2.1. Continued

	Gene/Accession ID	Gene name	Primer name	Primer sequence	Reference
<i>Vitis vinifera</i>	VIT_05s0077g01530	<i>VvPR10.1</i>	VvPR10.1-F	GCACATCCCGATGCCTATTAAG	Merz et al. 2015
			VvPR10.1-R	ACTTACTGAGACTGATAGATGCAATG AATA	
	VIT_05s0077g01560	<i>VvPR10.3</i>	VvPR10.3-F	GAAATCCTACAAGGACAGGGAGGT	Lebel et al. 2010
			VvPR10.3-R	CGGCCTTGGTGTGGTACTTTT	
	AF274281	<i>VvRS I</i>	VvRES I- F	CGAGGAATTTAGAAACGCTCAAC	Valsesia et al. 2005
			VvRES I- R	GCTGTGCCAATGGCTAGGA	
	VIT_08s0058g00790	<i>VvSIRD</i>	VvSIRD-F	TGAAGACACACTCGGAGCTG	This study
			VvSIRD-R	AGGATATCGAGGCGTCCGTA	
	VIT_16s0100g00950; VIT_16s0100g00990; VIT_16s0100g01010	<i>VvST29</i> (<i>VvST25</i> + <i>VvST2</i> 7+ <i>VvST29</i>)	VvST29-F	GGTTTTGGACCAGGCTTGACT	Höll et al. 2013
			VvST29-R	GAGATAAATACCTTACTCCTATTCAAC	
	VIT_16s0100g01130; VIT_16s0100g01160	<i>VvST41</i> (<i>VvST41</i> + <i>VvST45</i>)	VvST41-F	GAGTACTATTTGGTTTTGGACCT	Höll et al. 2013
			VvST41-R	AACTCCTATTTGATACAAAACAACGT	
	VIT_06s0004g00480	<i>VvTUB</i>	VvTUB-F	TGTTGGTGAAGGCATGGAGG	Giacomelli et al. 2012
			VvTUB-R	AGATGACACGCCTGCTGAACT	
VIT_08s0058g00690	<i>VvWRKY33</i>	VvWRKY33-F	ATTCAAGCACTAGTATGAACAGAGCA G	Merz et al. 2015	
		VvWRKY33-R	CCTTGTTCCTTGGCATGA		

Supplemental Table S2.2. Summary of reads mapping of the 15 RNA-Seq libraries. Ctrl, mock inoculated; Trt, *B. cinerea* inoculated; Bc, *Botrytis cinerea*; 1-3 indicate the three biological replicates; 24 and 96 indicate hours post inoculation.

Library	Total quality-trimmed reads	Reads mapped to <i>V. vinifera</i> reference	Reads uniquely mapped to <i>V. vinifera</i> reference	Reads mapped to <i>B. cinerea</i> reference	Reads uniquely mapped to <i>B. cinerea</i> reference
Ctrl 1-24	33,582,861	26,185,827 (77.97 %)	24,938,558 (74.26 %)	60,629 (0.18 %)	9,736 (0.03 %)
Ctrl 2-24	30,634,590	24,156,916 (78.86 %)	23,009,237 (75.11 %)	63,570 (0.21 %)	10,476 (0.03 %)
Ctrl 3-24	28,509,351	21,919,491 (76.89 %)	20,541,510 (72.05 %)	301,999 (1.06 %)	26,834 (0.09 %)
Ctrl 1-96	22,410,851	16,848,719 (75.18 %)	15,496,486 (69.15 %)	472,766 (2.11 %)	7,195 (0.03 %)
Ctrl 2-96	37,394,962	24,336,710 (65.08 %)	23,155,616 (61.92 %)	60,179 (0.16 %)	7,598 (0.02 %)
Ctrl 3-96	27,843,357	21,949,631 (78.83 %)	20,838,437 (74.84 %)	92,550 (0.33 %)	11,458 (0.04 %)
Trt 1-24	27,812,146	19,069,689 (68.57 %)	16,282,036 (58.54 %)	1,281,100 (4.6 %)	35,213 (0.12 %)
Trt 2-24	31,644,086	25,622,237 (80.97 %)	24,469,696 (77.33 %)	134,816 (0.43 %)	72,414 (0.23 %)
Trt 3-24	30,211,586	24,631,219 (81.53 %)	23,391,950 (77.43 %)	164,851 (0.55 %)	77,040 (0.26 %)
Trt 1-96	25,919,449	21,240,182 (81.95 %)	20,270,161 (78.20 %)	77,351 (0.34 %)	16,453 (0.06 %)
Trt 2-96	26,077,701	20,388,725 (78.18 %)	19,359,716 (74.24 %)	116,774 (0.45 %)	54,139 (0.21 %)
Trt 3-96	23,503,720	18,957,227 (80.66 %)	18,077,115 (76.91 %)	79,818 (0.34 %)	28,891 (0.12 %)
Bc 1	22,223,388	76,740 (0.35 %)	21,423 (0.01 %)	20,072,229 (90.32 %)	14,108,503 (63.48 %)
Bc 2	21,289,297	47,738 (0.22 %)	28,559 (0.13 %)	19,256,732 (90.45 %)	16,603,159 (77.99 %)
Bc 3	22,254,222	50,719 (0.23 %)	17,798 (0.08 %)	20,086,452 (90.25 %)	16,522,732 (74.24 %)

Supplemental Table S2.3. Differentially expressed genes of *V. vinifera* flowers upon *B. cinerea* infection (Provided as excel file)

Supplemental Table S2.4. List of genes used to validate the RNA-Seq expression values by q-PCR assay. Gene identification, gene description, and fold change from RNA-seq and qPCR are provided.

Gene ID	Description	RNA-seq (Log2 fold change)		qPCR (Log2 fold change)	
		24 hpi	96 hpi	24 hpi	96 hpi
VIT_04s0044g00580	Actin 7 (ACT7) / actin 2	-0.25	0.02	-0.05	-0.04
VIT_06s0004g00480	Tubulin alpha	0.05	0.10	0.05	0.04
VIT_08s0058g00690	WRKY DNA-binding protein 33	1.65	-0.04	1.14	-0.25
VIT_14s0060g00120	Germin-like protein 2	0.27	-0.04	0.40	-0.13
VIT_07s0005g03340	Myb domain protein 14	1.87	-0.05	1.46	-0.32
VIT_03s0088g00750	Pathogenesis related protein 1 precursor	1.45	0.21	1.07	-0.15
VIT_03s0088g00710	Pathogenesis-related protein 1 precursor	0.75	0.34	0.80	0.39
VIT_05s0077g01530	Pathogenesis protein 10 [Vitis vinifera]	4.94	1.56	3.89	2.13
VIT_19s0093g00320	Glutathione S-transferase 25 GSTU25	2.11	0.56	1.57	1.30
VIT_05s0094g00360	Chitinase class IV	2.35	0.23	1.90	0.49
VIT_01s0146g00480	TIFY 9 (Jasmonate ZIM domain-containing protein 10)	1.06	-0.82	1.07	-0.43
VIT_08s0007g08330	Polygalacturonase PG1	-4.80	-2.40	-3.18	-1.07
VIT_01s0010g02020	Peroxidase	7.12	2.09	5.46	2.77
VIT_07s0031g01380	Ferulate 5-hydroxylase	2.04	0.96	2.48	1.47
VIT_11s0052g01110	4-coumarate-CoA ligase 1	1.96	0.06	2.20	-0.27
VIT_03s0063g00140	Caffeoyl-CoA O-methyltransferase	1.33	0.25	1.43	0.19
VIT_16s0098g00850	Caffeic acid O-methyltransferase	0.68	-0.06	0.91	0.34
VIT_08s0040g00550	Pinorexinol-lariciresinol reductase	1.37	-0.63	1.28	0.08
VIT_14s0066g01150	Cinnamoyl-CoA reductase	1.15	0.05	1.35	0.74
VIT_08s0058g00790	Secoisolariciresinol dehydrogenase	1.51	0.31	1.77	1.08

Supplemental Table S2.5. Gene ontology terms enriched in the differentially expressed grapevine genes upon *B. cinerea* infection. Enriched GO terms at 24 and 96 hours post inoculation are presented. BP, biological process; MF, molecular function; CC, cellular component.

Hours post inoculation	GO term	Ontology	Description	No. of genes in reference set with any GO term assigned	No. of genes in test set with any GO term assigned	Number in input list	Number in reference list	p-value	FDR	Enrichment
24	GO:0019748	BP	secondary metabolic process	23,531	1,092	87	374	8.00E-35	2.60E-32	5.0
24	GO:0009607	BP	response to biotic stimulus	23,531	1,092	35	233	1.50E-09	6.90E-08	3.2
24	GO:0009875	BP	pollen-pistil interaction	23,531	1,092	24	185	6.70E-06	1.70E-04	2.8
24	GO:0006464	BP	protein modification process	23,531	1,092	147	2,097	2.60E-06	8.70E-05	1.5
24	GO:0007049	BP	cell cycle	23,531	1,092	25	193	4.50E-06	1.30E-04	2.8
24	GO:0009056	BP	catabolic process	23,531	1,092	81	1,084	4.10E-05	8.80E-04	1.6
24	GO:0003774	MF	motor activity	23,531	1,092	25	118	2.10E-10	4.40E-09	4.6
24	GO:0030246	MF	carbohydrate binding	23,531	1,092	40	403	8.60E-06	1.50E-04	2.1
24	GO:0016301	MF	kinase activity	23,531	1,092	132	2,132	1.10E-03	9.50E-03	1.3
24	GO:0004871	MF	signal transducer activity	23,531	1,092	98	1,475	4.90E-04	5.80E-03	1.4
24	GO:0016740	MF	transferase activity	23,531	1,092	263	4,541	6.40E-04	6.80E-03	1.2
24	GO:0005576	CC	extracellular region	23,531	1,092	73	887	4.10E-06	5.60E-04	1.8
96	GO:0005576	CC	extracellular region	23,531	244	31	887	2.60E-08	1.80E-06	3.4
96	GO:0005618	CC	cell wall	23,531	244	15	319	2.40E-06	8.10E-05	4.5

Supplemental Table S2.6. MapMan BINs enriched in the differentially expressed grapevine genes upon *B. cinerea* infection. Over- and under-represented functions are presented. NA, not available.

Hours post inoculation	MapMan Bin code	MapMan Bin Name	Representation	FDR
24	16	secondary metabolism	overrepresented	<1E-20
24	16.1	secondary metabolism.isoprenoids	overrepresented	6.11E-07
24	16.1.5	secondary metabolism.isoprenoids.terpenoids	overrepresented	1.26 E-2
24	16.2	secondary metabolism.phenylpropanoids	overrepresented	1.02E-04
24	16.2.1	secondary metabolism.phenylpropanoids.lignin biosynthesis	overrepresented	4.89E-05
24	16.2.1.1	secondary metabolism.phenylpropanoids.lignin biosynthesis.PAL	overrepresented	2.17E-05
24	16.8	secondary metabolism.flavonoids	overrepresented	1.55E-14
24	16.8.2	secondary metabolism.flavonoids.chalcones	overrepresented	<1E-20
24	16.8.2.3	Secondary metabolism.flavonoids.chalcones.stilbene synthase	overrepresented	<1E-20
24	20	stress	overrepresented	1.75 E-2
24	20.1	stress.biotic	overrepresented	9.40 E-2
24	20.1.7	stress.biotic.PR-proteins	overrepresented	2.07E-04
24	26	misc	overrepresented	9.75E-05
24	26.8	nitrile lyases, berberine bridge enzymes, reticuline oxidases, troponine reductases	overrepresented	2.11 E-3
24	26.9	misc.glutathione S transferases	overrepresented	6.25 E-2
24	27.3.32	RNA.regulation of transcription.WRKY domain transcription factor family	overrepresented	9.07 E-2
24	31	cell	underrepresented	3.08E-07
24	31.1	cell.organisation	underrepresented	2.28E-06
24	30	signalling	overrepresented	3.67 E-2
24	30.2	signalling.receptor kinases	overrepresented	7.54 E-2
24	30.2.99	signalling.receptor kinases.misc	overrepresented	3.24 E-3
96	NA	NA	NA	NA

Supplemental Table S2.7. List of differentially expressed *V. vinifera* genes belonging to the biotic stress functional categories. (Provided as excel file)

Supplemental Table S2.8. Concentration of polyphenolic secondary metabolites in mock (Ctrl) and *B. cinerea* (Trt) inoculated grapevine flowers. The amount is given in $\mu\text{g/g}$ fresh weight. LOD, limit of detection; hpi, hour post inoculation; SE, standard error.

Secondary metabolites	LOD($\mu\text{g/g}$)	12 hpi				24 hpi				48 hpi				72 hpi				96 hpi			
		Ctrl		Trt		Ctrl		Trt		Ctrl		Trt		Ctrl		Trt		Ctrl		Trt	
		mean	SE	Trt	SE	mean	SE	Trt	SE	mean	SE	Trt	SE	mean	SE	Trt	SE	mean	SE	Trt	SE
<i>p</i> -hydroxybenzoic acid	0.005	0.6	0.06	1.0	0.15	0.5	0.09	1.2	0.26	1.4	0.06	1.6	0.24	0.8	0.18	1.7	0.37	0.7	0.02	1.8	0.42
vanillic acid	0.0025	0.1	0.01	0.1	0.05	0.0	0.01	0.0	0.00	0.1	0.01	0.1	0.01	0.1	0.00	0.1	0.01	0.1	0.01	0.1	0.01
gallic acid	0.025	5.0	0.87	9.1	4.25	4.8	1.28	12.1	3.25	8.7	0.46	13.4	1.49	3.6	4.82	18.0	1.36	5.9	0.78	19.5	5.57
2,6-diOH-benzoic acid	0.0025	0.1	0.03	0.1	0.02	0.1	0.06	0.1	0.06	0.1	0.03	0.1	0.04	0.1	0.01	0.1	0.02	0.0	0.00	0.2	0.09
fraxin	0.0025	0.1	0.01	0.2	0.03	0.1	0.01	0.2	0.08	0.2	0.02	0.2	0.02	0.1	0.09	0.2	0.05	0.1	0.03	0.1	0.01
caftaric acid	0.0125	444.7	98.32	630.4	204.68	268.9	35.17	646.4	182.70	584.5	35.48	929.0	56.76	450.3	207.44	949.7	203.86	579.7	47.01	1227.7	408.41
fertaric acid	0.0025	59.0	4.51	85.6	19.15	54.0	6.65	116.4	33.16	150.5	2.57	176.4	17.75	107.7	3.28	135.1	11.17	42.0	2.27	116.3	16.46
<i>trans</i> -coutaric acid	0.025	118.6	10.38	177.3	36.59	73.3	14.57	184.8	51.64	175.2	13.95	267.4	25.73	135.4	53.47	257.5	49.83	115.6	0.19	297.5	59.57
phlorizin	0.0025	2.3	0.26	3.5	1.08	1.6	0.26	4.3	1.21	3.8	0.13	6.1	1.07	2.3	2.59	7.6	2.19	2.4	0.06	6.4	1.88
luteolin	0.0025	0.1	0.01	0.2	0.05	0.0	0.01	0.1	0.02	0.1	0.01	0.1	0.03	0.1	0.01	0.1	0.02	0.0	0.02	0.1	0.04
luteolin-7-O-Glc	0.0025	1.3	0.14	1.7	0.55	0.6	0.17	2.0	0.58	1.6	0.13	2.5	0.21	1.0	0.60	2.7	0.67	1.2	0.15	3.2	1.01
naringenin	0.0025	0.3	0.04	0.6	0.11	0.1	0.02	0.4	0.04	0.4	0.15	0.4	0.10	0.4	0.05	0.4	0.02	0.5	0.12	0.8	0.42
catechin	0.025	39.9	5.36	61.3	15.69	61.1	7.02	136.4	27.12	141.3	13.07	136.2	25.71	97.7	2.03	207.1	44.66	86.0	5.65	158.9	26.18
epicatechin	0.025	3.9	0.57	5.6	1.34	5.1	0.86	10.3	2.14	13.5	0.46	13.1	2.00	9.8	0.40	17.4	3.13	8.0	1.74	18.7	0.43
epigallocatechin	1.25	2.6	0.10	4.1	0.97	2.4	0.22	4.7	1.14	4.9	0.15	5.5	0.53	3.5	0.93	7.2	1.54	3.3	0.08	6.0	1.11
galocatechin	0.25	2.2	0.07	2.4	0.62	2.2	0.57	3.9	0.19	2.8	0.17	4.0	0.67	2.9	0.53	8.4	2.25	8.1	0.41	10.4	3.34
epigallocatechin gallate	0.25	2.1	0.06	2.4	0.45	2.9	0.66	3.8	0.44	3.9	0.07	2.4	0.31	2.7	1.87	7.4	1.92	3.6	1.93	4.3	1.00
epicatechin gallate	0.025	8.0	1.48	8.4	3.60	9.3	2.67	23.0	4.91	23.1	5.15	25.9	8.71	19.5	3.56	24.0	1.83	28.7	7.89	50.3	14.11
procyanidin B1	0.0125	147.1	15.25	180.1	54.86	109.4	15.24	263.9	73.12	236.7	7.98	335.1	36.84	167.8	72.37	407.4	97.80	168.0	23.45	421.4	123.10
procyanidin B2 + B4	0.125	6.8	0.12	7.2	1.80	7.8	1.05	16.3	3.29	16.0	0.90	20.4	3.00	15.2	0.65	29.7	5.91	17.5	0.57	36.0	8.00
procyanidin B3 (as B1)	0.0125	76.8	1.38	99.2	32.19	64.5	13.30	180.5	31.26	156.6	16.92	207.7	36.15	119.5	2.33	295.5	71.83	139.5	35.74	373.3	138.36
kaempferol	0.0025	0.1	0.00	0.2	0.11	0.0	0.01	0.1	0.03	0.2	0.03	0.1	0.00	0.0	0.01	0.1	0.01	0.0	0.00	0.0	0.00
quercetin	0.05	1.3	0.06	1.9	0.10	1.1	0.19	2.8	0.47	2.3	0.06	3.3	0.85	2.9	0.69	3.5	0.23	1.1	0.15	2.2	0.24
taxifolin	0.0025	71.3	4.43	102.7	23.60	60.4	6.37	137.8	37.11	131.5	9.17	145.4	13.55	85.4	31.46	148.1	25.60	38.4	11.83	89.0	6.62

Supplemental Table S2.8. Continued

Secondary metabolites	LOD($\mu\text{g/g}$)	12 hpi				24 hpi				48 hpi				72 hpi				96 hpi			
		Ctrl		Trt		Ctrl		Trt		Ctrl		Trt		Ctrl		Trt		Ctrl		Trt	
		mean	SE	Trt	SE	mean	SE	Trt	SE	mean	SE	Trt	SE	mean	SE	Trt	SE	mean	SE	Trt	SE
myricetin	1.25	4.3	0.34	6.3	1.53	3.6	0.32	7.5	2.08	7.5	0.19	9.1	0.84	5.3	2.43	11.3	2.46	4.3	0.19	8.9	1.48
quercetin-3-Rha	0.005	12.6	1.26	16.2	2.78	7.6	0.29	16.3	5.38	17.6	1.11	19.4	1.01	13.6	5.98	20.4	2.78	3.4	0.02	7.7	0.05
kaempferol-3-Glc	0.0025	6.0	0.12	6.4	0.71	5.1	0.97	11.6	2.88	9.8	0.48	11.7	1.69	9.5	2.54	16.0	2.64	2.6	0.72	7.2	0.74
quercetin-3-Glc+quercetin-3-Gal (as que-3-glc)	0.0025	106.0	1.16	120.9	14.81	82.3	4.01	146.3	44.92	157.3	19.36	194.0	16.94	120.9	63.80	218.9	40.00	48.7	3.43	111.9	10.15
isorhamnetin-3-Glc	0.0025	2.2	0.13	2.8	0.29	1.8	0.14	3.7	0.97	3.7	0.07	5.3	0.55	2.8	0.28	4.6	0.71	1.3	0.29	3.4	0.76
kaempferol-3-rutinoside	0.005	2.7	0.36	4.6	1.08	1.2	0.07	2.6	0.61	5.0	0.67	3.3	0.22	1.8	1.17	3.1	0.55	0.5	0.15	1.2	0.11
quercetin-3-Glc-Ara	0.005	0.7	0.06	1.0	0.06	0.4	0.04	0.8	0.27	1.0	0.03	1.3	0.16	0.5	0.40	1.4	0.35	0.2	0.02	0.5	0.04
rutin	0.0025	24.0	1.06	31.6	1.98	12.9	0.86	29.2	9.80	35.1	2.88	40.1	2.07	20.1	13.54	40.4	8.30	6.9	0.07	16.3	1.31
isorhamnetin-3-rutinoside	0.005	0.4	0.08	1.0	0.33	0.2	0.01	0.7	0.13	1.1	0.10	0.6	0.00	0.3	0.03	0.6	0.11	0.1	0.02	0.2	0.01
quercetin-3-glucuronide	0.0125	294.9	14.05	476.6	66.20	247.4	22.56	542.5	72.97	508.6	28.91	551.0	52.89	324.9	180.12	694.9	151.05	197.6	20.52	475.7	72.83
kaempferol-3-glucuronide	0.005	13.8	0.98	23.1	4.78	13.9	2.50	30.1	8.14	29.1	1.94	23.0	3.27	17.7	10.60	17.2	0.19	5.9	1.94	18.0	0.63
arbutin	0.005	7.2	1.29	7.2	2.11	8.2	1.26	14.8	4.45	12.8	1.13	17.9	0.88	7.1	1.96	11.5	1.79	4.2	0.33	11.5	0.60
<i>trans</i> -resveratrol	0.005	0.3	0.02	2.2	0.88	0.4	0.13	1.6	0.42	0.3	0.04	1.4	0.50	0.2	0.58	0.7	0.21	0.0	0.01	1.7	0.81
<i>cis</i> -resveratrol	0.0025	0.0	0.00	0.0	0.00	0.0	0.00	0.0	0.00	0.0	0.00	0.0	0.01	0.0	0.00	0.0	0.00	0.0	0.00	0.0	0.00
piceatannol	0.0025	0.3	0.11	2.0	0.83	0.4	0.10	2.1	0.59	0.3	0.02	1.3	0.32	0.4	0.38	0.7	0.12	0.0	0.01	0.8	0.14
<i>trans</i> -piceide	0.0125	11.5	2.87	17.8	6.85	8.9	0.93	23.8	5.45	15.0	2.43	34.6	5.95	11.7	6.92	25.0	5.45	16.1	4.38	45.7	17.60
<i>cis</i> -piceide	0.0025	4.6	2.90	1.5	0.47	1.9	0.53	5.2	2.60	0.9	0.12	1.9	0.52	0.8	0.93	2.4	0.67	1.5	0.81	7.9	3.56
astringin	0.005	5.8	0.65	14.9	1.84	17.6	1.76	31.0	6.79	23.0	1.13	28.0	5.48	17.7	0.79	21.6	1.58	4.7	0.06	19.5	7.24
isorhapontin	0.005	0.3	0.03	0.5	0.02	0.8	0.06	0.7	0.29	0.9	0.07	0.8	0.11	0.6	0.06	0.6	0.00	0.3	0.06	0.9	0.05
<i>trans</i> - ϵ -viniferin	0.005	0.1	0.02	0.9	0.34	0.0	0.01	8.7	1.62	0.3	0.14	8.0	0.95	0.1	0.02	3.8	1.52	0.0	0.00	13.4	4.05
<i>cis</i> + <i>trans</i> -o-viniferin	0.0125	0.0	0.00	0.5	0.14	0.0	0.01	3.5	0.66	0.1	0.02	2.9	0.49	0.1	0.01	1.1	0.42	0.0	0.00	5.7	1.01

Supplemental Table S2.8. Continued

Secondary metabolites	LOD($\mu\text{g}/\text{g}$)	12 hpi				24 hpi				48 hpi				72 hpi				96 hpi			
		Ctrl		Trt		Ctrl		Trt		Ctrl		Trt		Ctrl		Trt		Ctrl		Trt	
		mean	SE	Trt	SE	mean	SE	Trt	SE	mean	SE	Trt	SE	mean	SE	Trt	SE	mean	SE	Trt	SE
caffeic acid+catechin condensation	0.05	6.3	0.10	9.6	1.91	8.8	0.44	19.3	5.67	18.2	0.46	17.2	2.84	22.1	3.60	10.2	4.85	5.6	0.53	15.0	3.39
pallidol	0.005	1.0	0.20	6.3	0.42	1.5	0.23	29.3	8.60	2.4	0.39	18.4	2.16	2.2	0.58	12.5	4.19	0.4	0.05	20.3	3.73
ampelopsin D+quadranularin A	0.025	0.2	0.03	5.3	0.78	0.3	0.13	32.0	6.28	0.5	0.23	19.6	1.83	0.0	0.00	15.7	6.41	0.1	0.02	18.1	1.86
α -viniferin	0.0125	0.4	0.12	2.8	1.58	0.1	0.03	137.5	50.16	1.1	0.63	90.9	3.62	0.2	0.03	96.9	39.49	0.1	0.06	151.8	38.50
E-cis-miyabenol	0.0125	0.2	0.02	1.5	0.20	0.0	0.02	35.5	9.02	0.3	0.11	15.8	2.07	0.2	0.06	15.8	6.35	0.0	0.01	53.0	4.95
Z-miyabenol C	0.05	0.1	0.03	1.2	0.25	0.1	0.01	33.1	9.56	0.3	0.22	14.7	1.60	0.1	0.03	16.0	6.51	0.1	0.00	46.4	6.95
isohopeaphenol	0.0125	0.1	0.03	0.2	0.11	0.0	0.01	13.9	7.24	0.2	0.10	17.6	0.45	0.1	0.01	11.1	4.49	0.0	0.00	20.9	1.99
sinapaldehyde	0.00125	0.1	0.01	0.1	0.06	0.0	0.01	0.0	0.01	0.1	0.02	0.1	0.01	0.1	0.03	0.1	0.01	0.0	0.00	0.2	0.06
5-hydroxyferulic acid	0.00125	2.3	0.34	2.3	0.29	1.3	0.20	1.6	0.34	2.6	0.37	2.5	0.10	2.3	0.66	1.9	0.28	1.2	0.02	1.5	0.10
L-phenylalanine	0.00125	42.7	0.12	62.6	3.90	76.8	7.01	131.2	16.34	129.8	0.87	99.8	13.42	81.5	3.95	110.5	2.46	82.8	3.46	73.7	5.35
cinnamic acid	0.0025	0.0	0.02	0.0	0.00	0.0	0.01	0.1	0.01	0.0	0.01	0.0	0.00	0.1	0.00	0.1	0.00	0.1	0.01	0.1	0.01
p-coumaric acid	0.0025	1.2	0.32	1.3	0.47	0.6	0.22	0.5	0.14	0.6	0.11	0.8	0.05	0.8	0.52	0.5	0.23	0.2	0.01	0.2	0.04
caffeic acid	0.00125	0.7	0.05	0.6	0.12	0.4	0.03	0.3	0.08	0.4	0.04	0.5	0.02	0.4	0.09	0.4	0.08	0.5	0.02	0.4	0.03
ferulic acid	0.00125	1.3	0.57	2.7	0.50	0.7	0.19	0.6	0.13	1.5	0.19	1.0	0.25	0.5	0.07	0.8	0.47	0.1	0.02	0.1	0.08
coniferyl alcohol	0.00125	0.1	0.02	0.1	0.01	0.1	0.05	0.2	0.01	0.1	0.04	0.2	0.05	0.2	0.08	0.3	0.07	0.2	0.03	0.4	0.07

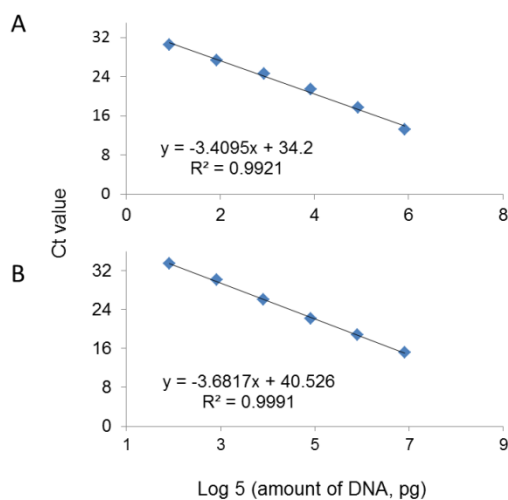
Supplemental Table S2.9. *B. cinerea* genes expressed *in planta*. (Provided as excel file)

Supplemental Table S2.10. Gene ontology (GO) annotation of *B. cinerea* genes expressed *in planta*. (Provided as excel file)

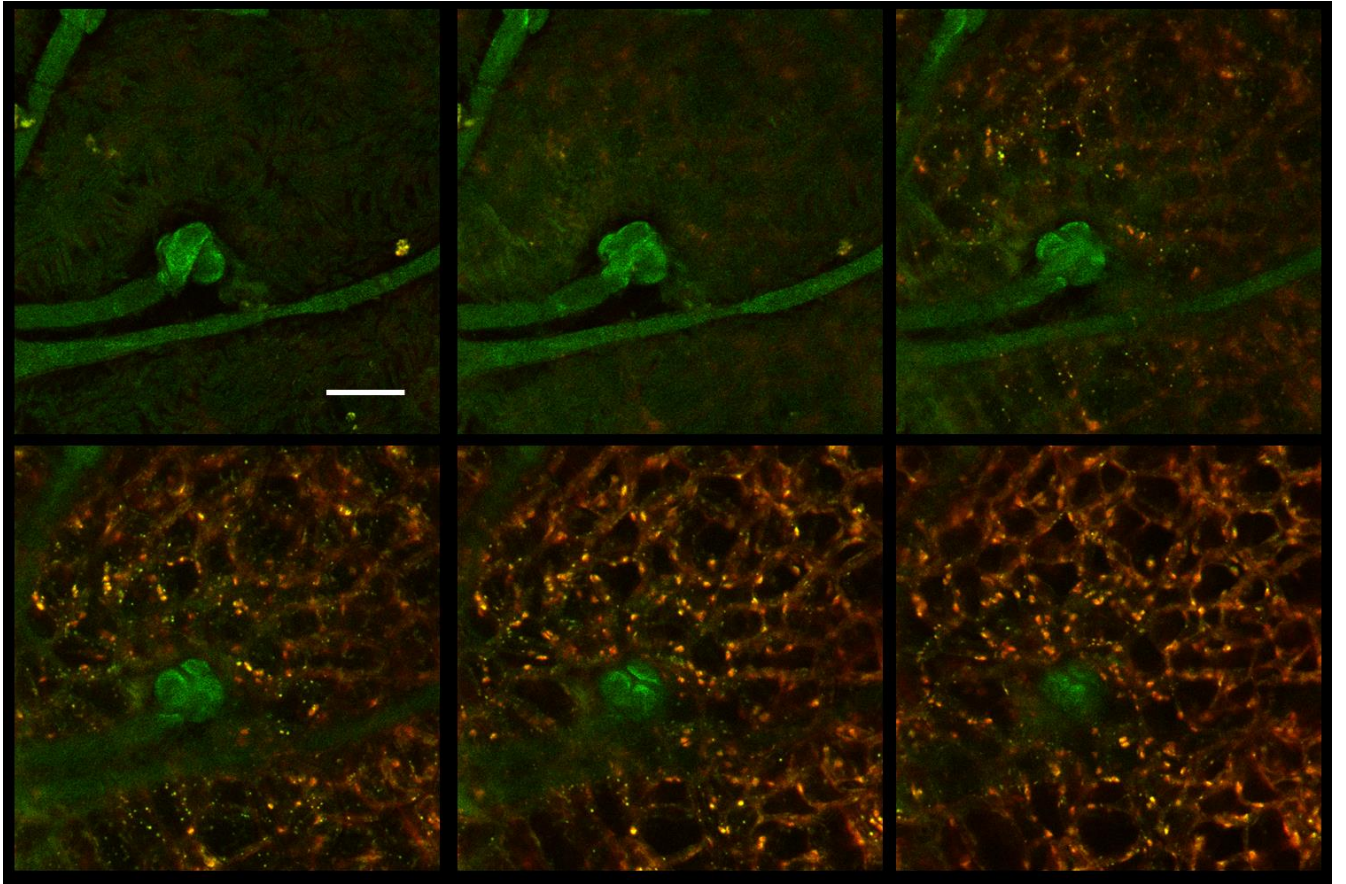
2.8.2. Supplemental figures



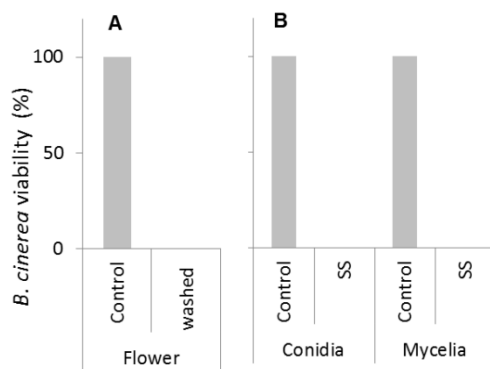
Supplemental Figure S2.1. Optical microscopy images of *B. cinerea* conidia cultured for 12 hours in PDB. Right panel shows a higher magnification view. This growth stage was used as control for the fungal transcriptomic study. C, conidia; Gt, germ tube; the bar represents 10 μm .



Supplemental Figure S2.2. Standard curves used for grapevine and *B. cinerea* genomic DNA quantification. Curves were generated by amplifying the *Bc3* (ribosomal IGS spacer) (A) and the *VvRS I* (resveratrol synthase gene I) (B) genes, in a 5-fold serially diluted genomic DNA of *B. cinerea* and grapevine, respectively. The standard curves show good linear relationship ($R^2 = 0.99$) between the log₅ value of the starting DNA concentration and the threshold cycle (Ct), both in the fungus and the plant.



Supplemental Figure S2.3. Z stack images of GFP-labeled B05.10 *Botrytis* infecting a grapevine flower. The confocal microscope image shows six layers of a Z stack with a pass of 1 μm each. The figure indicates that the *Botrytis* appressorium penetrates only the first epidermal layers within 24 hpi. The white bar represents 15 μm .

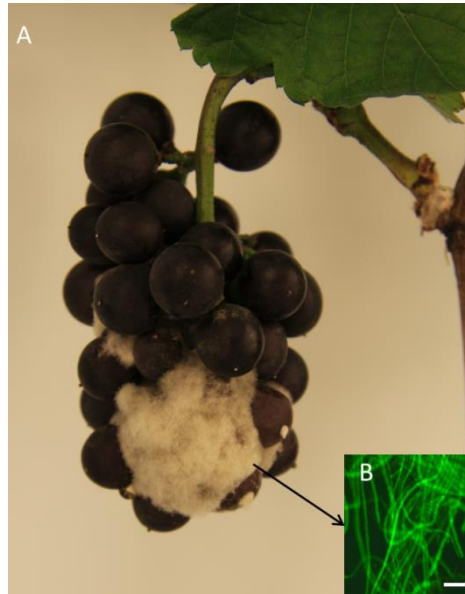


Supplemental Figure S2.4. Effects of washing within 6 hpi (A) and surface sterilization (SS) (B) on the viability of *B. cinerea*.

Description of Supporting Information Fig. S4

A preliminary study was conducted to know the effect of grapevine flowers washing and surface sterilization (SS) on the viability of *B. cinerea*. Grapevine flowers were collected from fruiting cuttings at cap-off stage, 16 flowers from each of 3 fruiting cuttings (replicates). Flowers were then inoculated with 300 conidia of GFP-labelled B05.10 strain and incubated in Petri dishes with moistened paper towel for 6 hours, a time span within which the conidium will not germinate. The inoculated flowers were further incubated for one week on selective media (PDA with 70 µg/ml Hygromycin B), before or after washing. Washing was carried out as described in Materials and Methods section. As shown in 2A, mycelial growth was observed on 100 % of the flowers that were plated out without washing, but on none of the washed flowers, indicating that washing was effective in removing ungerminated conidia.

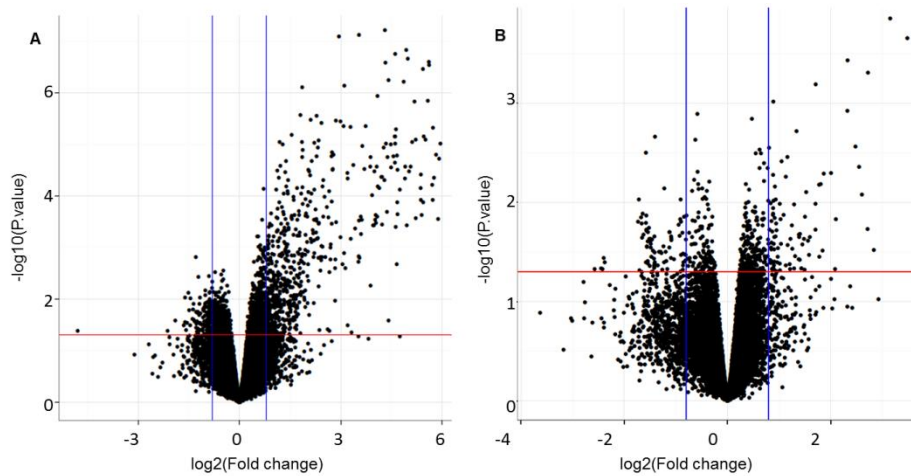
To check the effect of surface sterilization on the viability of *B. cinerea*, conidia and mycelia (harvested from Petri dishes of the same strain mentioned above) were treated as described in Materials and Methods and then allowed to grow on selective media. As shown in of Supporting Information Fig. S4B, conidia and mycelia did not grow after sterilization.



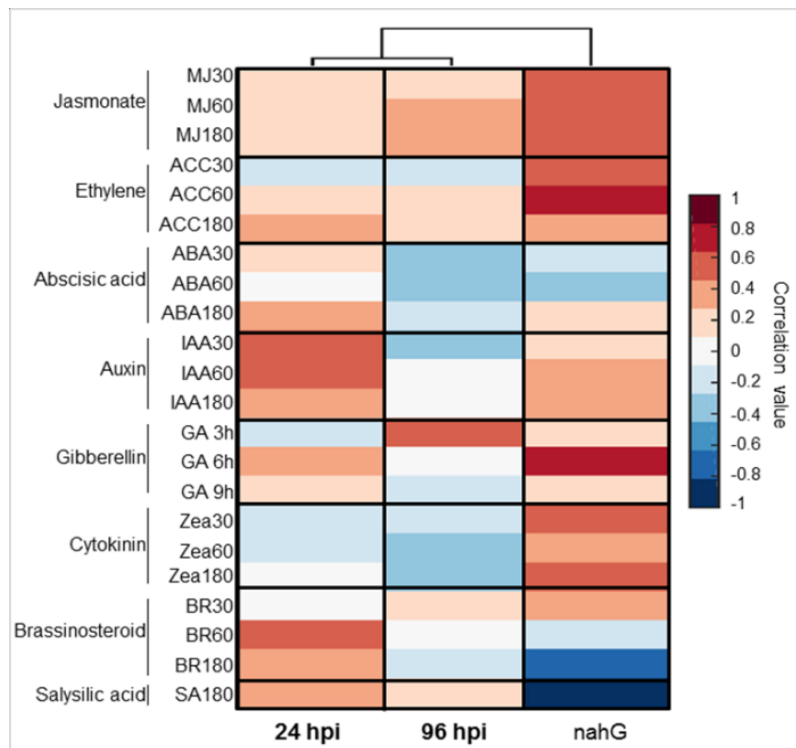
Supplemental Figure S2.5. Egression of *B. cinerea* at ripening (A), inoculated at full cap-fall stage, and fluorescence of mass of *B. cinerea* mycelia isolated from the rotting bunch (B). The white bar represents 25 μm .



Supplemental Figure S2.6. *B. cinerea* egression test on immature berries. Immature berries at pepper-corn stage, which were inoculated with *B. cinerea* at flower cup-off stage, were bagged for 2 weeks. No egression was observed during the period.



Supplemental Figure S2.7. Volcano plots of grapevine gene expression values at 24 hpi (A) and 96 hpi (B). Genes in the left top rectangle [$\log_{10}(P. \text{value}) > 1.12$ and $\log_2(\text{fold change}) < -0.585$] were selected as downregulated; whereas, genes in the right top rectangle were selected as upregulated [$\log_{10}(P. \text{value}) > 1.12$ and $\log_2(\text{fold change}) > 0.585$].



Supplemental Figure S2.8. Hormonal Signatures based on transcriptomic data. HORMONOMETER software was used to compare gene expression data of our experiment, as query experiment, with data sets of hormone responses. Transcriptomes of *Arabidopsis* mutant, *nahG*, with known alteration in salicylic acid level was used as control. The scale bar shows the correlation between the query transcriptome and the hormone-treated indexed data set.

Description of Supporting Information Fig. S8

HORMONOMETER software (Volodarsky *et al.* 2009) was used to evaluate hormonal responses in grapevine inflorescence upon *B. cinerea* inoculation. Since the software accepts only *Arabidopsis thaliana* gene IDs as input, *Arabidopsis* orthologs of grapevine genes provided by Grimplet *et al.* (2012) were taken. Out of the expressed grapevine genes in our experiment, 10507 had *Arabidopsis* orthologs, and hence were used to investigate the hormonal profiles of grape flower due to *B. cinerea* inoculation. Gene expression data of *Arabidopsis* mutant with reduced salicylic acid levels, *nahG*, (GEO, GSE5727) was also included to validate the set of genes used in the analysis.

As depicted in Supportign Information Fig. S8, the HORMONOMETER profile of *Botrytis*-inoculated flowers showed positive correlations with salicylic acid, brassinosteroid, gibberellin, auxin, abscisic acid (ABA), and ethylene treatments at 24 hpi and with jasmonate treatment at 96 hpi. Whereas, a negative correlation was observed with ABA and cytokinin treatments at 96 hpi; the latter one also showed similar trend at 24 hpi. Although the role of cytokinin in plant defense is largely unknown, the profile shown by the HORMONOMETER could be related to the cell cycle network enriched in the downregulated genes shown in Table 2. With regard to ABA, its role in plant defense appears to vary among different types of plant-pathogen interactions (Bari and Jones, 2009). In tomato, the induction of ABA biosynthetic genes was reported to facilitate *B. cinerea* colonization by inducing senescence, and on the other hand, ABA-deficient *sitiens* mutant was shown to be more resistant to the pathogen (Audenaert *et al.* 2002; Blanco-Ulate *et al.* 2013).

3. INTERACTION BETWEEN GRAPE BERRY AND *B. cinerea* DURING QUIESCENT AND EGRESSED INFECTIONS

3.1. Abstract

Botrytis cinerea is an important pathogen in vineyards where primary infections are mostly initiated by airborne conidia from overwintered sources around bloom. The fungus often remains quiescent from bloom until maturity and egresses at ripe where it causes bunch rot. Studying the interaction between the fungus and the host during quiescent and egressed infection stages help understand the cross talk between the two organisms. Therefore, flowers from fruiting cuttings of the cv. Pinot noir were inoculated with GFP labelled *B. cinerea* at full cap-off stage, and molecular analyses were carried out at 4 weeks post inoculation (wpi), fungus quiescent state, on hard-green berries and at 12 wpi, fungus pre-egression and egression states, on ripe berries. During the quiescent state, the expressed fungal transcriptome highlighted that the fungus was undergoing basal metabolic activities besides remodeling its cell wall to evade plant chitinases. Hard-green berries responded by differentially regulating genes encoding for different PR proteins and genes involved in monolignol, flavonoid and stilbenoid biosynthesis pathways which kept the pathogen quiescent. At 12 wpi, the transcripts of *B. cinerea* in the pre-egressed samples showed that virulence-related genes were expressed, suggesting infection process was initiated. The egressed *B. cinerea* expressed almost all virulence and growth related genes that enabled the pathogen to colonize the berries. In response to egression, ripe berries reprogramed different defense responses, though futile. Our results indicated that hard-green berries defense program was capable to contain *B. cinerea*; however, ripening associated fruit's cell wall self-disassembly together with high humidity created the opportunity for the fungus to egress and cause bunch rots.

3.2. Introduction

Botrytis cinerea is responsible for a significant economic damage in vineyards by causing bunch rot. The disease is mostly observed on ripe berries, following rainfalls or long periods of high humidity close to harvest, and develops into gray mold. Primary infections are usually initiated by airborne conidia from overwintered sources (Nair et al., 1995; Elmer and Michailides, 2004), which mostly happens at bloom leading to quiescent infection (McClellan and Hewitt, 1973; Keller et al., 2003; Pezet et al., 2003b). Quiescent infection is an interesting phenomenon in *B. cinerea*-plant interaction where the pathogen spends prolonged time in the host tissue asymptotically, without being aggressive (Williamson et al., 1987; McNicol and Williamson, 1989; Coertze and Holz, 2002; Shaw et al., 2016). Besides *Botrytis*, several species of fungal pathogens belonging to the genera *Alternaria*, *Botryosphaeria*, *Colletotrichum*, *Lasiodiplodia*, *Monilinia*, *Phomopsis*, and *Sclerotinia*, have been reported to pass through a quiescent state in the cuticular wax or intercellular space of their hosts until conditions favor egression (Reviewed by Prusky et al., 2013).

In grapevine, *B. cinerea* egression, causing bunch rot, was observed at ripening from the artificial inoculation made at bloom, where the pathogen stayed quiescent in the developmental stages between fruitlets to maturity (see in Chapter 2). What drives and keeps *B. cinerea* into quiescence until berry ripening is not fully known, but preformed and induced defense mechanisms, including immature berries skin features such as polyphenols in the berry skin cell wall and the thickness of epidermal cell layer complex, have been proposed as part of the ontogenic resistance to *B. cinerea* (Deytieux-Belleau et al., 2009; Goetz et al., 1999; Keller et al., 2003). Recently, it has been shown that upon contact with the grapevine flower, *B. cinerea* induces genes encoding known virulence factors (like *BcBOA6*, *BcBOT*, *BcPG2*, and *BcSOD1*) and proteins contributing to the infection program (like *BcOAH*, *BcXYN11A*, and *BcGST1*) to cause disease. However, no visible disease progress was observed despite the confirmed presence of the pathogen on the immature berries (Chapter 2). As a response to the infection attempt, grapevine flowers react by reprogramming the expression of genes encoding antimicrobial proteins (mainly PR-proteins), monolignol biosynthesis (*VvPAL*, *VvCOMT*, *VvCCoAMT* and *VvCAD*), stilbenoids (*VvSTS*), and prompting oxidative burst (*VvGLP3*). The conjugated actions of these induced defense responses contribute for putting *B. cinerea* into quiescence (Chapter 2). In addition, the involvement of the salicylic acid (SA) dependent defense pathway together with the accumulation of ROS and the

activation of stilbene and lignin biosynthesis was reported as the possible reasons of *B. cinerea* progress arrest in berries at véraison while ripe berries were fully susceptible to the pathogen (Kelloniemi et al., 2015).

The transition from a quiescent to an active infection mostly occurs during senescence/fruit ripening. Physiological and biochemical changes that occur in the host during ripening, together with favorable climatic conditions at ripening are suggested to take a part in triggering the transition (Prusky, 1996; Barnes and Shaw, 2002; Prusky et al., 2013). Cell wall loosening and appearance of disassembled cell wall substrates (Cantu et al., 2008), decrease in preformed and inducible host defense responses and change in hormonal balance and pH (Prusky, 1996; Prusky et al., 2013) are the major changes happening in the processes of berry ripening that could enhance the outgrowth of a quiescent necrotrophic pathogen. Egression impairs product quantity, quality, and appearance.

Global expression profiling of both the pathogen and the host at quiescent and egression stages of the infection enables to gain insight into the signaling, the metabolic pathways, the transcriptional control, and the defense responses involve in the cross talk. Hence, the objective of this study was to understand the molecular mechanisms associated with *B. cinerea* and grapevine berry interaction during quiescent and egression stages. Here we report the simultaneous transcriptome and secondary metabolite analyses of the two organisms at berry hard-green and ripe stages, after host inoculation with *B. cinerea* conidial at full cap-off stage (EL25/26).

3.3. Materials and methods

3.3.1. Fungal isolate, plant material and inoculation

A genetically transformed *Botrytis cinerea* strain, B05.10, expressing a green fluorescent protein (GFP), was used due to its ability to grow on selective medium (potato dextrose agar [PDA] + 70 µg/ml Hygromycin B) besides giving a green fluorescent signal when observed under fluorescence microscopy. Grapevine fruiting cuttings were used from cv. Pinot Noir. Winter woody cuttings were collected and grown to raise flowers as described in (Chapter 2).

Flowers at full cap-fall stage (EL25/26, according to Eichorn and Lorenz [1977]) were inoculated by placing a 1.5 µl droplet of either conidia solution of GFP-labeled B05.10 ($2 \times 10^5 \text{ ml}^{-1}$) or distilled water (mock inoculation) close to the receptacle area. Conidia were obtained from

Botrytis grown on PDA at 25 °C for 10 days, and the concentration was determined using a hemacytometer under light microscope. Inoculation was made on three biological replicates, considering the inflorescence from a fruiting cutting as one biological replicate. After inoculation, the whole pot was immediately bagged in a clear plastic bag sprayed with water, for 24 h, in order to ensure high humidity around the inoculated inflorescence, which is an essential factor for conidial germination. Inoculated inflorescences were regularly inspected for gray mold growth until fruit ripening. At full coloring (approximately 10 weeks post inoculation, wpi), bunches were bagged for two weeks with plastic bags, to create favorable humidity for *B. cinerea* to egress.

Samples were collected at two time points, at 4 wpi, hard green berry, and at 12 wpi, from ripe clusters where *Botrytis* egression was evident on a subset of berries. For the latter time point, two kinds of samples were collected: berries with visible egressed *Botrytis* and berries without visible *Botrytis* sign. Samples without visible *Botrytis* sign are hereafter called berries with “pre-egressed” *Botrytis*. Samples were snap frozen in liquid nitrogen and stored at -80 °C until use.

3.3.2. RNA extraction, qPCR and RNA-seq

Extraction of RNA, synthesis of cDNA, and quantitative polymerase chain reaction (qPCR) assay were carried out as described in (Chapter 2). For qPCR assay, each amplification reaction was run in triplicate, and *VvACT* and *VvGAPDH*, and *BcRPL5* and *BcTUBA* genes were selected using GeNORM (Vandesompele et al., 2002) as reference for grapevine and *B. cinerea*, respectively, for normalization. Amplification efficiencies of each primer pair were calculated with LinReg software (Ruijter et al., 2009). The obtained amplification efficiency was used to calculate the relative quantity (RQ) and normalized relative quantity (NRQ) according to Hellemans et al. (2007). All primers and corresponding gene identifiers are listed in Supplemental Table S3.1.

Single-end reads of 100 bp long sequences were obtained for each sample using a Next Generation Sequencing Platform HiSeq 1500 (Illumina, San Diego, CA). Approximately 20 million strand-specific sequences, except for pre-egressed samples (above 45 million), was obtained. For pre-egressed samples, the sequence depth was doubled in order to obtain more reads of *Botrytis* origin. The quality of the reads was checked using FastQC (version 0.11.2) software and pre-processed by cutadapt (version 1.8.1; Martin, [2011]) for adapter. Genome

assemblies of grapevine (12Xv1, <http://genomes.cribi.unipd.it/>) and *B.cinerea* (strain B05.10) (<http://fungi.ensembl.org>) were used as reference sequences. The alignment was made by Subread aligner (Liao, et al., 2013) and raw read counts were extracted using the featureCount read summarization program (Liao, et al., 2014).

The RNA sequences of *B. cinerea* (B05.10), from the PDB cultured conidia (used in Chapter 2) were also used in this study as a control for differential expression analysis for the *in planta* *Botrytis* transcripts.

3.3.3. Secondary metabolites extraction and analysis

Extraction of polyphenol and Ultra High Performance Liquid Chromatography - Diode Array Detection - Mass Spectrometry (UHPLC-DAD-MS) analysis were carried out as described in (Chapter 2). For 4 wpi, the samples used for polyphenol and RNA extraction were independent.

3.3.4. Statistical analysis

Statistical analyses of the qPCR results were made after $\log_2(\text{NRQ})$ transformation (Rieu and Powers, 2009). Statistical significance was calculated by Tukey's Honestly Significant Difference test or an unpaired heteroscedastic Student's *t* test, considering each technical replicate as an individual sample.

Differential expression analysis was performed after precision weight was given, by the voom method (Law, et al., 2014), for each observation that was fed into the limma empirical Bayes analysis pipeline (Smyth, 2004). Two-sample t-test was used for transcripts of grapevine at 4 wpi (mock inoculated vs *Botrytis* inoculated) and *B. cinerea* at egression (PDB-cultured *Botrytis* vs egressed *Botrytis*), whereas one-way ANOVA for grapevine transcripts at 12 wpi (mock inoculated vs pre-egressed *Botrytis* vs egressed *Botrytis*). Genes were considered differentially expressed (DE) if they fulfill a *p*-value < 0.01 and an absolute fold change of ≥ 2.0 .

Principal component analysis (PCA) was performed using prcomp package in R on precision weight given counts. *K*-means clustering of differentially expressed genes based on fold change values (using cosine distance) and precision weight given counts (using Euclidean distance) was performed using akmeans package in R.

3.3.5. Functional classification based on Gene Ontology, VitisNet, and MapMan

DE genes were subjected to enrichment analyses using: i) VitisNet annotation within the VESPUCCI grapevine gene expression compendium (<http://vespucci.colombos.fmach.it>) (Grimplet et al., 2012; Moretto et al., 2016), p -value < 0.01; ii) customized GO annotation and annotated reference, taken from CRIBI annotation (<http://www.cribi.unipd.it/>), using AgriGO analysis tool (<http://bioinfo.cau.edu.cn/agriGO/analysis.php>; Du et al., 2010). Enriched GO terms (FDR < 0.01) were visualized using the ‘Reduce + Visualize Gene Ontology’ (REViGO) webserver (<http://revigo.irb.hr>; Supek et al., 2011). Additionally, the differentially expressed genes were visualized in the context of biotic stress pathway using the GrapeGen 12Xv1 annotations version (Lijavetzky et al., 2012) with the help of MapMan tool (Thimm et al., 2004)



Figure 3.1. *Botrytis cinerea* infected grapevine flowers and their growth until maturity. **A**, Flowers 24 h after inoculation with GFP-labelled B05.10 at full cap-fall stage (EL25/26). **B**, Healthy looking, asymptomatic, hard-green berry at 4 weeks post inoculation (wpi) **C**, Egression of *B. cinerea* at ripening (12 wpi). **D**, Fluorescence of mass of mycelia isolated from the outgrown *B. cinerea*; white bar represents 50 μ m.

3.4. Results

3.4.1. *Botrytis cinerea* inoculation of grapevine

Grapevine flowers were inoculated with a GFP-labeled B05.10 strain at full cap-off stage by placing 300 conidia around the receptacle area, and the infection was monitored until ripening, for 12 weeks (Figure 3.1). No visible symptom or sign of the fungus was observed until full coloring, though appressorium assisted penetration of floral epidermis at 24 hours post inoculation has been observed and described in detail in Chapter 2. The proportion berries still carrying *B. cinerea* at hard-green berry stage (4 wpi; Figure 3.1C) derived from flower inoculation was checked by plating out on selective media (Figure 3.2). *B. cinerea* was present on 80 % of the asymptomatic berries quiescently when samples were washed or not with water; the proportion dropped to 40 % when berries were surface sterilized, suggesting that the fungus mostly resides in the first few outer epidermal cell layers. At 10 wpi, full color change, bunches were bagged with plastic bags, to increase humidity and favor *B. cinerea* growth. Two weeks later, egression of *B. cinerea* was observed (Figure 3.1C), and cross checking the strain using fluorescence microscope, on mass of mycelia taken from the rotting bunch, confirmed that the strain was the GFP-labeled B05.10 inoculated at cap-off stage (Figure 3.1D). Egression was observed on about 40 % (39 ± 9 %) of the inoculated berries.

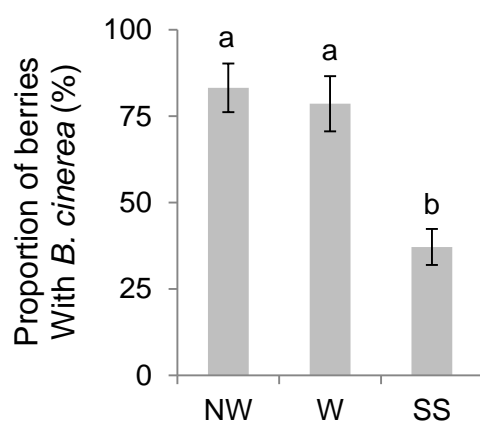


Figure 3.2. Proportion of berries with *B. cinerea* at 4 wpi, following flower inoculation with the fungus, as determined by plating out. Plating out was made on selective media (PDA with Hygromycin B, 70 $\mu\text{g/ml}$) to check the presence of quiescent *B. cinerea* before (NW) or after washing (W), or after surface sterilization (SS). Mean proportion of berries (8-10 berries from each of 6 biological replicates) showing GFP-labeled B05.10 growth on the selective media. Error bars indicate standard error. Mean proportions followed by a common letter are significantly not different, according to Tukey's Honestly Significant Difference test ($P \leq 0.05$), using one way ANOVA.

3.4.2. Transcriptional profiling of grapevine berry responses to *B. cinerea*

Hard green (4 wpi) and ripe berries (12 wpi), which were mock- or *Botrytis*-inoculated at cap-off stage, were harvested in 3 biological replicates for dual (plant and fungus) transcriptome analysis using the RNA-seq method. The fraction of reads from *Botrytis*- and mock-inoculated samples

mapped to the *V. vinifera* reference genome ranged from 13 to 88 %, the smaller proportion being from samples with egressed *B. cinerea*. However, in the case of *Botrytis*-inoculated samples mapped to *B. cinerea* reference genome, the fraction of mapped reads was below 1 % for the 4 wpi and pre-egressed samples, and up to 68 % for egressed *B. cinerea* samples (Supplemental Table S3.2).

The biological variability of all the samples was assessed using principal component analysis (PCA) on the gene expression data. Concerning grapevine data, samples were largely separated by growth stage along the first principal component, but within each growth stage most of the variation in gene expression was explained by the infection process (Figure 3.3A). With regard to *B. cinerea*, PDB grown and egressed samples were compared by PCA, highlighting the amazing difference in gene expression between the egression stage on berries at ripening and the growth in liquid PDB medium (Figure 3.3B)..

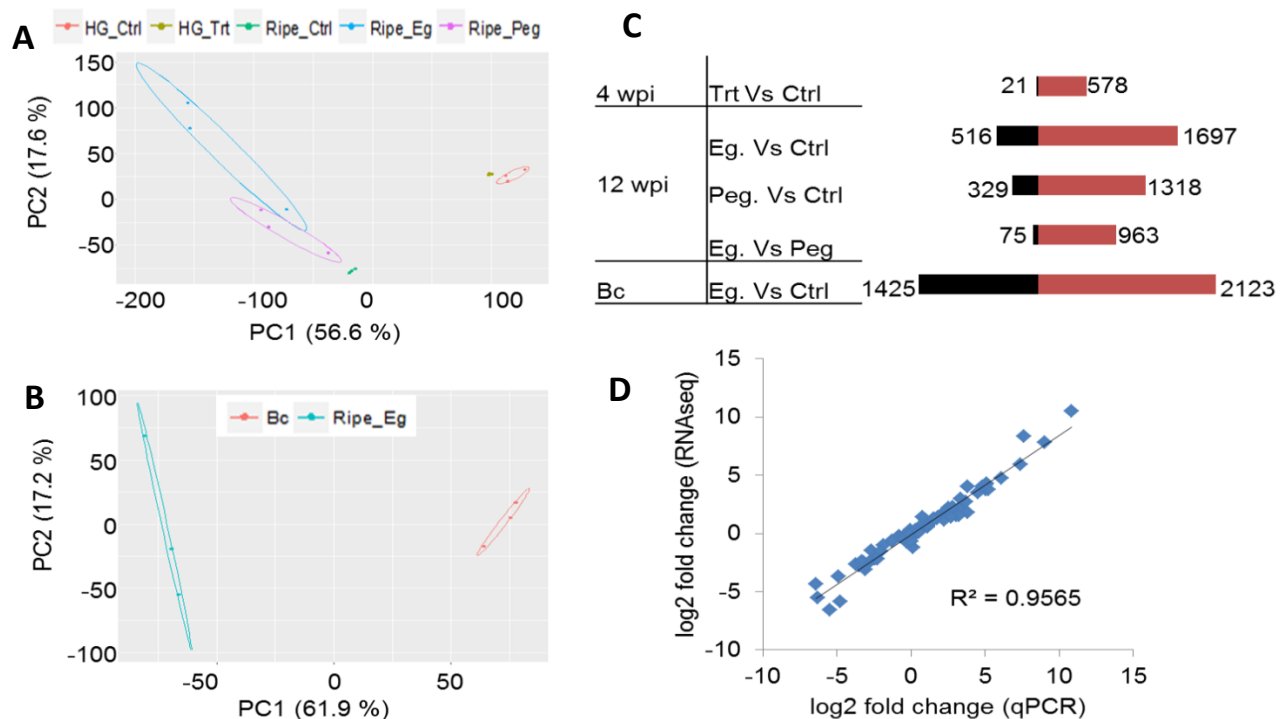


Figure 3.3. Global evaluation of the RNA-seq data and of the differentially expressed (DE) genes. PCA displaying the biological variations among samples, for grapevine genes (A) and *B. cinerea* genes (B). Ctrl, mock inoculated; Trt, *B. cinerea* inoculated; Bc, *Botrytis cinerea*; HG, hard-green berry; Eg, *B. cinerea* egression state; Peg, *B. cinerea* pre-egression state. Raw count data were used after precision weight was calculated by the voom method (Law et al., 2014). C, Number of DE genes ($P < 0.01$, absolute fold change > 2.0) upon *B. cinerea* infection at 4 weeks post inoculation (wpi) and 12 wpi; upregulated genes (red) and downregulated genes (black). Bc, *Botrytis cinerea*. D, Correlation of gene expression values obtained by RNA-seq and qPCR. Relative expression levels were calculated for 18 *Vitis* genes and an R^2 value of 0.96 was obtained comparing the results obtained with the two techniques.

Differential expression of genes was computed between *Botrytis*- and mock-inoculated berries at hard green stage (4 wpi) and at ripening (12 wpi) imposing a p -value < 0.01 and an absolute fold change > 2 (Supplemental Figure S3.1). At 4 wpi, 599 genes of grapevine were differentially expressed (DE) due to *B. cinerea* infection (Supplemental Table S3.3), whereas the number increased to 2,311 at ripening (Figure 3.3C and Supplemental Table S3.4). Only 158 genes were common between the two stages, suggesting an apparent different reaction of the host. For *B. cinerea* during egression, as compared to PDB cultured *Borytis*, there were 3,548 DE genes (Figure 3.3C and Supplemental Table S3.5). However, for 4 wpi and pre-egressed samples, due to limited amount of fungal RNA in the samples (Supplemental Table S3.6 and S3.7), it was not possible to gain insight into the differential expression of transcriptome of the fungus in the host using the RNA-seq results. To overcome the technical problem, qPCR assay was used to study the expression profile of selected genes.

The gene expression values obtained from RNA-seq were validated using qPCR assay. To this end, the expression of 18 grapevine genes (Supplemental Table S3.8) having different expression profile (differentially expressed or not) from RNA-seq were analyzed and a strong correlation ($R^2 = 0.96$) was observed between the results obtained from the two techniques (Figure 3.3D).

The total DE genes of the grapevine berries (2,752), considering both hard-green and ripe stages, were clustered into 12 distinct groups based on their expression pattern (Figure 3.4). Based on the expression trend of the DE genes, the clusters fell into 6 major expression profiles: profile A consisted only cluster 1, the upregulation extent of the majority of the 220 genes were higher at hard green stage as compared to ripe stage; profile B consisted cluster 2 and 5, the majority of the 464 genes was slightly upregulated or not affected at quiescence and pre-egression stage but highly upregulated during egression of *B. cinerea*; profile C consisted cluster 3 and 4, where majority of the 323 genes were upregulated at hard green stage and downregulated or not affected at ripe; profile D consisted cluster 7, having only 14 genes downregulated more at hard green than at ripe stage; profile E consisted cluster 6, 9 and 10, and majority of the 1176 genes were upregulated during ripening only; and profile F consisted cluster 8, 11 and 12, where the expression of majority of the 555 genes was not affected at hard green stage but downregulated during ripening. The molecular networks enrichment analysis of the gene set of each profile, based on VitisNet annotation, showed an abundance of transcripts in functional classes which are

usually affected by biotic stress. A considerable number of genes annotated for phenylpropanoid biosynthesis and transcriptional factors (TF) were represented in all expression profiles except for profile D and F. Signal transduction, such as ethylene and jasmonate signaling and plant-pathogen interaction, was represented in profile B and C. Several transcripts involved in amino acid metabolism, including glutathione metabolism, were represented in expression profile E.

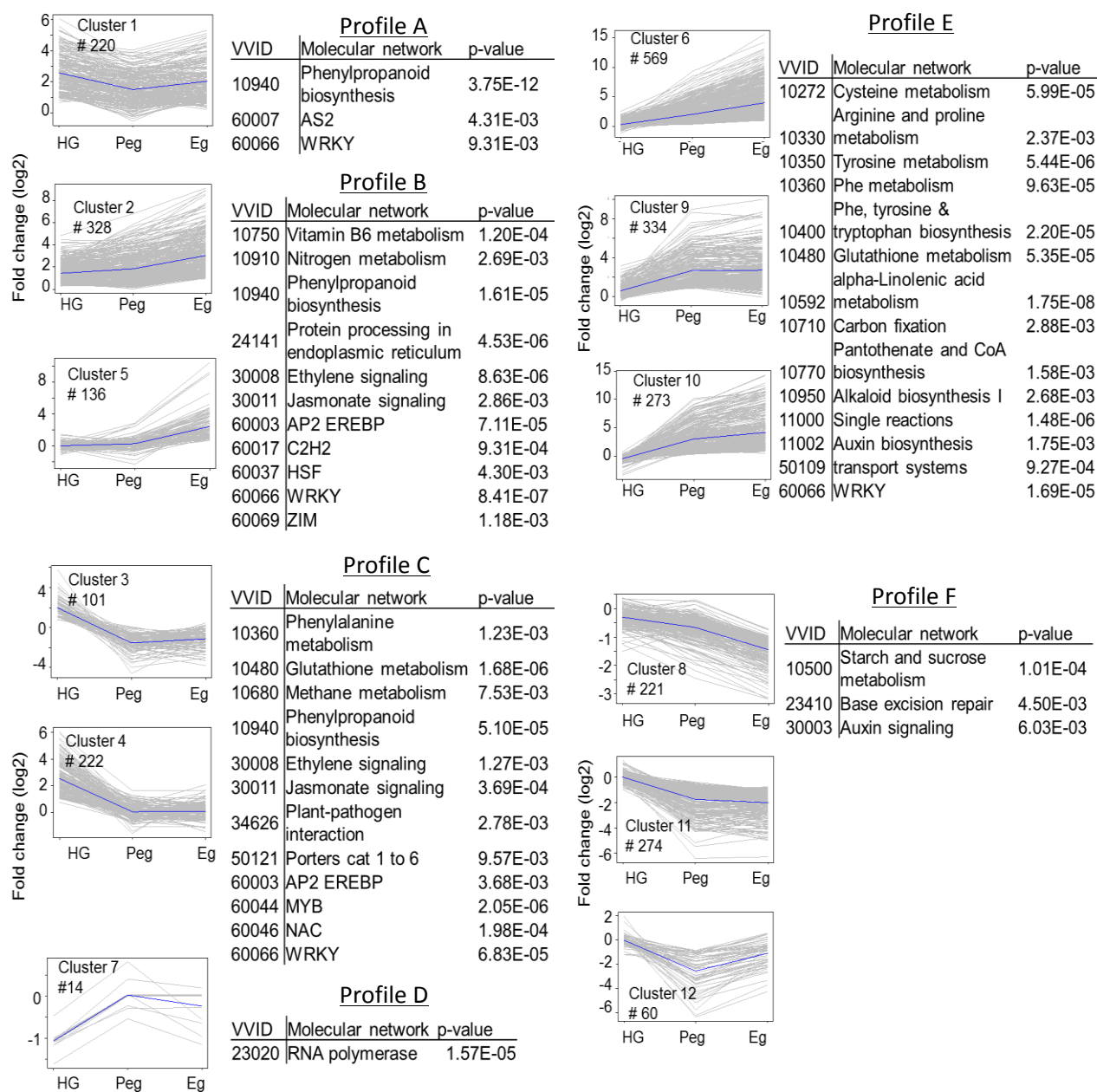


Figure 3.4. Profiles of grapevine berry transcripts at hard-green and ripe stages in response to *B. cinerea* inoculation. K-means clustering of grapevine genes based on the cosine distance of their log₂ (fold change) values. Genes that showed at least twofold expression difference with p-value < 0.01 were considered, and clustered into 12 clusters. The clusters were grouped into 6 major profiles (A, B, C, D, E and F). Molecular enrichment analysis based on VitisNet is provided for each group.

3.4.3. Transcriptional alterations of *B. cinerea* during quiescent infection, at 4 wpi

The signal of *B. cinerea* transcriptome detected in the inoculated samples at 4 wpi was very low; the reason could largely be linked to a reduced fungal biological activity as well as to the little fungal mass present at the quiescent stage. Only about 20 % of *B. cinerea* genes (1,926) had at least 1 raw reads in all of the three biological replicates. Within this set, those represented by an average of at least 10 reads (289), considered as expressed fungal transcript at 4 wpi and functionally annotated using Blast2GO (Conesa et al., 2005) and Amselem et al. (2011) (Supplemental Table S3.6). Using the Combined Graph Function of Blast2GO, metabolic processes, structural constituent of ribosome, and intracellular GO slim terms were represented most in the 289 genes (Supplemental Table S.3.9). Twenty-two genes from this group, selected based on their function, are presented in Table 3.1; the expression profile of 9 of them, involved in functions such as cell wall metabolism, redox-reaction, and transcriptional regulation, was further examined using qPCR assay (Figure 3.5). As depicted in Figure 3.5, all but *Bcin07g01540* and *Bcin13g05810* had a higher relative expression during quiescent infection at hard green stage than during initial infection at flowering and pre-egression and egression stages at ripe.

Table 3.1. RNA-seq reads of selected *B. cinerea* transcripts with different biological functions at quiescence in the hard-green berry (4 wpi)

Gene ID	Function (Blast2GO)	RNA-seq reads (average)					
		24 hpi	96 hpi	4 wpi	12 wpi		PDB culture
					Ripe_Peg*	Ripe_Eg	
Bcin01g09570	yt521-b-like splicing	9	8	15	119	2,685	2,177
Bcin02g06140	CP2 transcription factor protein	2	6	12	2	1,773	3,193
Bcin02g06930	1,3-beta-glucan synthase	49	27	20	24	15,886	12,324
Bcin03g01920	catalase	19	6	32	12	7,577	1,314
Bcin03g06170	40S ribosomal protein	108	62	21	42	18,774	34,625
Bcin03g07630	60S ribosomal protein	97	48	21	19	14,335	26,262
Bcin03g07670	NAD-specific glutamate dehydrogenase	30	20	31	10	2,937	11,142
Bcin04g01310	GPI-anchored cell wall organization Ecm33	97	34	45	37	31,061	17,374
Bcin07g01540	elongation factor 2	114	68	42	25	21,912	35,265
Bcin07g03980	chitin- domain 3	22	12	67	7	3,776	2943
Bcin08g05540	ASG1; CND1, similar to Gas1-like protein	129	54	410	35	24,761	35,778
Bcin09g00200	glucan endo-1,3-beta-glucosidase eglC	15	15	31	8	5,578	8,505
Bcin10g01180	ABC transporter ATP-binding ARB1	21	14	20	19	10,154	5,384
Bcin11g04800	chitin deacetylase	10	3	67	4	2,385	210
Bcin11g04930	Stress response ish1	7	6	21	19	15,610	348
Bcin12g06170	allergen; Peptide transport PTR2	8	2	20	1	682	86
Bcin13g05580	alcohol dehydrogenase 1	100	47	21	4	4,198	37,002
Bcin13g05810	aldehyde dehydrogenase	238	46	48	25	10,689	4,569
Bcin14g04260	cell surface; Gas2, regulated by Bmp1 MAP kinase cascade	18	4	112	23	21,022	41
Bcin14g03970	1,3-beta-glucanosyltransferase gel1; glycolipid-anchored surface protein 5 precursor	76	42	26	14	14,303	11,200
Bcin15g02080	ATP synthase beta chain	107	67	27	24	19,251	36,547
Bcin16g02430	carbohydrate-binding module family 5	13	14	28	5	4,352	7,622

* The sequence depth of the samples was double; only two biological replicates were considered.

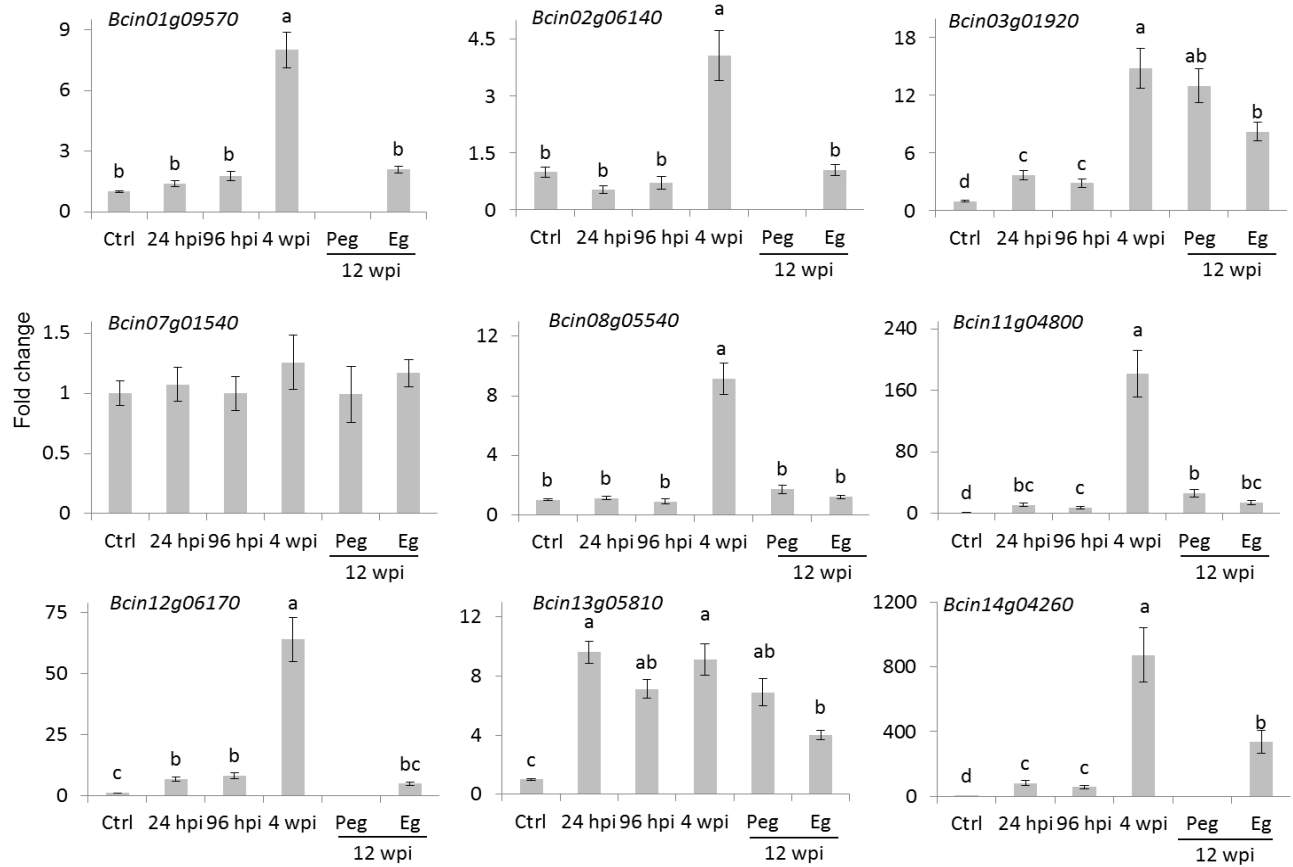


Figure 3.5. Expression profile of selected *Botrytis cinerea* genes having higher raw reads at hard-green berry stage relative to PDB-cultured *B. cinerea*. Bars represent fold change of samples at 24 and 96 hours post inoculation (hpi; flower infection), 4 weeks post inoculation (wpi; quiescent infection at hard-green berry stage), and 12 wpi (pre-egression, Peg, and egression, Eg, stages of *B. cinerea* at ripening) relative to the PDB-cultured *B. cinerea* (Ctrl). Normalization based on the expression levels of ribosomal protein L5, *BcRPL5*, and α tubulin, *BcTUBA*, was carried out before calculating fold changes. Error bar represents standard error of the mean of three biological replicates. Expression values followed by a common letter are significantly not different between samples, according to Tukey's Honestly Significant Difference test ($P \leq 0.05$), using one way ANOVA of $\log_2(\text{NRQ})$.

The qPCR results suggested that the biological activities of the fungus were not totally switched off during quiescent infection. The expression of *Bcin01g09570* and *Bcin07g01540* gene, which encode putative yt521-b-like splicing and elongation factor 2 proteins, respectively, and the numerous genes encoding for ribosomal proteins (Table 3.1 and Supplemental Table S3.6) indicated that protein synthesis activities were carried out during quiescent infection stage. The expression of stress and defense related genes, such as *Bcin12g06170*, encoding a protein similar to allergen, and *Bcin11g04800*, which encodes a putative chitin deacetylase protein, highlighted that the interaction between the pathogen and the plant was not passive. Chitin deacetylase

activity has been speculated to be involved in protecting the fungal cell wall from degradation by plant chitinases in other fungi (Deising and Siegrist, 1995; El Gueddari et al., 2002). In addition, genes encoding putative proteins involved in cell wall remodeling and integrity (for example, *Bcin04g01310* and *Bcin14g03970*) seemed also active during fungal quiescence (Table 3.1 and Supplemental Table S3.6). Stress usually causes ROS production that can lead to accumulation of aldehydes and alcohols in fungal cells (Asiimwe, et al., 2012). *Bcin13g05810* and *Bcin13g05580*, encoding putative aldehyde dehydrogenase and alcohol dehydrogenase, respectively, involved in the detoxification of alcohols and aldehydes, as well as *Bcin03g01920*, encoding a putative catalase, were speculated to help overcome stress from the berries' defense. Moreover, *Bcin08g05540*, encoding putative CND1 protein, *Bcin14g04260*, annotated for a putative cell surface protein and Gas2, and *Bcin02g06140*, encoding a putative CP2 transcription factor protein, all these genes probably involved in maintaining cell wall, (Garrett-Engele et al., 1995; Paré et al., 2012), appeared to be relatively expressed more during quiescent infection at 4 wpi as compared to initial and egression stages of infection (Figure 3.5).

The extremely low number of *B. cinerea* genes expressed *in planta* seconded by absence of any macroscopically noticeable disease progress at 4 wpi suggests that the pathogen was at its basal metabolic activity despite specific stress related genes were expressed.

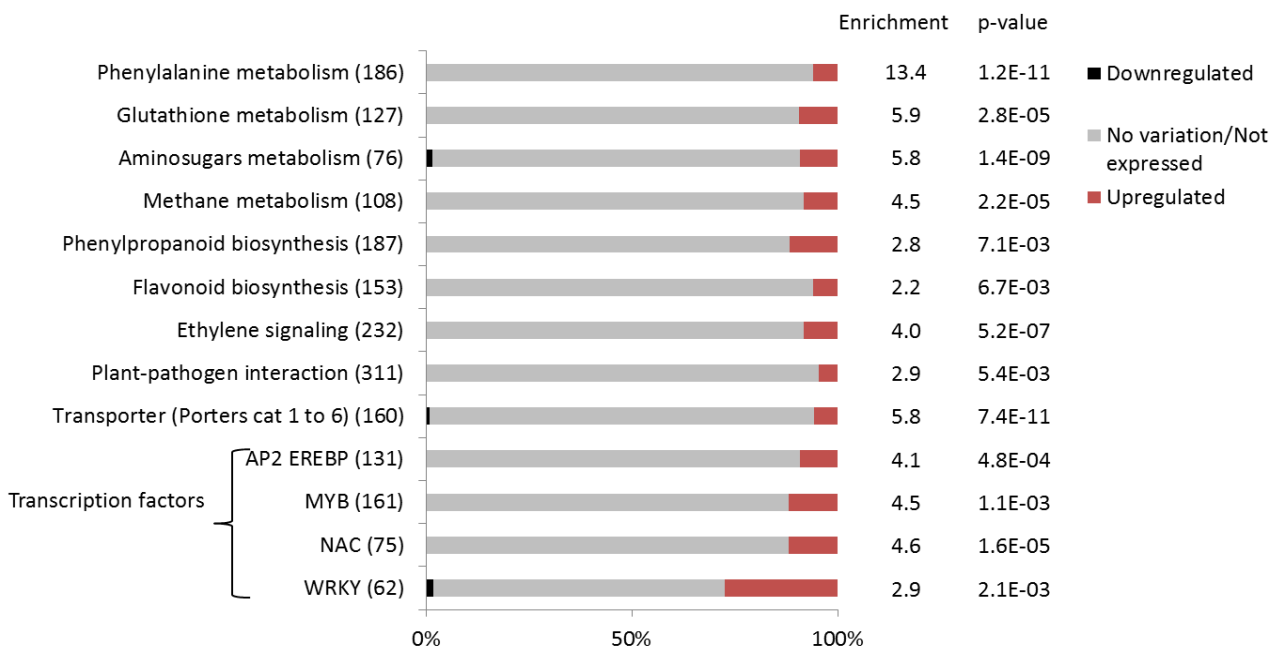


Figure 3.6. VitisNet functional classes enriched in the differentially expressed genes at hard-green berry stage due to quiescent *Botrytis cinerea*. The number presented in the parentheses is the total number of *V. vinifera* genes within each category. The portion of upregulated and downregulated genes within a category is represented by red and black bars, respectively

3.4.4. Response of hard-green berries to quiescent *B. cinerea*, at 4 wpi

In contrast to the fungus for which not many transcripts were observed, 599 grapevine genes were differentially regulated due to the quiescent presence of *B. cinerea*, of which only 21 genes were downregulated (Figure 3.3C and Supplemental Table S3.3). In this set of *Botrytis*-induced genes functional classes related to responses to stress, amino acid metabolism for redox activity and phenylpropanoid pathways, signaling, and TFs were overrepresented (Figure 3.6 and Supplemental Table S3.10). The visualization of individual gene responses in biotic stress pathway using MapMan tool also indicated a remarkable induction of genes related to signaling, TFs, proteolysis, PR-proteins and secondary metabolism (Figure 3.7). Genes involved in some defense pathways, which were activated at initial infection stage (24 hpi) but returned to basal level toward the entry of quiescence (96 hpi) during flower infection (Chapter 2), seemed to be reactivated at 4 wpi, such as genes in the phenylpropanoid biosynthesis pathway for stilbenoids, flavonoids and lignin precursors synthesis.

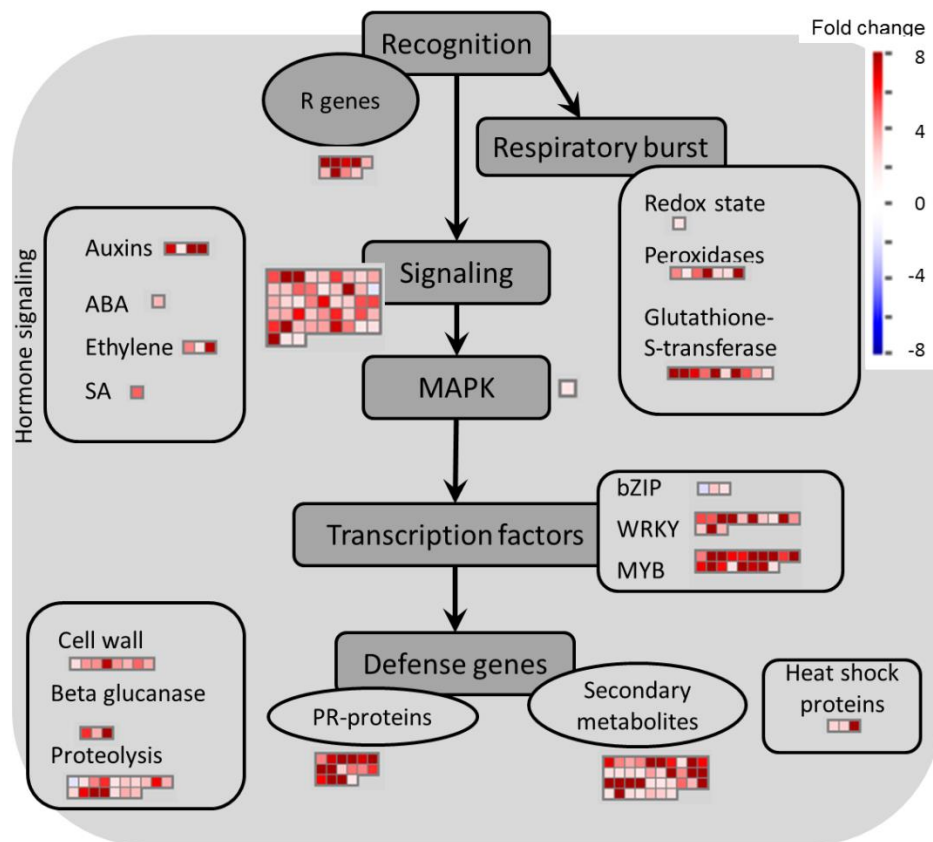


Figure 3.7. Biotic stress overview of hard-green berries due to quiescent *B. cinerea* infection, 4 wpi, as visualized by MapMan. Upregulated and downregulated genes are shown in red and blue, respectively. The scale bar displays fold change values. ABA, abscisic acid; MAPK, mitogen-activated protein kinase; SA, salicylic acid.

Table 3.2. Selected differentially expressed grapevine genes due to quiescent *B. cinerea* infection (at 4 wpi)

ID	Fold change (log2)	Functional annotation	ID	Fold change (log2)	Functional annotation
Recognition and signaling			Cell wall		
VIT_05s0020g04680	1.07	Auxin-induced protein 22D	VIT_01s0127g00070	1.17	Nitrate transporter 2.5
VIT_12s0055g01280	1.98	Brassinosteroid insensitive 1-associated receptor kinase 1	VIT_17s0000g09470	1.40	Nitrate transporter 3.1
VIT_14s0030g02150	4.22	Calmodulin	VIT_03s0091g01050	1.53	Nucleobase-ascorbate transporter 4
VIT_03s0038g01380	1.02	Calcium-binding EF hand	VIT_05s0049g00010	1.23	Cellulose synthase CSLG2
VIT_08s0056g00290	1.07	Calcium-binding protein CML	VIT_00s0340g00050	2.60	Endo-1,4-beta-glucanase korrigan (KOR)
VIT_04s0008g00440	1.78	Clavata1 receptor kinase (CLV1)	VIT_14s0128g00690	4.20	Germin protein 3
VIT_11s0016g03080	2.51	Clavata1 receptor kinase (CLV1)	VIT_06s0004g01990	3.06	Proline-rich extensin-like family protein
VIT_06s0004g06210	5.07	CYP86A1	VIT_12s0055g00200	2.20	UDP-glucose glucosyltransferase
VIT_11s0118g00160	3.65	Disease resistance protein	Response to stress and secondary metabolism		
VIT_17s0000g07560	1.10	EDS1 (Enhanced disease susceptibility 1)	VIT_11s0052g01110	2.69	4-coumarate-CoA ligase 1
VIT_08s0040g00920	3.67	Glutathione S-transferase 25 GSTU7	VIT_16s0050g02220	3.18	Acidic endochitinase (CHIB1)
VIT_04s0044g01990	1.42	Lectin protein kinase	VIT_03s0017g02110	3.16	Anthocyanidin 3-O-glucosyltransferase
VIT_18s0072g00990	1.30	Leucine-rich repeat protein kinase	VIT_08s0007g06060	2.55	Beta 1-3 glucanase
VIT_18s0122g01260	1.68	Protein kinase 1B	VIT_16s0098g00850	1.40	Caffeic acid O-methyltransferase
VIT_10s0071g00150	1.60	R protein disease resistance protein	VIT_03s0063g00140	1.19	Caffeoyl-CoA O-methyltransferase
VIT_00s0262g00010	2.25	Receptor kinase RK20-1	VIT_16s0100g00860	4.82	Chalcone synthase
VIT_17s0000g02360	2.42	Receptor protein kinase	VIT_05s0094g00340	2.17	Chitinase class IV
VIT_16s0039g01310	2.18	Receptor serine/threonine kinase PR5K	VIT_09s0070g00240	1.19	Cinnamoyl-CoA reductase
VIT_16s0148g00140	1.47	Ser/Thr receptor-like kinase1	VIT_06s0004g01010	3.95	Dirigent protein pDIR9
VIT_17s0000g04400	3.10	Wall-associated kinase 1 (WAK1)	VIT_07s0031g01380	3.72	ferulate 5-hydroxylase
VIT_17s0000g03340	1.08	Wall-associated kinase 4	VIT_16s0098g00860	2.31	Flavanone 3-hydroxylase
Transcription factors			VIT_02s0109g00310	1.84	flavonoid 3-monooxygenase
VIT_05s0049g00510	2.01	Ethylene response factor ERF1	VIT_10s0003g00470	2.15	Isoflavone methyltransferase
VIT_05s0049g01020	1.55	Myb domain protein 14	VIT_13s0067g01970	2.78	Laccase
VIT_15s0046g00170	1.21	MYBPA1 protein	VIT_17s0000g06290	4.78	Lipase GDSL
VIT_04s0008g02710	4.25	NAC domain containing protein 39	VIT_02s0025g04250	4.12	Osmotin
VIT_12s0028g00860	3.00	NAC domain containing protein 42	VIT_05s0077g01570	4.37	Pathogenesis protein 10 [Vitis vinifera]
VIT_04s0008g05760	1.81	WRKY DNA-binding protein 18	VIT_03s0088g00710	3.50	Pathogenesis-related protein 1 precursor (PRP 1)
VIT_08s0058g00690	1.61	WRKY DNA-binding protein 33	VIT_04s0023g02570	2.15	Peroxidase 72
VIT_08s0058g01390	1.74	WRKY DNA-binding protein 70	VIT_16s0039g01100	4.90	Phenylalanin ammonia-lyase [Vitis vinifera]
Transport			VIT_02s0025g00750	3.49	Pinoresinol forming dirigent protein
VIT_08s0040g02840	4.46	ABC transporter G member 29	VIT_00s0480g00030	2.75	Polyphenol oxidase
VIT_08s0058g00150	2.54	Ammonium transporter 2	VIT_16s0100g01200	5.33	Stilbene synthase
VIT_04s0069g00540	1.90	Glutamate receptor protein	VIT_02s0025g02850	1.16	Subtilisin protease
			VIT_02s0025g04270	4.33	Thaumatococin

Receptor-like protein kinases (RLKs) regulate recognition and responses to both internal and external signals, and also take part in defense and symbiosis. From the differentially expressed genes, about one-sixth of them were those involved in signaling, dominated by RLKs (Table 3.2 and Supplemental Table S3.3). Membrane-localized RLKs which were switched on during infection initiation at flowering, like *Clavata1 receptor kinase (CLV1)*, *Brassinosteroid insensitive 1– associated kinase 1 (BAK1)*, and *Wall-associated kinase 1 (WAK1)*, were also upregulated during the interaction at quiescent infection. The involvement of *WAK1*, a damage associated pattern receptor which recognize plant cell wall–derived oligogalacturonides due to cell wall degradation (Brutus et al., 2010), at this stage of interaction was not obvious, however. From the transcriptional alteration on RLKs, lectin protein kinase and protein kinase 1, seem to be quiescent-stage-specific. The putative orthologue in other species are associated to plant immunity, in particular the latter is known to mediate signaling in response to *B. cinerea* (Abuqamar et al., 2008). In addition, transcripts related to Ca^{2+} mediated signaling (such as calcium- and calmodulin-binding proteins) and oxidative stress (mainly GST and cytochrome P450 monooxygenases) were also found to involve in the ongoing berry immunity.

Key TFs that play an important role in plant-microbe interaction, which were also upregulated at initial infection during flowering, were still tuned on in the presence of asymptomatic *B. cinerea*, at 4 wpi (Table 3.2 and Supplemental Table S3.3). Most prominent was the MYB TF family: 21 genes encoding 14 different MYB proteins, including *MYB14* and *MYBPA1* which respectively regulate stilbene and proanthocyanidin biosynthesis. From the WRKY and NAC TFs *WRKY33*, which regulates plant defense reaction against pathogens (Birkenbihl et al., 2012; Merz et al., 2015), *NAC042*, known to regulate phytoalexin biosynthesis (Saga et al., 2012), *WRKY51*, mediating the repression of JA signaling in a SA- and low-oleic-acid-dependent manner (Gao et al., 2011), and *NAC036*, *WRKY18* and *WRKY70*, regulate SA biosynthesis and SA signal transduction (Wang et al., 2006) were involved. The upregulation of SA signaling marker genes, such as *PRI* and *EDS1*, is a further indication of SA involvement in enhancing the defense ability of the hard-green berry. In addition, the upregulation of 3 *ACC oxidase* and 12 *AP2/ERF* genes underlines that also ET signaling is in place during the interaction at quiescent state. *AP2/ERF* are vital in plant-pathogen interactions (Gutterson and Reuber, 2004; Licausi et al., 2013). Genes related to auxin metabolism were also modulated, suggesting that also this phytohormone is likely involved.

Intriguingly, differential regulation was observed for genes coding for various PR proteins and enzymes of the phenylpropanoid pathway and of flavonoid and stilbenoid biosynthesis during quiescent infection (Table 3.2 and Supplemental Table S3.3). For some of the genes, the upregulation was nearly 50 fold. PR proteins encoding genes included: PR 10s and the regulator WRKY33, involve in defense against *B. cinerea* and *Plasmopara viticola* in grapevine (Merz et al., 2015; ?firstpaper?); β -1,3-glucanase and different classes of chitinases, to attack fungal cell wall; and osmotin and thaumatin, known to interfere with the growth of *Phomopsis viticola* and *Botrytis cinerea* mycelia (Monteiro et al., 2003). Besides, a gene encoding cystatin, proteinaceous inhibitors of cystein proteases which is suggested to inhibit the growth of *B. cinerea* (Pernas et al., 1999), was also upregulated.

Table 3.3. Concentration ($\mu\text{g/g}$ fresh weight) of selected polyphenolic secondary metabolites in mock (Ctrl) and *B. cinerea* (Trt) inoculated grapevine at hard-green berry stage, 4 wpi.

Class	Secondary metabolites	LOD($\mu\text{g/g}$)	Hard green berry (4 wpi)	
			Ctrl	Trt
stilbenoids	<i>trans</i> -resveratrol	0.005	n.d.	1.52 \pm 0.47
	<i>trans</i> -piceide*	0.0125	0.97 \pm 0.09	10.08 \pm 1.83
	<i>cis</i> -piceide*	0.0025	0.34 \pm 0.05	1.7 \pm 0.40
	astringin*	0.005	0.14 \pm 0.03	1.55 \pm 0.26
	isorhapontin	0.005	n.d.	0.21 \pm 0.06
	arbutin*	0.005	0.13 \pm 0.01	0.90 \pm 0.19
	<i>trans</i> - ϵ -viniferin	0.005	n.d.	9.86 \pm 2.16
	<i>cis</i> + <i>trans</i> - <i>o</i> -viniferin	0.0125	n.d.	0.30 \pm 0.07
	pallidol	0.005	n.d.	0.60 \pm 0.19
	ampelopsin D+quadrangularin A	0.025	n.d.	2.78 \pm 0.81
	α -viniferin	0.0125	n.d.	1.86 \pm 0.66
	E- <i>cis</i> -miyabenol	0.0125	n.d.	0.91 \pm 0.34
	Z-miyabenol C	0.05	n.d.	0.40 \pm 0.12
	isohopeaphenol	0.0125	n.d.	0.16 \pm 0.05
Flavonoids	naringenin*	0.0025	0.01 \pm 0.00	0.08 \pm 0.01
	catechin	0.025	17.75 \pm 1.23	26.06 \pm 3.55
	epicatechin*	0.025	4.40 \pm 0.44	9.33 \pm 1.19
	epicatechin gallate*	0.025	0.10 \pm 0.02	1.67 \pm 0.29
	procyanidin B1	0.0125	67.98 \pm 4.47	136.63 \pm 28.81
	taxifolin	0.0025	6.54 \pm 0.95	13.40 \pm 3.46

LOD, limit of detection; wpi, week post inoculation; values after \pm are standard error.

Asterisks (*) indicate statistically significant difference ($P < 0.05$)

n.d., not determined. For metabolites that were not determined in control sample, no statistical comparison was made.

In the case of secondary metabolites biosynthesis, though there was generally a smaller number of DE genes involved as compared to the initial infection during flowering, still the monoglignol, flavonoid and stilbenoid biosynthesis pathways were somehow active. Genes encoding enzymes in the biosynthetic pathway, for example, phenylalanine ammonia-lyase, stilbene synthase, anthocyanidin 3-O-glucosyltransferase, chalcone synthase, and cinnamoyl-CoA reductase were differentially regulated (Supplemental Table S3.3). Many compounds of the phenylpropanoid pathway were also quantified by UHPLC-DAD-MS (Supplemental Table S3.11). The strongest effect was recorded on flavonoids and stilbenoids (Table 3.3), in particular on compounds known to mediate defense against pathogens: resveratrol, viniferin, ampelopsin, miyabenol, isohopeaphenol, catechin, and proanthocyanidins (Jersch et al., 1989; Goetz et al., 1999; Pezet et al., 2003a; Favaron et al., 2007; Hammerbacher et al., 2011). For the stilbenoid class, most of the compounds were below the detection limit in control samples. Here it should be noted that there is ontogenic reduction of the polyphenols' concentration between flower and hard-green developmental stages (Supplemental Table S2.8 and S3.11).

In sum, even though we did not observe any known virulence related genes of the pathogen which can provoke response from the berries at 4 wpi, it seemed, however, that the berries are at primed state with enhanced immunity as it recognizes nonself organism, which in turn help the berry to contain the pathogen. This gives an interesting insight that there is a molecular communication going on between the quiescent *B. cinerea* and the berry.

3.4.5. *B. cinerea* transcriptome during pre-egression and egression stages, at ripening

At ripening, two kinds of berries were collected from *Botrytis*-treated samples: berries without visible *B. cinerea* outgrowth (samples with pre-egressed *B. cinerea*) and berries with visible signs of *B. cinerea* outgrowth (named egressed *B. cinerea*). Both samples were subjected to RNA-seq to analyze the dual transcriptome (fungus and plant) at these stages. In the samples with pre-egressed *B. cinerea*, as in flower and hard-green berry samples, the number of fungal transcripts was unfortunately very low, even though the sequencing depth was doubled. Moreover, in one of the biological replicates (replicate 2) the growth of the fungus was advanced than the rest two, as inferred from the number of fungal transcripts obtained from the RNA-seq experiment (Supplemental Table S3.2 and S3.7). Taking similar threshold previously used in the flower and hard-green berry samples (an average of at least 10 reads) in the two biological replicates,

excluding the sample with advanced *B. cinerea* growth, 431 genes were selected for further analysis. The functional annotation and the most represented functional classes in these set of genes are provided in Supplemental Table S3.7 and S3.12, respectively.

Within the 431 genes, there were several genes encoding proteins functionally associated to the infection process: dyp-type peroxidase and galactose oxidase, involved in generation and detoxification of ROS (Schumacher et al., 2015); polygalacturonase, deployed in pectin degradation; glyoxal oxidase and oxalate decarboxylase, both catalyze oxalate; different types of oxidoreductases; and cerato-platanin *BcSPL1*, a small protein required for full virulence (Frías et al., 2011, 2014). Interestingly, these genes showed a low number of raw reads or were not expressed at all at 4 wpi (Table 3.4), indicating that the physiological state of the fungus in the ripe berry before egression was different from that in the hard-green one.

Table 3.4. RNA-seq reads of selected *B. cinerea* transcripts having more reads at pre-egression (12 wpi, on ripe berry) than at quiescence (4 wpi, on hard-green berry).

Gene ID	Function (Blast2GO)	Further description	RNA-seq reads (average)		
			4 wpi	12 wpi (Peg)*	PDB culture
Bcin13g05720	Dyp-type peroxidase	BcPRD1, Dyp-type peroxidase	2	42	312
Bcin13g05710	Galactose oxidase beta-propeller	BcGOX1, Galactose oxidase	4	30	609
Bcin12g02040	acid protease	BcAP8, aspartic proteinase	1	12	1,064
Bcin14g00850	polygalacturonase	Pectin degradation	0	30	147,821
Bcin07g01150	ubiquitin-60S ribosomal L40	Polyubiquitin	11	23	30,510
Bcin06g01930	glyoxal oxidase	Glyoxal oxidase	3	31	6,239
Bcin15g02380	acid protease partial	Glutamic protease	0	42	56
Bcin01g09650	glucose-6-phosphate 1-dehydrogenase	Glucose-6-phosphate dehydrogenase	15	36	6,740
Bcin03g00500	probable rot1 PRECURSOR	Cerato-platanin family protein BcSpl1	5	29	64,662
Bcin01g11220	glycoside hydrolase family 17	b-1,3-Glucosidase	4	16	4,617
Bcin07g00160	glycoside hydrolase family 18	CAZyme	5	42	2,386
Bcin04g05650	oxalate decarboxylase family bicupin		1	41	38
Bcin11g02720	aldo keto reductase	Oxidoreductase	9	35	3,377
Bcin04g05700	nadp-dependent alcohol dehydrogenase	Oxidoreductase	1	21	4,844
Bcin06g04940	short-chain dehydrogenase	Oxidoreductase	2	34	338
Bcin09g03090	lipid phosphate phosphatase 1	Oxidoreductase	2	25	152
Bcin16g04720	C-5 sterol desaturase		5	23	14,517
Bcin11g02630	phytanoyl- dioxygenase	Oxidoreductase	0	23	22
Bcin15g03620	glycosyltransferase family 35	CAZyme	8	20	12,308
Bcin11g06080	ATP synthase H mitochondrial precursor		3	40	6,851

* The sequence depth of the samples was double; only two biological replicates were considered.

In the egressed sample, 86 % of total *B. cinerea* transcriptome was expressed, which is a sign of utmost metabolic activity. Interestingly, the number of genes expressed were similar between egressed and PDB cultured *B. cinerea*, about 10,000 of the total 11701 predicted genes (van Kan et al., 2016). Such en masse transcriptional activity was never seen in the other evaluated infection stages, possibly due to the low measurable signal linked to the little amount of the fungus, but likely also to a reduced transcriptional activity at these stages. In other words, at ripening, the time, the status of the host tissue, and the environmental conditions, components of the disease pyramid, were conducive for *B. cinerea* to egress and grow vigorously, as observed from Figure 3.1C.

Table 3.5. RNA-seq reads of selected virulence *B. cinerea* genes which were not differentially expressed in comparison to PDB culture d *B. cinerea*

Gene ID	Gene name	RNA-seq reads (average)					
		24hpi	96hpi	4 wpi	12 wpi		PDP culture
					Peg*	Eg	
Bcin14g00850	Polygalacturonase1 (BcPG1)	209	175	0	30	24,289	147,821
Bcin10g00740	Glutathione S-transferase (BcGST1)	9	1	3	4	1,496	2,655
Bcin01g00060	Botcinic acid6 (BcBOA6)	13	2	0	1	740	1,048
Bcin03g00500	Cerato-platanin family protein (BcSPL1)	138	75	5	29	29,201	64,662

* The sequence depth of the samples was double; only two biological replicates were considered.

Compared to the transcriptional changes of *B. cinerea* cultured in PDB, 3,548 genes were differentially regulated during egression at ripening (Figure 3.3C and Supplemental Table S3.5). These DE genes are overrepresented in metabolic processes, ion binding, catalytic and oxidoreductase activities, cytoplasm, intracellular part functional classes (Supplemental Table S3.13). Genes encoding carbohydrate-active enzymes and others involved in plant cell wall degradation (Espino et al., 2010; Blanco-Ulate et al., 2014), such as *Bcin10g06130* and *Bcin14g01630*, encoding pectinases, *Bcin03g01680*, encoding a polygalacturonase, and *Bcin07g06480* and *Bcin15g03080*, encoding cutinases, were expressed more during egression than in PDB medium. Other virulence and/or growth related genes having similar expression trend as those mentioned above were: ROS producers and scavengers like *Bcin03g03390*, *Bcin13g05710*, and *Bcin13g05720* (Rolke et al., 2004; Schumacher et al., 2015); characterized aspartic proteases (*Bcin12g02040* and *Bcin12g00180*, ten Have et al., 2010); membrane

transporters, mostly the ATP-binding cassette; and botcinic acid and botrydial phytotoxins (*Bcin12g06390* and *Bcin12g06380*, Siewers et al., 2005; Dalmais et al., 2011). On the other hand, known virulence genes like *BcPG1* (*Bcin14g00850*), *BcGST1* (*Bcin10g00740*), *BcBOA6* (*Bcin01g00060*), and *BcSPL1* (*Bcin03g00500*) had similar or lower expression level during egression as compared to PDB cultured *Botrytis*. This, however, does not mean that they do not play a role in the necrotrophic stage of infection during egression at ripening, as the number of reads of these genes was reasonably high at this stage (Table 3.5).

3.4.6. Response of ripe berry for *B. cinerea*'s pre-egression and egression state

Grapevine berries responded to the necrotrophic colonization of the fungus, during egression, by reprogramming the transcription of 2,213 genes (Figure 3.3C and Supplemental Table S3.4). Of these genes, 1,564 were already differentially regulated in pre-egressed samples, together with additional 83 genes. The GO enrichment analysis computed on these DE genes of pre-egressed and egressed samples showed a high overlap in the enriched biological process: secondary metabolic process, response to stimulus, catabolic process and transport functional classes were among the enriched functional classes (Supplemental Table S3.14). In the case of the genes modulated between egression and pre-egression states (Eg. Vs. Peg), only 15 genes were not part of the DE genes obtained in the Peg Vs. Ctrl and Eg. Vs Ctrl comparisons (Figure 3.3C).

The differentially expressed genes, 2,311 in total at 12 wpi, were clustered into 8 groups based on their expression pattern considering control, pre-egressed, and egressed samples as shown in Supplemental Figure S3.2. Several functional classes as amino acid metabolism, protein processing, carbohydrate and lipid metabolism, phytohormone (auxin, ET, and JA) signaling were overrepresented, combining the 8 clusters into into four main expression profiles (A-D in Supplemental Figure S3.2).

Almost all of the DE genes in the pre-egressed samples were also in the egressed samples, and there existed a general similar expression direction (up- or down-regulation) in these genes Supplemental Table S3.4 and Supplemental Figure S3.2). As a result, we used the the DE genes of the egressed stage only to visualize the biotic stress pathway (Figure 3.8), *via* MapMan, as it can give enough insight of the pre-egressed stage as well. Figure 3.8 depicted the transcriptional changes involved in biotic stress were huge. Although it might seem surprising, it is not uncommon to see such modulation of defense related genes in infected plant tissues even when

the pathogen wins the battle (Alkan et al., 2014; Agudelo-Romero et al., 2015; Kelloniemi et al., 2015). This could be due to the futile attempts of the infected tissue reacting against the pathogen and/or to the transcriptome attributes of other cell layers, not yet colonized, as it is impossible to spatially resolve. From the biotic stress pathway visualization, however, the presence of many downregulated genes in the PR protein and secondary metabolite categories, and the involvement of a lot of genes in JA and ET signaling and cell wall modification (Figure 3.8) were unique of the ripe berry transcriptome as compared to flower and hard-green berry due to *B. cinerea* (Figure 2.4 and Figure 3.7).

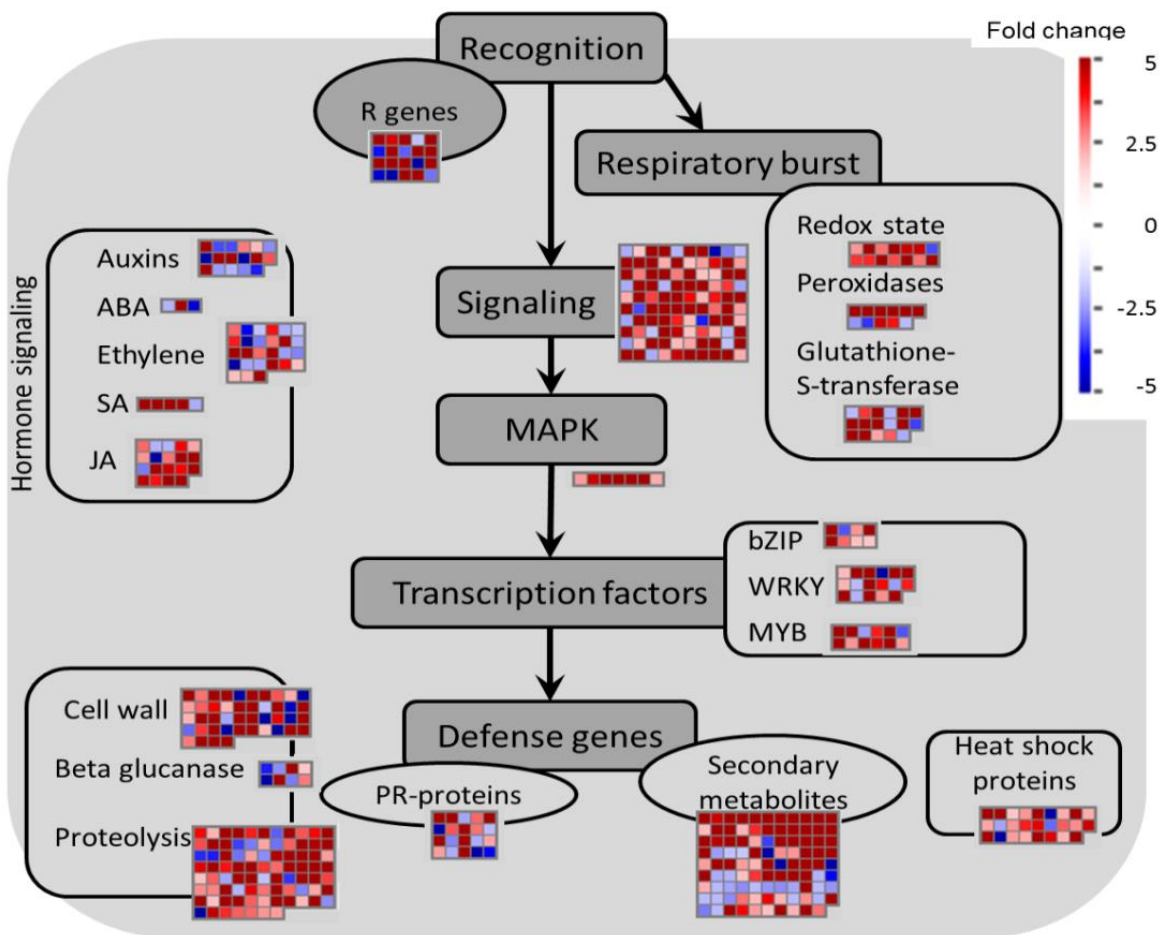


Figure 3.8. Biotic stress overview of ripe berries due to egressed *B. cinerea*, 12 wpi, as visualized by MapMan. Upregulated and downregulated genes are shown in red and blue, respectively. The scale bar displays fold change value. ABA, abscisic acid; JA, jasmonic acid; MAPK, mitogen-activated protein kinase; SA, salicylic acid.

The PR proteins, which were differentially expressed by the infection during flowering and hard-green berry stages, were also regulated in ripe berry when during *Botrytis* egression, but to a different extent or direction and/or with reduced number of gene copies (Table 3.6). For example, two *PR10* genes, namely VIT_05s0077g01580 (upregulated) and VIT_05s0077g01690 (downregulated) were among the PRs in ripe berry; however, during initial infection at flowering, 5 colocalized PR10 genes, including VIT_05s0077g01690, were highly upregulated (up to 25 fold). Similar trend was observed for other PR genes as osmotin, thaumatin, and chitinases (Supplemental Table S2.3, S3.3 and S3.4). In addition, endochitinase and chitinase class I, which were upregulated during initial (flower) and quiescent (hard-green berry) infections, were found down regulated during *B. cinerea* egression.

The results also suggested that during *B. cinerea* egression the SA pathway was repressed, but the JA pathway was actively functioning. The expression of genes encoding PR1, an SA marker, and EDS1, a defense regulator involving SA signaling (Wiermer et al., 2005), were downregulated or not affected. On the other hand, genes encoding jasmonate ZIM-domain1, a JA marker, and MYC2, involved in the activation of JA signaling (Lorenzo et al., 2004), were upregulated (Supplemental Table S3.4).

Table 3.6. Selected differentially expressed grapevine genes during pre-egression and egression of *B. cinerea* on ripe berries (12 wpi).

<u>Fold change (log 2)</u>				<u>Fold change (log 2)</u>			
ID	Peg	Eg	Functional annotation	ID	Peg	Eg	Functional annotation
Transcription factors				Response to stress and secondary metabolism			
VIT_07s0141g00690	3.3	6.5	ERF/AP2 transcription factor sub B-1	VIT_08s0007g06040	4.6	6.7	Beta-1,3-glucanase
VIT_10s0003g00580	2.9	2.8	ERF/AP2 transcription factor sub B-3	VIT_18s0001g14790	-4.0	-4.4	Lipase 3 (EXL3) family II extracellular
VIT_02s0234g00130		-1.1	Ethylene responsive element binding factor 1	VIT_17s0000g10060	-1.5	-2.3	Lipase GDSL
VIT_07s0005g03340	2.8	2.9	Myb domain protein 14	VIT_01s0137g00700		1.5	Lipase GDSL
VIT_19s0027g00870	-1.3	-0.9	NAC domain-containing protein 42	VIT_14s0128g00080	4.5	5.6	Lipase GDSL
VIT_06s0004g07500	2.4	2.1	WRKY DNA-binding protein 33	VIT_16s0039g01320	4.98	5.07	Phenylalanin ammonia-lyase
Cell wall				VIT_08s0040g01710	2.34	1.53	Phenylalanine ammonia-lyase
VIT_09s0002g01320	-1.0	-1.2	Germin-like protein	VIT_00s2849g00010	5.84	4.39	Phenylalanine ammonia-lyase
VIT_14s0060g02750	-2.0	-3.3	Germin-like protein 3	VIT_02s0025g03660	-1.5	-0.9	4-coumarate-CoA ligase
VIT_14s0128g01020	-0.8	-1.5	Germin-like protein 3	VIT_16s0050g00390	3.1	4.2	4-coumarate-CoA ligase
VIT_06s0009g02570	0.9	2.9	Pectinesterase family	VIT_03s0063g01690	-1.2	-1.8	flavonoid 3-monooxygenase
VIT_02s0154g00600	1.1	3.1	Pectinesterase family	VIT_18s0001g14310	0.8	1.0	Flavonone- 3-hydroxylase
VIT_04s0044g01020	4.5	11.6	Pectinesterase family	VIT_04s0023g01290	-0.9	-1.5	Anthocyanidin 3-O-glucosyltransferase
VIT_07s0005g00720	4.7	8.5	Pectinesterase family	VIT_03s0017g02000	3.7	6.7	Anthocyanidin 3-O-glucosyltransferase
VIT_08s0007g07770	4.8	7.2	Polygalacturonase PG1	VIT_03s0038g01460	0.7	1.2	Chalcone synthase
VIT_08s0007g07760	5.0	8.3	Polygalacturonase PG1	VIT_02s0012g01570	-1.5	-0.7	Cinnamoyl-CoA reductase
VIT_11s0052g01180	0.7	3.2	Xyloglucan endotransglucosylase	VIT_14s0066g01150	0.5	4.6	Cinnamoyl-CoA reductase
VIT_05s0062g00240	1.1	2.1	Xyloglucan endotransglucosylase	VIT_00s0218g00010	-0.4	-1.2	Cinnamyl alcohol dehydrogenase
Response to stress and secondary metabolism				VIT_13s0067g00680	0.3	2.1	Cinnamyl alcohol dehydrogenase
VIT_04s0023g03550	1.9	4.2	Thaumatococin	VIT_06s0080g01000	-2.0	-1.6	Secoisolariciresinol dehydrogenase
VIT_07s0005g02560		-1.1	Chitinase Class I	VIT_08s0058g00790	1.0	1.8	Secoisolariciresinol dehydrogenase
VIT_05s0094g00360	-0.8	-1.5	Chitinase class IV	VIT_01s0010g01960	8.01	3.82	Anionic peroxidase
VIT_05s0094g00200		3.4	Chitinase class IV	VIT_12s0055g00810	-1.83	-1.50	Cationic peroxidase
VIT_03s0038g03400		-1.2	Endochitinase 1, basic	VIT_08s0058g00970	1.98	0.96	Cationic peroxidase
VIT_05s0077g01690		-1.1	Pathogenesis protein 10	VIT_16s0100g00830		1.1	Stilbene synthase
VIT_05s0077g01580		1.6	Pathogenesis protein 10	VIT_16s0100g01200	7.1	10.5	Stilbene synthase
VIT_03s0088g00700		-1.2	Pathogenesis related protein 1 precursor	VIT_16s0100g01190	-1.0	-2.0	Stilbene synthase
VIT_03s0088g00690	-3.4	-3.5	Pathogenesis-related protein 1 precursor	VIT_16s0100g01160	-0.8	-1.2	Stilbene synthase
VIT_05s0077g01150		1.5	Beta-1,3-glucanase	VIT_16s0100g01140	-0.8	-1.4	Stilbene synthase 2
				VIT_16s0100g00990	1.0	2.1	Stilbene synthase 2

The secondary metabolites biosynthesis pathway, polyphenols in specific, was also generally affected by the egression of *B. cinerea* at ripening (Table 3.6 and Supplemental Table S3.4), although the transcription of genes encoding dihydroflavonol-4-reductase and flavanone 3-hydroxylase, both involved in flavonoid biosynthesis, was not affected. In line with this evidence, almost all of the quantified flavonoids were significantly lower or not different in the berries with egressed *B. cinerea* as compared to the control (Table 3.7). Whereas, for other key enzymes in the biosynthesis pathway mixed regulation (both up- and down regulation of genes encoding a given transcript) was observed, as in cinnamate 4-hydroxylase, 4-coumarate-CoA ligase 1, and stilbene synthase genes. For stilbene synthase, for example, from the 23 differentially-regulated stilbene synthase genes, 16 of them were downregulated. Overall, the trend of stilbenoids content of the samples was: for monomeric stilbenes (like trans-resveratrol, trans-piceide, and astringin), no appreciated difference between berries with egressed *Botrytis* and control; and for oligomeric stilbenes (like viniferin, E-cis-miyabenol, and isohopeaphenol), the concentration was highest in berries with pre-egressed *Botrytis*, followed by berries with egressed *Botrytis* and the lowest in healthy berries, control (Table 3.7).

Most of the genes involved in monolignol biosynthesis (such as CCR and CAD) were differentially regulated (Table 3.6 and Supplemental Table S3.4), though not all in the same direction—the mixed regulation mentioned above. However, a few but important genes like CCoAMT and F5H encoding genes were not differentially regulated. CCoAMT is involved in ferulic esterification and lignification process in response to pathogen attack in grapevine (Busam et al., 1997). From the secondary metabolite analysis, caffeate and ferulate, substrate for CCoAMT were not detected in any samples at ripening (Table 3.7). Perhaps, lignification is not an option in plant defense during ripening. The downregulation of all the differentially expressed genes encoding GLP3, an important protein in the oxidative cross-linking to strengthen cell wall during pathogen threat (Bradley et al., 1992; Godfrey et al., 2007), adds to the suggestion that cell wall apposition was downplayed at ripening. Rather, a number genes encoding proteins which involve in ripening-associated cell wall extensibility and disassembly like xyloglucan endotransglucosylase and polygalacturonase and pectinesterases (Nunan et al., 2001; Deytieux-Belleau et al., 2008) were highly upregulated in ripe berries with pre-egressed and egressed *Botrytis*. Pectinesterases is actually suggested to be involved both in cell wall loosening and strengthening (Micheli, 2001); however it seemed here it was involved in cell wall loosening as

there were a lot of upregulated polygalacturonases which degrade polygalacturonans, made accessible by the pectinesterases.

Table 3.7. Concentration ($\mu\text{g/g}$ fresh weight) of polyphenolic secondary metabolites in mock (Ctrl) and berries with pre-egressed (peg) and egressed (eg) *B. cinerea* at ripe, 12 wpi.

Class	Compounds	LOD($\mu\text{g/g}$)	Ripe berry (12 wpi)		
			Ctrl	Peg	Eg
benzoic acids	p-hydroxybenzoic acid	0.005	0.61 \pm 0.27	0.33 \pm 0.04	1.2 \pm 0.36
	vanillic acid	0.0025	0.00 \pm 0.00 ^b	0.16 \pm 0.02 ^b	0.72 \pm 0.14 ^a
	gallic acid	0.025	0.43 \pm 0.01	0.18 \pm 0.03	0.44 \pm 0.16
	2,6-diOH-benzoic acid	0.0025	0.22 \pm 0.15	0.05 \pm 0.02	0.04 \pm 0.02
	methyl gallate	0.01	0.01 \pm 0.01	0.02 \pm 0.01	0.02 \pm 0.01
Phenylpropanoids	caftaric acid	0.0125	848.1 \pm 84.86 ^a	473.41 \pm 16.29 ^b	208.69 \pm 60.81 ^c
	fertaric acid	0.0025	16.63 \pm 2.35 ^a	15.47 \pm 0.62 ^a	6.14 \pm 2.87 ^b
	trans-coutaric acid	0.025	256.85 \pm 8.89 ^a	162.12 \pm 10.76 ^b	67.21 \pm 20.07 ^c
Dihydrochalcones	phlorizin	0.0025	1.82 \pm 0.11 ^a	1.6 \pm 0.08 ^a	0.7 \pm 0.16 ^b
	luteolin-7-O-Glc	0.0025	0.24 \pm 0.02	0.15 \pm 0.03	0.07 \pm 0.05
flavonoids	naringenin	0.0025	0.24 \pm 0.05 ^a	0.04 \pm 0.01 ^b	0.03 \pm 0.01 ^b
	catechin	0.025	18.89 \pm 6.61	6.29 \pm 2.00	34.43 \pm 19.75
	epicatechin	0.025	11.19 \pm 1.33	7.86 \pm 0.89	8.57 \pm 2.9
	epigallocatechin	1.25	14.35 \pm 0.96 ^a	6.14 \pm 0.61 ^b	2.64 \pm 0.63 ^c
	gallocatechin	0.25	51.21 \pm 5.8 ^a	6.6 \pm 0.83 ^b	3.89 \pm 2.14 ^b
	epigallocatechin gallate	0.25	1.68 \pm 0.04	1.3 \pm 0.25	2.28 \pm 1.35
	epicatechin gallate	0.025	1.33 \pm 0.14	1.54 \pm 0.28	12.12 \pm 9.35
	procyanidin B1	0.0125	81.82 \pm 7.33	36.1 \pm 8.23	44.26 \pm 35.02
	procyanidin B2 + B4	0.125	4.81 \pm 0.45	1.47 \pm 0.17	8.21 \pm 3.3
	procyanidin B3 (as B1)	0.0125	28.78 \pm 11	7.56 \pm 0.84	24.58 \pm 19.56
	quercetin	0.05	0.52 \pm 0.04 ^a	0.32 \pm 0.07 ^{ab}	0.17 \pm 0.04 ^b
	taxifolin	0.0025	98.19 \pm 12.81 ^a	40.59 \pm 0.79 ^b	19.54 \pm 12.49 ^b
	myricetin	1.25	8.66 \pm 1.89 ^a	4.3 \pm 0.94 ^{ab}	2.34 \pm 0.39 ^b
	quercetin-3-Rha	0.005	0.13 \pm 0.03	0.23 \pm 0.03	0.13 \pm 0.07
	quercetin-3-Glc+	0.0025	14.14 \pm 1.77	14.97 \pm 4.87	4.31 \pm 1.59
	quercetin-3-Gal				
	isorhamnetin-3-Glc	0.0025	2.22 \pm 0.26 ^b	10.65 \pm 2.46 ^a	2.79 \pm 0.95 ^b
	rutin	0.0025	2.06 \pm 0.31 ^a	1.28 \pm 0.14 ^{ab}	0.55 \pm 0.26 ^b
	isorhamnetin-3-rutinoside	0.005	0.27 \pm 0.01	0.48 \pm 0.13	0.14 \pm 0.03
	quercetin-3-glucuronide	0.0125	31.2 \pm 0.53 ^a	7.51 \pm 0.59 ^b	2.17 \pm 0.78 ^c
isorhamnetin	0.4	0.01 \pm 0.00	0.01 \pm 0.01	0.02 \pm 0	
syringetin	0.025	0.06 \pm 0.02	0.03 \pm 0.01	0.01 \pm 0	
myricitrin	0.5	1.13 \pm 0.18 ^a	1.03 \pm 0.25 ^a	0.31 \pm 0.13 ^b	
syringetin-3-Glc+	0.05	6.01 \pm 0.66 ^b	17.51 \pm 2.15 ^a	5.12 \pm 1.43 ^b	
syringetin-3-Gal					
stilbenoids	arbutin	0.005	4.96 \pm 1.48	5.93 \pm 1.52	3.74 \pm 2.05
	trans-resveratrol	0.005	40.5 \pm 9.34	36.94 \pm 10.34	47.56 \pm 23.86
	cis-resveratrol	0.0025	0.42 \pm 0.07 ^a	0.13 \pm 0.06 ^b	0.05 \pm 0.02 ^b
	piceatannol	0.0025	17.82 \pm 6.04	22.24 \pm 7.41	5.67 \pm 2.95
	trans-piceide	0.0125	24.01 \pm 2.01 ^b	50.77 \pm 3.69 ^a	21.58 \pm 9.08 ^b
	cis-piceide	0.0025	13.04 \pm 5.59 ^a	11.59 \pm 3.24 ^a	2.97 \pm 1.05 ^b

Table 3.7. Continued.

Class	Compounds	LOD($\mu\text{g/g}$)	Ripe berry (12 wpi)		
			Ctrl	Peg	Eg
stilbenoids	astringin	0.005	4.21 \pm 0.57 ^b	13.67 \pm 1.52 ^a	4.85 \pm 2.81 ^b
	isorhapontin	0.005	0.54 \pm 0.04 ^b	3.33 \pm 0.38 ^a	1.19 \pm 0.31 ^b
	trans- ϵ -viniferin	0.005	4.65 \pm 0.57 ^c	41.86 \pm 3.82 ^a	12.12 \pm 4 ^b
	cis+trans-o-viniferin	0.0125	1.12 \pm 0.33 ^c	22.43 \pm 0.01 ^a	3.28 \pm 0.27 ^b
	pallidol	0.005	61.04 \pm 13.54 ^b	215.63 \pm 5.87 ^a	68.96 \pm 6.62 ^b
	ampelopsin D+ quadangularin A	0.025	0.25 \pm 0.04 ^c	5.49 \pm 0.15 ^a	0.79 \pm 0.17 ^b
	E-cis-miyabenol	0.0125	0.04 \pm 0.03 ^c	18.58 \pm 0.57 ^a	2.55 \pm 0.46 ^b
	Z-miyabenol C	0.05	0.04 \pm 0.00 ^b	18.77 \pm 5.45 ^a	1.68 \pm 0.35 ^b
	isohopeaphenol	0.0125	0.15 \pm 0.14 ^c	132.30 \pm 25.67 ^a	35.84 \pm 12.15 ^b
	α -viniferin	0.0125	0.01 \pm 0.00 ^c	59.68 \pm 6.44 ^a	10.83 \pm 4.03 ^b
	ampelopsin H + vaticanol C-like isomer	0.01	0.45 \pm 0.35 ^c	49.83 \pm 4.78 ^a	10.73 \pm 2.86 ^b
	caffeic acid+catechin condensation	0.05	10.75 \pm 1.32 ^a	1.31 \pm 0.24 ^b	1.31 \pm 0.97 ^b

LOD, limit of detection; Ctrl, control; Peg, pre-egression; Eg, egression; values after \pm are standard error. Concentration amounts followed by a common letter are significantly not different between samples, according to Tukey's Honestly Significant Difference test ($P \leq 0.05$), using one way ANOVA

3.5. Discussion

Grapevine flowers were challenged by placing suspension of *B. cinerea* conidia, to induce infection. Following that, fungal genes encoding known virulence factors and proteins contribute to the infection program were highly upregulated, as described in Chapter 2. Consequently, the flowers reprogrammed their transcriptome which resulted in increased expression levels of genes involved in reduction-oxidation process, encoding different families of antimicrobial proteins, and those involved in activating polyphenolic metabolites biosynthesis pathway that brought about the production of phytoalexin and precursors for cell wall toughening. These defense reactions of the flowers were unbreakable, forcing *B. cinerea* into quiescence. To know more on the fate of the fungus, we further inspected the inoculated flower until ripening, with an in-depth look of their molecular communication at hard-green (4 wpi) and at ripe (12 wpi) stages.

In the very early stage of quiescence in the flowers, at 96 hpi, ribosomal genes were prevalent in the *in planta* expressed *B. cinerea* genes (78 of the 574 genes, Supplemental Table S2.9). A similar high proportion of ribosomal genes were also observed in the hard-green berry at 4 wpi, 48 out the 289 *in planta* expressed genes (Supplemental Table S3.6). Nevertheless, there was not

any known virulence-related gene in these 289 genes, which could suggest that pathogenesis was “suspended”. Yet, other biological activities help the fungus stay “alive” were being carried out since elongation factors, ATP synthesis, and ATP-dependent molecular functions related genes were transcriptionally active. Glyceraldehyde-3-phosphate dehydrogenase (*Bcin15g02120*) and malate dehydrogenase (*Bcin16g04800*), both are highly abundant inside mycelium (Fernández-Acero et al., 2006; 2007) and also involved in glycolysis and tricarboxylic acid cycle for energy metabolism, were expressed. Also among expressed were an ATP-dependent cell division cycle protein 48 (p97/valosin-containing protein, *Bcin08g03700*) gene, involved in cell cycle and transcriptional regulation (Wang et al., 2004), and a number of ATP-dependent membrane transporter genes. To the question where and how the quiescent *B. cinerea* manages to get energy sources, out of the 34 CAZyme genes expressed at the quiescent stage, 4 of them were glycosidases, which can act on cellulose and hemicellulose of plant cell wall. In addition, the upregulation of plant receptors that mediate signaling in response to *B. cinerea*, *PROTEIN KINASE 1* (Abuqamar et al., 2008), and *WAK 1*, which recognizes cell wall-derived oligogalacturonides, (Brutus et al., 2010), indirectly suggest that the quiescent *B. cinerea* was able to obtain energy sources from the plant to carry out its basal metabolic activity.

Notwithstanding the absence of detectable pathogenic progression of the quiescent *B. cinerea*, fruit transcripts that involved in plant defense at initial infection stage (at bloom) continued to be upregulated at 4 wpi. Such continued activation of defense pathways between appressoria formation and quiescent stages of infection was also reported in unripe green tomato infection by *Colletotrichum gloeosporioides* (Alkan et al., 2014). The expressions of *WRKY33* gene, whose expression correlates with the expression of *PR10* genes in response to defense in grapevine (Merz et al., 2015; Chapter 2), and genes of different families of PR proteins, including PR10, were highly induced in the hard-green berry due to the quiescently present *B. cinerea* (Supplemental Table S3.3). The grapevine *WRKY33* functional homologue *AtWRKY33* has been shown to involve in response to biotic and abiotic stresses (Zheng et al., 2006; Jiang and Deyholos, 2009; Li et al., 2011; Birkenbihl et al., 2012). Five genes, encoding a GDSL lipase, whose expression was not affected during flower infection, were strongly upregulated (up to 25-fold) during quiescent infection. There is no previous report associating the lipases encoded by these genes with defense against pathogen. However, they are annotated for catalyzing acyltransfer or hydrolase reactions with lipid and non-lipid substrates, i.e. they have broad

substrate and may interfere with the fungal activity. Other lipases having similar motif, for example, GDSL Lipase 1, targets fungal cell walls and possesses antimicrobial activity (Oh et al., 2005), was shown to be involved in defense against *Alternaria brassicicola* and *B. cinerea* in *Arabidopsis* in an ET dependent manner regulated by *WRKY33* (Oh et al., 2005; Kwon et al., 2009; Birkenbihl et al., 2012).

The upregulation of osmotin, thaumatin, β -1,3-glucanase, and chitinases of the hard-green berry compelled the quiescent *B. cinerea* to undergo a survival cell wall remodeling. The qPCR assay confirmed that *Bcin11g04800*, a gene encoding chitin deacetylase was highly upregulated during quiescent phase (Figure 3.5). Deacetylation of chitin is a mechanism used by plant pathogens as well as endophytic fungi to protect their cell wall from being attacked by plant chitinases (Deising and Siegrist, 1995; El Gueddari et al., 2002). Depolymerisation of chitin into deacetylated chitosan oligomer avoid binding by plant receptors and the consequential plant immune responses (Petutschnig et al., 2010; Liu et al., 2012). Very recently, Cord-Landwehr and colleagues demonstrated that chitosan oligomer, deacetylated chitin extracted from an endophytic fungus *Pestalotiopsis* sp., elicited no plant immunity in rice cell suspension culture (Cord-Landwehr et al., 2016). Thus, the enzyme might play an important role, particularly during quiescent phase, to reduce the recognition of the quiescent *B. cinerea* from the plant immunity. In addition to chitin deacetylase, other genes encoding glycolipid-anchored surface protein and GPI-anchored cell wall organization *Ecm33*, which in yeast are linked to cell wall integrity to ensure viability (Pardo et al., 2004), were also expressed during the quiescent phase, suggesting that the fungus is also actively defending itself besides the basal metabolic activity.

The activation of stilbenoid and flavonoid biosynthetic pathways by grapevine in response to active pathogenic infection is well documented (Langcake, 1981; Jeandet et al., 1995; Keller et al., 2003; Agudelo-Romero et al., 2015; Kelloniemi et al., 2015; Chapter 2). Here we observed that the genes encoding essential enzymes of the pathways, such as stilbene synthase, chalcone synthase, flavanone 3-hydroxylase, and anthocyanidin 3-O-glucosyltransferase, were actively engaged during quiescent infection. The transcription factor regulating stilbene biosynthesis, MYB14 (Höll et al., 2013) was also modulated. Polyphenols, as measured by HPLC-DAD-MS, too, were found at higher concentration in the inoculated samples. Nonetheless, compared to the infection initiation state at bloom (12-96 hpi), the concentration of the polyphenols was less at 4

wpi in the hard-green berry. The content of resveratrol and its monomeric (for example astringin, isorhapontin, and piceide) and oligmeric (for example miyabenol, isohopeaphenol, and viniferin) derivatives, which are known defense compounds (Langcake, 1981; Pezet, et al., 2003a; Favaron et al., 2007; Hammerbacher et al., 2011), was higher in hard-green berry with quiescent *Botrytis* than control.

Relevant transcripts for the synthesis of monolignols precursors (PAL, COMT, CCoAMT), which increase penetration resistance of the plant tissues (Bhuiyan et al., 2009), and other lignin forming enzymes like GLP3 and EXT, were also induced in the hard-green berry. The result from initial infection in the flower suggested that lignification at the site of penetration as one of the major defense mechanism grapevine flowers use to stop *B. cinerea* progress. The activation of monolignol biosynthetic pathway and the upregulation of GLP3 and EXT together with H₂O₂ accumulation that we observed at the site of penetration in the flower were similar mechanisms that véraison berry and green tomatoes employed to stop *B. cinerea* growth (Cantu et al., 2009; Kelloniemi et al., 2015). It is interesting to observe the pathway being active at 4 wpi in the hard-green berry.

The ability of the grape berries to keep the pathogen under quiescence is however broken at ripening (Figure 3.1C). Egression of *B. cinerea* was observed after bagging bunches for two weeks starting at full coloring (approximately 10 wpi), to create high humidity around the bunch. Creating similar high humidity around the bunch, before full coloring, was shown causing no *B. cinerea* egression (Supplemental Figure S2.6). At the very start of the egression process, an outgrowth of *B. cinerea* (or egression) was observed on about 40 % of the berries. Basically, at ripe stage, a single berry with active *B. cinerea* growth could be enough to cause rot on the whole bunch; it will be just a matter of time as the tissue is senescing and therefore its susceptibility to pathogen increases (Kretschmer et al., 2007; Prusky et al., 2013). Since it gets confusing with time to identify berries with “truly” egressed *B. cinerea* or progression thereof around the egression spot, samples were immediately collected to avoid disease progression into asymptomatic spots. As per the state of the fungus in berries that showed no visible symptom/sign (pre-egressed *B. cinerea*), the “initiation” of virulence-related genes, like ceratoplatanin *BcSPL1*, required for full virulence (Frías et al., 2011, 2014), that were not expressed in the hard-green berry signaled that the state of the pre-egressed *B. cinerea* in ripe berries was different from that of the quiescent one in the hard-green berry.

During egression about 86 % of the *B. cinerea* transcriptome was expressed, and compared to PDB cultured *B. cinerea* 3,548 of the genes were differentially expressed during egression at ripening. These genes encompasses functional annotations of ROS producers and scavengers, CWDE, proteases, and phytotoxic secondary metabolites, which are all what *B. cinerea* requires for full pathogenicity (as reviewed in Nakajima and Akutsu, 2014). *Botrytis* transcripts belonging to these functional classes were shown to involve during successful infection of ripe grapevine berries and other hosts (De Cremer et al., 2013; Smith et al., 2014; Kelloniemi et al., 2015). However, the expression level of *BcPG6* and *BcPEL-like1*, pectinases which were extremely upregulated during initial infection at bloom (Figure 2.9), was much less both at ripe and in PDB culture. *BcPG6* was shown acting as endo-hydrolases, releasing monomers and dimers of D-galacturonate instead of oligomers unlike other PGs (Kars et al., 2005). In general, as expected, the transcriptional activity of the pathogen was high during egression. Indeed, what made the quiescent *B. cinerea* egress is the trickiest research question of this study. But ripening associated signals are speculated triggering the transition from the prolonged quiescent to egression phase.

The changes in physical and chemical properties occurring at ripening, such as activation of phytohormone biosynthesis, cuticular changes, cell wall loosening, conversion of acids into sugars, and a steadily diminishing of antifungal compounds (both preformed and inducible secondary metabolites) are hypothesized to favor pathogen egression (Prusky, 1996; Prusky et al., 2013). It has been shown that the protective role of berry cuticle on *B. cinerea* infection decreased with ripening (Commenil et al., 1997; Mlikota-Gabler et al., 2003). The structural changes in the cell wall polysaccharides that lead to fruit softening were also reported to cause susceptibility to necrotrophic pathogens at fruit ripening (Cantu et al., 2008). In their study, suppression of the ripening-associated cell wall loosening genes reduced the susceptibility of ripe tomato to *B. cinerea* (Cantu et al., 2008). A shift in plant-hormone synthesis and signaling balance happening during ripening can also trigger fungal pathogenicity factors (Prusky, 1996; Prusky et al., 2013). In grapevine, alongside the decline in resistance during ripening, the sugars and organic acids exudates appearing on the berry surface can stimulate and promote *B. cinerea* outgrowth (Padgett and Morrison, 1990; Pezet et al., 2003b; Kretschmer et al., 2007).

Considering the transcriptional alterations underwent in the ripe berry, as a response to *Botrytis* egression, a wide array of defense responses were noticed, suggesting that the tissue under

colonization “never gives up” rearranging its defense mechanisms. The expression level of genes of PR proteins, secondary metabolites, cell wall modification, and phytohormones (biosynthesis and signaling) were affected. Even though hormonal cross-talks in response to pathogen attack are complex (Ferrari et al., 2003, 2007; Rowe et al., 2010), we observed egression of *Botrytis* activated ET and JA pathways while SA pathway was repressed. Similar interplay between JA and SA in grapevine-*Botrytis* interaction was reported by Kelloniemi et al. (2015): JA pathway being activated during compatible berry-*Botrytis* interaction at ripe and SA pathway during incompatible interaction at véraison. With regard to stilbenic secondary metabolites, surprisingly oligomerization was majorly driven by the presence of the fungus. Oligomerization, according to Pezet et al. (2003a), increases toxicity. The amount of oligomeric resveratrol was very little in control than treated berries (with pre-egressed and egressed *Botrytis*); from the treated berries, lesser being in berries with egressed *Botrytis* than pre-egressed one. The *B. cinerea* LACCASE 2 (encoded by *Bcin14g02510*) that oxidizes resveratrol (Schouten et al., 2002) was extremely upregulated (128 fold) in the egressed *Botrytis*. This could probably be one of the reasons that the concentration of oligomeric resveratrols was significantly lower in berries having immense *Botrytis* growth than pre-egressed one.

Last, the evolution of the berry skin tissue is an important component of the berry-*Botrytis* interaction. It has been noticed that the extent of the expression of cell wall modifying genes increased toward maturity. It is actually a phenological cue that once the seeds are mature, ripening-associated softening kicks off. The differential accumulation of xyloglucan endotransglucosylases, involve in cell wall extensibility (Miedes et al., 2011) and polygalacturonases and pectinases, involved in berry softening (Deytieux-Belleau et al., 2008), are phenomenal during berry ripening (Nunan et al., 2001; Lijavetzky et al., 2012). These cell wall modifying genes were remarkably upregulated in ripe berries with both pre-egressed and egressed *B. cinerea*, suggesting that the fungus used advantage of the onset of the fruit’s cell wall self-disassembly, exploiting endogenous developmental programs to activate its own virulence CWDE. In tomato, the ripening associated genes polygalacturonase and expansin have been shown to facilitate susceptibility to *B. cinerea* (Cantu et al., 2008, 2009). It has also been suggested that the fungus can induce unripe fruit’s cell wall-modifying proteins to initiate the induction of susceptibility (Cantu et al., 2009). We, however, haven’t observed any hastening of

ripening process in *Botrytis*-inoculated samples. Both mock- and *Botrytis*-inoculated bunches ripen on similar time after inoculation.

On the other side of cell wall modification, the downregulation of genes encoding GLP3, involved in cell wall strengthening by oxidative cross-linking of cell wall components (Bradley et al., 1992; Godfrey et al., 2007), together with the non-differential regulation of monolignol genes as CCoAMT and F5H, involved in cell wall apposition in response to pathogen attack (Busam et al., 1997; Bhuiyan et al., 2009), strongly suggest that cell wall fortification was not involved.

Taken together cell wall strengthening process is the most missed component from the defense responses at ripening.

3.6. Conclusions

The *B. cinerea* inoculated at bloom was quiescent for 12 weeks and egressed at ripening, suggesting that the defense responses of the berries were efficient to halt the growth of the fungus only until maturity. Our study revealed that the defense responses of immature berries (at 4 wpi) that put *B. cinerea* quiescent involved different classes of PR proteins and increased activities of the flavonoid, stilbenoid, and monolignol biosynthesis pathways, for phytoalexins and cell wall strengthening. These responses are similar to the responses of the plant to the pathogen at bloom. In this period, the fungus had cryptic interaction with the berry keeping its basal metabolic activities and deacetylating its cell wall. However, at ripe (at 12 wpi) the pathogen managed to egress and cause bunch rot, using the advantage of the fruit's cell wall self-disassembly and fulfilment of other conditions (including humidity). Consequently, there were different defense responses except cell wall strengthening by the ripe berries, but futile and did not keep the pathogen from its advancement to colonize the berries. The study seems to indicate that, in grapevine-*Botrytis* interaction, cell wall associated defense is principal in keeping *B. cinerea* quiescent.

3.7. References

- Abuqamar S, Chai M-F, Luo H, Song F, Mengiste T** (2008) Tomato protein kinase 1b mediates signaling of plant responses to necrotrophic fungi and insect herbivory. *Plant Cell* **20**: 1964–83
- Agudelo-Romero P, Erban a., Rego C, Carbonell-Bejerano P, Nascimento T, Sousa L, Martinez-Zapater JM, Kopka J, Fortes a. M** (2015) Transcriptome and metabolome reprogramming in *Vitis vinifera* cv. Trincadeira berries upon infection with *Botrytis cinerea*. *J Exp Bot.* doi: 10.1093/jxb/eru517
- Alkan N, Friedlander G, Ment D, Prusky D, Fluhr R** (2014) Simultaneous transcriptome analysis of *Colletotrichum gloeosporioides* and tomato fruit pathosystem reveals novel fungal pathogenicity and fruit defense strategies. **205**: 801–815
- Amselem J, Cuomo C a., van Kan J a L, Viaud M, Benito EP, Couloux A, Coutinho PM, de Vries RP, Dyer PS, Fillinger S, et al** (2011) Genomic analysis of the necrotrophic fungal pathogens *Sclerotinia sclerotiorum* and *Botrytis cinerea*. *PLoS Genet.* doi: 10.1371/journal.pgen.1002230
- Asiimwe T, Krause K, Schlunk I, Kothe E** (2012) Modulation of ethanol stress tolerance by aldehyde dehydrogenase in the mycorrhizal fungus *Tricholoma vaccinum*. *Mycorrhiza* **22**: 471–484
- Barnes SE, Shaw MW** (2002) Factors affecting symptom production by latent *Botrytis cinerea* in *Primula* × *polyantha*. 746–754
- Bézier A, Lambert B, Baillieux F** (2002) Study of defense-related gene expression in grapevine leaves and berries infected with *Botrytis cinerea*. *Eur J Plant Pathol* **108**: 111–120
- Bhuiyan NH, Selvaraj G, Wei Y, King J** (2009) Gene expression profiling and silencing reveal that monolignol biosynthesis plays a critical role in penetration defence in wheat against powdery mildew invasion. *J Exp Bot* **60**: 509–521
- Birkenbihl RP, Diezel C, Somssich IE** (2012) Arabidopsis WRKY33 is a key transcriptional regulator of hormonal and metabolic responses toward *Botrytis cinerea* infection. *Plant Physiol* **159**: 266–285
- Blanco-Ulate B, Morales-Cruz A, Amrine KCH, Labavitch JM, Powell ALT, Cantu D** (2014) Genome-wide transcriptional profiling of *Botrytis cinerea* genes targeting plant cell walls during infections of different hosts. *Front Plant Sci* **5**: 1–16
- Bradley DJ, Kjellbom P, Lamb CJ** (1992) Elicitor-Induced and Wound-Induced Oxidative Cross-Linking of a Proline-Rich Plant-Cell Wall Protein - a Novel, Rapid Defense Response. *Cell* **70**: 21–30
- Brutus A, Sicilia F, Macone A, Cervone F, De Lorenzo G, Lorenzo G De** (2010) A domain swap approach reveals a role of the plant wall-associated kinase 1 (WAK1) as a receptor of oligogalacturonides. *Proc Natl Acad Sci U S A* **107**: 9452–7
- Busam G, Junghanns KT, Kneusel RE, Kassemeyer HH, Matern U** (1997) Characterization and expression of caffeoyl-coenzyme A 3-O-methyltransferase proposed for the induced resistance response of *Vitis vinifera* L. *Plant Physiol* **115**: 1039–48
- Cantu D, Blanco-Ulate B, Yang L, Labavitch JM, Bennett AB, Powell ALT** (2009) Ripening-regulated susceptibility of tomato fruit to *Botrytis cinerea* requires NOR but not RIN or ethylene. *Plant Physiol* **150**: 1434–1449
- Cantu D, Vicente AR, Greve LC, Dewey FM, Bennett AB, Labavitch JM, Powell ALT** (2008) The intersection between cell wall disassembly, ripening, and fruit susceptibility to *Botrytis cinerea*. *Proc Natl Acad Sci U S A* **105**: 859–864

- Coertze S, Holz G** (2002) Epidemiology of *Botrytis cinerea* on Grape: Wound Infection by Dry , Airborne Conidia. *S Afr J Enol Vitic* **23**: 72–77
- Commenil P, Brunet L, Audran J** (1997) The development of the grape berry cuticle in relation to susceptibility to bunch rot disease. *J Exp Bot* **48**: 1599–1607
- Conesa A, Götz S, García-Gómez JM, Terol J, Talón M, Robles M** (2005) Blast2GO: a universal tool for annotation, visualization and analysis in functional genomics research. *Bioinformatics* **21**: 3674–6
- Conn S, Curtin C, Bézier A, Franco C, Zhang W** (2008) Purification, molecular cloning, and characterization of glutathione S-transferases (GSTs) from pigmented *Vitis vinifera* L. cell suspension cultures as putative anthocyanin transport proteins. *J Exp Bot* **59**: 3621–3634
- Cord-Landwehr S, Melcher RLJ, Kolkenbrock S, Moerschbacher BM** (2016) A chitin deacetylase from the endophytic fungus *Pestalotiopsis* sp. efficiently inactivates the elicitor activity of chitin oligomers in rice cells. *Sci Rep* 1–11
- Dalmais B, Schumacher J, Moraga J, Le Pecheur P, Tudzynski B, Collado IG, Viaud M** (2011) The *Botrytis cinerea* phytotoxin botcinic acid requires two polyketide synthases for production and has a redundant role in virulence with botrydial. *Mol Plant Pathol* **12**: 564–579
- De Cremer K, Mathys J, Vos C, Froenicke L, Michelmore RW, Cammue BP a, De Coninck B** (2013) RNAseq-based transcriptome analysis of *Lactuca sativa* infected by the fungal necrotroph *Botrytis cinerea*. *Plant Cell Environ* **36**: 1992–2007
- Deising H, Siegrist J** (1995) Chitin deacetylase activity of the rust. *FEMS Microbiol Lett* **127**: 207-212
- Deytieux-Belleau C, Geny L, Roudet J, Mayet V, Donèche B, Fermaud M** (2009) Grape berry skin features related to ontogenic resistance to *Botrytis cinerea*. *Eur J Plant Pathol* **125**: 551–563
- Deytieux-Belleau C, Vallet A, Donèche B, Geny L** (2008) Pectin methylesterase and polygalacturonase in the developing grape skin. *Plant Physiol Biochem* **46**: 638–646
- Du Z, Zhou X, Ling Y, Zhang Z, Su Z** (2010) agriGO: a GO analysis toolkit for the agricultural community. *Nucleic Acids Res* **38**: 64-70
- Eichorn KW, Lorenz DH** (977) Phänologische entwicklungsstadien der rebe. *Nachrichtenbl. Deut Pflanzenschutz* **29**: 119-120
- Elmer PAG, Michailides TM** (2004) Epidemiology of *Botrytis cinerea* in orchard and vine crops. In: Elad Y, Williamson B, Tudzynski P, Delan N, eds. *Botrytis: Biology, Pathology and Control*. Dordrecht, The Netherlands: Kluwer Academic, 243–72
- Espino JJ, Gutiérrez-Sánchez G, Brito N, Shah P, Orlando R, González C** (2010) The *Botrytis cinerea* early secretome. *Proteomics* **10**: 3020–3034
- Favaron F, Lucchetta M, Odorizzi S, Cunha ATP, Sella L** (2007) The role of grape polyphenols on trans-resveratrol activity against *Botrytis cinerea* and of fungal laccase on the solubility of putative grape pr proteins. **91**: 579–588
- Fernández-Acero FJ, Jorge I, Calvo E, Vallejo I, Carbú M, Camafeita E, Garrido C, López JA, Jorrin J, Cantoral JM** (2007) Proteomic analysis of phytopathogenic fungus *Botrytis cinerea* as a potential tool for identifying pathogenicity factors, therapeutic targets and for basic research. *Arch Microbiol* **187**: 207–215
- Fernández-Acero FJ, Jorge I, Calvo E, Vallejo I, Carbú M, Camafeita E, López JA, Cantoral JM, Jorrin J** (2006) Two-dimensional electrophoresis protein profile of the phytopathogenic fungus *Botrytis*

cinerea. Proteomics **6 Suppl 1**: S88-96

Ferrari S, Galletti R, Denoux C, De Lorenzo G, Ausubel FM, Dewdney J (2007) Resistance to *Botrytis cinerea* induced in Arabidopsis by elicitors is independent of salicylic acid, ethylene, or jasmonate signaling but requires PHYTOALEXIN DEFICIENT3. *Plant Physiol* **144**: 367–79

Ferrari S, Plotnikova JM, De Lorenzo G, Ausubel FM (2003) Arabidopsis local resistance to *Botrytis cinerea* involves salicylic acid and camalexin and requires EDS4 and PAD2, but not SID2, EDS5 or PAD4. *Plant J* **35**: 193–205

Frías M, Brito N, González M, González C (2014) The phytotoxic activity of the cerato-platanin BcSpl1 resides in a two-peptide motif on the protein surface. *Mol Plant Pathol* **15**: 342–351

Frías M, González C, Brito N (2011) BcSpl1, a cerato-platanin family protein, contributes to *Botrytis cinerea* virulence and elicits the hypersensitive response in the host. *New Phytol* **192**: 483–495

Gao Q-M, Venugopal S, Navarre D, Kachroo A (2011) Low oleic acid-derived repression of jasmonic acid-inducible defense responses requires the WRKY50 and WRKY51 proteins. *Plant Physiol* **155**: 464–476

Garrett-Engle P, Moilanen B, Cyert MS (1995) Calcineurin, the Ca²⁺/calmodulin-dependent protein phosphatase, is essential in yeast mutants with cell integrity defects and in mutants that lack a functional vacuolar H⁽⁺⁾-ATPase. *Mol Cell Biol* **15**: 4103–14

Giacomelli L, Nanni V, Lenzi L, Zhuang J, Serra MD, Banfield MJ, Town CD, Silverstein K a. T, Baraldi E, Moser C (2012) Identification and Characterization of the Defensin-Like Gene Family of Grapevine. *Mol Plant Microbe Interact* **25**: 1118–1131

Godfrey D, Able AJ, Dry IB (2007) Induction of a grapevine germin-like protein (VvGLP3) gene is closely linked to the site of *Erysiphe necator* infection: a possible role in defense? *Mol Plant Microbe Interact* **20**: 1112–1125

Goetz G, Fkyerat A, Métais N, Kunz M, Tabacchi R, Pezet R, Pont V (1999) Resistance factors to grey mould in grape berries: Identification of some phenolics inhibitors of *Botrytis cinerea* stilbene oxidase. *Phytochemistry* **52**: 759–767

Grimplet J, Van Hemert J, Carbonell-Bejerano P, Díaz-Riquelme J, Dickerson J, Fennell A, Pezzotti M, Martínez-Zapater JM (2012) Comparative analysis of grapevine whole-genome gene predictions, functional annotation, categorization and integration of the predicted gene sequences. *BMC Res Notes* **5**: 213

El Gueddari NE, Rauchhaus U, Moerschbacher BM, Deising HB (2002) Developmentally regulated conversion of surface-exposed chitin to chi-tosan in cell walls of plant pathogenic fungi. *New Phytol* **156**: 103–112

Gutterson N, Reuber TL (2004) Regulation of disease resistance pathways by AP2/ERF transcription factors. *Curr Opin Plant Biol* **7**: 465–471

Hammerbacher A, Ralph SG, Bohlmann J, Fenning TM, Gershenzon J, Schmidt A (2011) Biosynthesis of the major tetrahydroxystilbenes in Spruce, astringin and isorhapontin, proceeds via resveratrol and is enhanced by fungal infection. *Plant Physiol* **157**: 876–890

ten Have A, Espino JJ, Dekkers E, Van Sluyter SC, Brito N, Kay J, González C, van Kan J a L (2010) The *Botrytis cinerea* aspartic proteinase family. *Fungal Genet Biol* **47**: 53–65

Hellemans J, Mortier G, De Paep A, Speleman F, Vandesompele J (2007) qBase relative quantification framework and software for management and automated analysis of real-time quantitative

PCR data. *Genome Biol* **8**: R19

Höll J, Vannozzi A, Czempl S, D'Onofrio C, Walker AR, Rausch T, Lucchin M, Boss PK, Dry IB, Bogs J (2013) The R2R3-MYB transcription factors MYB14 and MYB15 regulate stilbene biosynthesis in *Vitis vinifera*. *Plant Cell* **25**: 4135–49

Jeandet P, Bessis R, Sbaghi M, Meunier P (1995) Production of the Phytoalexin Resveratrol by Grapes as a Response to *Botrytis* Attack Under Natural Conditions. *J Phytopathol* **143**: 135–139

Jersch S, Scherer C, Huth G, Schlösser E (1989) Proanthocyanidins as basis for quiescence of *Botrytis cinerea* in immature strawberry fruits *Z. Pflanzenkrankh Pflanzenschutz* **96**: 365–378

Jiang Y, Deyholos MK (2009) Functional characterization of Arabidopsis NaCl-inducible WRKY25 and WRKY33 transcription factors in abiotic stresses. *Plant Mol Biol* **69**: 91–105

Kars I, Krooshof GH, Wagemakers L, Joosten R, Benen J a E, Van Kan J a L (2005) Necrotizing activity of five *Botrytis cinerea* endopolygalacturonases produced in *Pichia pastoris*. *Plant J* **43**: 213–225

Keller M, Viret O, Cole FM (2003) *Botrytis cinerea* Infection in Grape Flowers : Defense Reaction , Latency , and Disease Expression. **93**: 316–322

Kelloniemi J, Trouvelot S, Héloir MC, Simon A, Dalmais B, Frettinger P, Cimerman A, Fermaud M, Roudet J, Baulande S (2015) Analysis of the molecular dialogue between gray mold (*Botrytis cinerea*) and grapevine (*Vitis vinifera*) reveals a clear shift in defense mechanisms during berry ripening. *Mol Plant-Microbe Interact* **X**: 1–14

Kretschmer M, Kassemeyer H-H, Hahn M (2007) Age-dependent grey mould susceptibility and tissue-specific defence gene activation of grapevine berry skins after infection by *Botrytis cinerea*. *J Phytopathol* **155**: 258–263

Kwon SJ, Jin HC, Lee S, Nam MH, Chung JH, Kwon S Il, Ryu CM, Park OK (2009) GDSL lipase-like 1 regulates systemic resistance associated with ethylene signaling in Arabidopsis. *Plant J* **58**: 235–245

Langcake P (1981) Disease resistance of *Vitis* spp. and the production of the stress metabolites resveratrol, ϵ -viniferin, α -viniferin and pterostilbene. *Physiol Plant Pathol* **18**: 213–226

Law CW, Chen Y, Shi W, Smyth GK (2014) voom: Precision weights unlock linear model analysis tools for RNA-seq read counts. *Genome Biol* **15**: R29

Li S, Fu Q, Chen L, Huang W, Yu D (2011) *Arabidopsis thaliana* WRKY25, WRKY26, and WRKY33 coordinate induction of plant thermotolerance. *Planta* **233**: 1237–1252

Liao Y, Smyth GK, Shi W (2013) The Subread aligner: Fast, accurate and scalable read mapping by seed-and-vote. *Nucleic Acids Res.* doi: 10.1093/nar/gkt214

Liao Y, Smyth GK, Shi W (2014) FeatureCounts: An efficient general purpose program for assigning sequence reads to genomic features. *Bioinformatics* **30**: 923–930

Licausi F, Ohme-Takagi M, Perata P (2013) APETALA2/Ethylene Responsive Factor (AP2/ERF) transcription factors: Mediators of stress responses and developmental programs. *New Phytol* 639–649

Lijavetzky D, Carbonell-Bejerano P, Grimplet J, Bravo G, Flores P, Fenoll J, Hellín P, Oliveros JC, Martínez-Zapater JM (2012) Berry flesh and skin ripening features in *Vitis vinifera* as assessed by transcriptional profiling. *PLoS One.* doi: 10.1371/journal.pone.0039547

Liu T, Liu Z, Song C, Hu Y, Han Z, She J, Fan F, Wang J, Jin C, Chang J, et al (2012) Chitin-induced dimerization activates a plant immune receptor. *Science* (80-) **336**: 1160–1164

- Lorenzo O, Chico JM, Sa´nchez-Serrano JJ, Solano R** (2004) JASMONATE-INSENSITIVE1 encodes a MYC transcription factor essential to discriminate between different jasmonate-regulated defense responses in *Arabidopsis*. *Plant Cell Online* **16**: 1938–1950
- Martin M** (2011) Cutadapt removes adapter sequences from high-throughput sequencing reads. *EMBnetjournal* **17**: 10–12
- McClellan WD, Hewitt WB** (1973) Early *Botrytis* rot of grapes: Time of infection and latency of *Botrytis cinerea* Pers. in L. *Phytopathology* **63**: 1151–1157
- McNicol RJ, Williamson B** (1989) Systemic infection of black currant flowers by *Botrytis cinerea* and its possible involvement in premature abscission of fruits. *Ann Appl Biol* **114**: 243–254
- Mehli L, Kjellsen TD, Dewey FM, Hietala AM** (2005) A case study from the interaction of strawberry and *Botrytis cinerea* highlights the benefits of comonitoring both partners at genomic and mRNA level. *New Phytol* **168**: 465–474
- Merz PR, Moser T, Höll J, Kortekamp A, Buchholz G, Zyprian E, Bogs J** (2015) The transcription factor VvWRKY33 is involved in the regulation of grapevine (*Vitis vinifera*) defense against the oomycete pathogen *Plasmopara viticola*. *Physiol Plant* 365–380
- Micheli F** (2001) Pectin methylesterases: Cell wall enzymes with important roles in plant physiology. *Trends Plant Sci* **6**: 414–419
- Miedes E, Zarra I, Hoson T, Herbers K, Sonnewald U, Lorences EP** (2011) Xyloglucan endotransglucosylase and cell wall extensibility. *J Plant Physiol* **168**: 196–203
- Mlikota-Gabler F, Smilanick JL, Mansour M, Ramming DW, Mackey BE** (2003) Correlations of Morphological, Anatomical, and Chemical Features of Grape Berries with Resistance to *Botrytis cinerea*. *Phytopathology* **93**: 1263–73
- Monteiro S, Barakat M, Piçarra-Pereira M a, Teixeira AR, Ferreira RB** (2003) Osmotin and thaumatin from grape: a putative general defense mechanism against pathogenic fungi. *Phytopathology* **93**: 1505–1512
- Moretto M, Sonogo P, Dierckxsens N, Brilli M, Bianco L, Ledezma-Tejeida D, Gama-Castro S, Galardini M, Romualdi C, Laukens K, et al** (2016) COLOMBOS v3.0: Leveraging gene expression compendia for cross-species analyses. *Nucleic Acids Res* **44**: D620–D623
- Nair N, Guilbaud-Oulton S, Barchia I, Emmet R, G N, Nair N, Guilbaud-Oulton S, Barchia I, Emmet R** (1995) Significance of carry over inoculum , flower infection and latency on the incidence of *Botrytis cinerea* in berries of grapevines at harvest in New South Wales. *Aust J Exp Agric* **35**: 1177–1180
- Nakajima M, Akutsu K** (2014) Virulence factors of *Botrytis cinerea*. *J Gen Plant Pathol* **80**: 15–23
- Nunan KJ, Davies C, Robinson SP, Fincher GB** (2001) Expression patterns of cell wall-modifying enzymes during grape berry development. *Planta* **214**: 257–264
- Oh IS, Park AR, Bae MS, Kwon SJ, Kim YS, Lee JE, Kang NY, Lee S, Cheong H, Park OK** (2005) Secretome analysis reveals an Arabidopsis lipase involved in defense against *Alternaria brassicicola*. *Plant Cell* **17**: 2832–2847
- Padgett M, Morrison JC** (1990) Changes in Grape Berry Exudates during Fruit Development and Their Effect on Mycelial Growth of *Botrytis cinerea*. **115**: 269–273
- Pardo M, Monteoliva L, Vázquez P, Martínez R, Molero G, Nombela C, Gil C** (2004) PST1 and ECM33 encode two yeast cell surface GPI proteins important for cell wall integrity. *Microbiology* **150**:

4157–4170

Paré A, Kim M, Juarez MT, Brody S, McGinnis W (2012) The functions of Grainy head-like proteins in animals and fungi and the evolution of apical extracellular barriers. *PLoS One*. doi: 10.1371

Pernas M, López-Solanilla E, Sánchez-Monge R, Salcedo G, Rodríguez-Palenzuela P (1999) Antifungal activity of a plant cystatin. *Mol Plant-Microbe Interact* **12**: 624–627

Petutschnig EK, Jones AME, Serazetdinova L, Lipka U, Lipka V (2010) The Lysin Motif Receptor-like Kinase (LysM-RLK) CERK1 is a major chitin-binding protein in *Arabidopsis thaliana* and subject to chitin-induced phosphorylation. *J Biol Chem* **285**: 28902–28911

Pezet R, Perret C, Jean-Denis JB, Tabacchi R, Gindro K, Viret O (2003a) δ -viniferin, a resveratrol dehydrodimer: One of the major stilbenes synthesized by stressed grapevine leaves. *J Agric Food Chem* **51**: 5488–5492

Pezet R, Viret O, Perret C, Tabacchi R (2003b) Latency of *Botrytis cinerea* Pers. : Fr. and Biochemical studies during growth and ripening of two grape berry cultivars, respectively susceptible and resistant to grey mould. *Phytopathology* **214**: 208–214

Prusky D (1996) Pathogen quiescence in postharvest diseases. *Annu Rev Phytopathol* **34**: 413–434

Prusky D, Lichter A (2007) Activation of quiescent infections by postharvest pathogens during transition from the biotrophic to the necrotrophic stage. *FEMS Microbiol Lett* **268**: 1–8

Prusky D, Alkan N, Mengiste T, Fluhr R (2013) Quiescent and necrotrophic lifestyle choice during postharvest disease development. *Annu Rev Phytopathol* **51**: 155–76

Ramírez-Suero M, Bénard-Gellon M, Chong J, Laloue H, Stempien E, Abou-Mansour E, Fontaine F, Larignon P, Mazet-Kieffer F, Farine S, et al (2014) Extracellular compounds produced by fungi associated with *Botryosphaeria* dieback induce differential defence gene expression patterns and necrosis in *Vitis vinifera* cv. Chardonnay cells. *Protoplasma* **251**: 1417–1426

Rieu I, Powers SJ (2009) Real-Time Quantitative RT-PCR: Design, Calculations, and Statistics. *Plant Cell Online* **21**: 1031–1033

Rolke Y, Liu S, Quidde T, Williamson B, Schouten A, Weltring K-M, Siewers V, Tenberge KB, Tudzynski B, Tudzynski P (2004) Functional analysis of H₂O₂-generating systems in *Botrytis cinerea*: the major Cu-Zn-superoxide dismutase (BCSOD1) contributes to virulence on French bean, whereas a glucose oxidase (BCGOD1) is dispensable. *Mol Plant Pathol* **5**: 17–27

Rowe HC, Walley JW, Corwin J, Chan EK, Dehesh K, Kliebenstein DJ (2010) Deficiencies in jasmonate-mediated plant defense reveal quantitative variation in *Botrytis cinerea* pathogenesis. *PLoS Pathog* **6**: e1000861

Ruijter JM, Ramakers C, Hoogaars WMH, Karlen Y, Bakker O, van den hof MJB, Moorman AFM (2009) Amplification efficiency: Linking baseline and bias in the analysis of quantitative PCR data. *Nucleic Acids Res*. doi: 10.1093/nar/gkp045

Saga H, Ogawa T, Kai K, Suzuki H, Ogata Y, Sakurai N, Shibata D, Ohta D (2012) Identification and Characterization of ANAC042, a Transcription Factor Family Gene Involved in the Regulation of Camalexin Biosynthesis in *Arabidopsis*. *Mol Plant-Microbe Interact* **25**: 684–696

Schouten A, Wagemakers L, Stefanato FL, van der Kaaij RM, van Kan J a L (2002) Resveratrol acts as a natural profungicide and induces self-intoxication by a specific laccase. *Mol Microbiol* **43**: 883–94

- Schumacher J, Simon A, Cohrs KC, Traeger S, Porquier A, Dalmais B, Viaud M, Tudzynski B** (2015) The VELVET Complex in the Gray Mold Fungus *Botrytis cinerea*: Impact of BcLAE1 on Differentiation, Secondary Metabolism, and Virulence. *Mol Plant Microbe Interact* **28**: 659–74
- Shaw MW, Emmanuel CJ, Emilda D, Terhem RB, Shafia A, Tsamaidi D, Emblow M, van Kan JAL** (2016) Analysis of Cryptic, Systemic Botrytis Infections in Symptomless Hosts. *Front Plant Sci* **7**: 625
- Siewers V, Viaud M, Jimenez-Teja D, Collado IG, Gronover CS, Pradier J-M, Tudzynski B, Tudzynski P** (2005) Functional Analysis of the Cytochrome P450 Monooxygenase Gene *bcbot1* of *Botrytis cinerea* Indicates That Botrydial Is a Strain-Specific Virulence Factor. *Mol Plant-Microbe Interact* **18**: 602–612
- Smith JE, Mengesha B, Tang H, Mengiste T, Bluhm BH** (2014) Resistance to *Botrytis cinerea* in *Solanum lycopersicoides* involves widespread transcriptional reprogramming. *PLoS One* **9**: 1–18
- Smyth GK** (2004) Linear Models and Empirical Bayes Methods for Assessing Differential Expression in Microarray Experiments. *Stat Appl Genet Mol Biol* **3**: 1–26
- Supek F, Bošnjak M, Škunca N, Šmuc T** (2011) Revigo summarizes and visualizes long lists of gene ontology terms. *PLoS One*. doi: 10.1371/journal.pone.0021800
- Thimm O, Bläsing O, Gibon Y, Nagel A, Meyer S, Krüger P, Selbig J, Müller LA, Rhee SY, Stitt M** (2004) MAPMAN: A user-driven tool to display genomics data sets onto diagrams of metabolic pathways and other biological processes. *Plant J* **37**: 914–939
- Vandesompele J, De Preter K, Pattyn F, Poppe B, Van Roy N, De Paepe A, Speleman F** (2002) Accurate normalization of real-time quantitative RT-PCR data by geometric averaging of multiple internal control genes. *Genome Biol* **3**: RESEARCH0034
- van Kan JAL, Stassen JHM, Mosbach A, Van Der Lee TAJ, Faino L, Farmer AD, Papanastasiou DG, Zhou S, Seidl MF, Cottam E, et al** (2016) A gapless genome sequence of the fungus *Botrytis cinerea*. *Mol Plant Pathol* **17**: 75–89
- Wang D, Amornsiripanitch N, Dong X** (2006) A genomic approach to identify regulatory nodes in the transcriptional network of systemic acquired resistance in plants. *PLoS Pathog* **2**: 1042–1050
- Wang Q, Song C, Li CCH** (2004) Molecular perspectives on p97-VCP: Progress in understanding its structure and diverse biological functions. *J Struct Biol* **146**: 44–57
- Wiermer M, Feys BJ, Parker JE** (2005) Plant immunity: The EDS1 regulatory node. *Curr Opin Plant Biol* **8**: 383–389
- Williamson BYB, Mecnicol RJ, Dolan A, Crop S, Do D** (1987) The effect of inoculating flowers and developing fruits with *Botrytis cinerea* on post-harvest grey mould of red raspberry. 285–294
- Zhang L, van Kan J a L** (2013) *Botrytis cinerea* mutants deficient in d-galacturonic acid catabolism have a perturbed virulence on *Nicotiana benthamiana* and *Arabidopsis*, but not on tomato. *Mol Plant Pathol* **14**: 19–29
- Zheng Z, Qamar SA, Chen Z, Mengiste T** (2006) Arabidopsis WRKY33 transcription factor is required for resistance to necrotrophic fungal pathogens. *Plant J* **48**: 592–605

3.8. Supplemental materials

3.8.1. Supplemental tables

Supplemental Table S3.1. List of qPCR primers. Gene identification, primer name, primer sequence, and source are listed.

	Gene ID	Primer name	Primer sequence	Reference
<i>Botrytis cinerea</i>	Bcin01g09620 (<i>BcRPL5</i>)	Bcrp15-F	GATGAGACCGTCAAATGGTTC	Zhang and vanKan, 2013
		Bcrp15-R	CAGAAGCCCACGTTACGACA	
	Bcin01g08040 (<i>BcTUBA</i>)	BctubA-F	TTTGAGCCAGGTACCATGG	Mehli <i>et al.</i> 2005
		BctubA-R	GTCGGGACGGAAGAGTTGAC	
	Bcin01g09570	Bcyt521-F	GTTGGAAGTGTCTGGAGGTGT	This study
		Bcyt521-R	GCCTTTTCATCAGCTGCTTT	
	Bcin02g06140	BcCP2-F	CGGATTCCCATCATTC AATC	This study
		BcCP2-R	AGGAGGTCCCATTC C C A T A C	
	Bcin03g01920	BcCAT-F	CAATGGTCCACTCCTTCTTCA	This study
		BcCAT-R	AACACGCTCTGGGATACGTT	
	Bcin07g01540	BcEF2-F	CTTTGGGTGACGTCCAAGTT	This study
		BcEF2-R	CACCGAATTTCTTGGCGTAT	
	Bcin08g05540	BcCND1-F	GCTACCGATGGTCTTGAAA	This study
		BcCND1-R	ATCAGTGGTGACGATGTGGA	
Bcin11g04800	BcCDA-F	CTTCCCTGTTGTTCCCTCAA	This study	
	BcCDA-R	TGTCTCATCCGGACTCACA		
Bcin12g06170	Bcalle-F	CGAAGTCCTTCCAGAGCAAC	This study	
	Bcalle-R	TGGGTCTCTCCGACAGTTCT		
Bcin13g05810	BcALD-F	ACGGAAAGGCAATCTCAATG	This study	
	BcALD-R	CTTATCTGCCATCCACCAT		
Bcin14g04260	BcMAS1-F	CGATGGAACTCCTCGTGATT	This study	
	BcMAS1-R	GATCATCTTGGCAGCACTGA		
<i>Vitis vinifera</i>	VIT_04s0044g00580 (<i>VvACT</i>)	VvACT-F	ATGTGCCTGCCATGTATGTTGCC	Bèzier <i>et al.</i> 2002
		VvACT-R	AGCTGCTCTTTGCAGTTCCAGC	
	VIT_06s0004g00480 (<i>VvTUB</i>)	VvTUB-F	TGTTGGTGAAGGCATGGAGG	Giacomelli <i>et al.</i> 2012
		VvTUB-R	AGATGACACGCCTGCTGAACT	
	VIT_01s0010g02020	VvPER-F	AGGGCAAGCAAGATGTGTGA	This study
		VvPER-R	TCCAGGGGTGCAAGATTGTC	
	VIT_01s0146g00480	VvJAZ10-F	TCCGAAGAATAATCCGCCGT	This study
		VvJAZ10-R	CAGGACTGTAAACCGGCAAC	
	VIT_02s0025g01670	Vv02-F	ACAAGGAAGCAAAAGGAGCA	This study
		Vv02-R	CCTCAGCAAGTTCAACCACA	
	VIT_03s0038g03130	VvFMO3-F	CTCCAAACACCCAAACCATT	This study
		VvFMO3-R	TGAACTTGATGTGCCTGAGC	
	VIT_04s0023g03230	VvSAUR9-F	TGGGAAGAAACCTGGCTATG	This study
		VvSAUR9-R	GGTGAGCCAACCATGAGATT	
	VIT_05s0094g00360	VvCHIT4c-F	TCGAATGCGATGGTGGAAA	Ramírez-Suero <i>et al.</i> 2014
		VvCHIT4c-R	TCCCCTGTGAAACACCAAG	
VIT_07s0005g03340	VvMYB14-F	TCTGAGGCCGGATATCAAAC	Höll <i>et al.</i> 2013	
	VvMYB14-R	GGGACGCATCAAGAGAGTGT		
VIT_08s0058g00690	VvWRKY33-F	ATTCAAGCACTAGTATGAACAGAGCAG	Merz <i>et al.</i> 2015	
	VvWRKY33-R	CCTTGTTGCCCTGGCATGA		

Supplemental Table S3.1.Continued.

Vitis vinifera	Gene ID	Primer name	Primer sequence	Reference
	VIT_08s0058g00790	VvSIRD-F	TGAAGACACACTCGGAGCTG	This study
		VvSIRD-R	AGGATATCGAGGCGTCCGTA	
	VIT_11s0052g01110	Vv4CL-F	TTCCCGACATCAACATCCCG	This study
		Vv4CL-R	TTACGTGCGGTGAGATGGAC	
	VIT_12s0059g01250	VvbGlu-F	GCGTTTCTCCTGACCGTCTA	This study
		VvbGlu-R	GCTCTTCATGGCCAACTGAC	
	VIT_13s0074g00390	VvCYP-F	ATCGAAAAGGGCCAGTCTTT	This study
		VvCYP-R	GCATGTTTTGCACCATGTTC	
	VIT_14s0066g01150	VvCCR-F	AGCAGAAACAGGGATGCCAT	This study
		VvCCR-R	AGAGAGCCTCCCATCTGACA	
	VIT_14s0171g00180	VvLRR-F	GCACTGGAAATTTGGGAGAA	This study
		VvLRR-R	GCAAATCCGCTGAAATCACT	
	VIT_17s0000g09770	VvCP-F	GGTTTTGGTTGTTGGGATTG	This study
		VvCP-R	TAAAGCGCTTGTGCTTCTCA	
	VIT_18s0001g14790	VvEXL3-F	GGCGGAAGAATAGTTGTTG	This study
VvEXL3-R		GATCCTCGGCACACTCTCTT		
VIT_19s0014g01780	VvBZIP-F	TTCTGGGTGGACGAGTTTC	This study	
	VvBZIP-R	ATGCCTAGCTTCCTCAACCA		
VIT_19s0093g00320	VvGST1-F	CAAAGAGCAAAGCCAAGT	Conn <i>et al.</i> 2008	
	VvGST1-R	TGTCCAGAAAACCCAAAGTC		

Supplemental Table S3.2. Summary of reads mapping of the 18 RNA-seq libraries Ctrl, mock inoculated; Trt, *B. cinerea* inoculated; Bc, *Botrytis cinerea*; HG, hard-green berry; Peg, pre-egression; Eg, egression; 1-3 indicate the three biological replicates.

Library	Total quality-trimmed reads	Reads mapped to <i>V. vinifera</i> reference	Reads uniquely mapped to <i>V. vinifera</i> reference	Reads mapped to <i>B. cinerea</i> reference	Reads uniquely mapped to <i>B. cinerea</i> reference
HG_Ctrl1	18,764,162	17,226,186 (91.80 %)	16,552,848 (88.22 %)	46,268 (0.25 %)	520 (0.01 %)
HG_Ctrl2	18,245,810	13,462,443 (73.78 %)	10,041,596 (55.04 %)	1,675,246 (9.18 %)	1,786 (0.00 %)
HG_Ctrl3	20,330,170	17,125,573 (84.24 %)	16,376,294 (80.55 %)	68,337 (0.34 %)	545 (0.00 %)
HG_Tr1	23,828,415	21,594,466 (90.62 %)	20,837,836 (87.45 %)	45,065 (0.19 %)	6,958 (0.03 %)
HG_Tr2	21,976,001	19,853,734 (90.34 %)	19,120,028 (87.00 %)	56,664 (0.26 %)	16,928 (0.08 %)
HG_Tr3	21,146,332	18,828,955 (89.04 %)	18,070,467 (85.45 %)	75,234 (0.35 %)	24,680 (0.12 %)
Ripe_Ctrl1	24,635,902	22,048,745 (89.50 %)	21,007,364 (85.27 %)	37,989 (0.15 %)	818 (0.00 %)
Ripe_Ctrl2	26,843,805	24,151,620 (89.97 %)	23,069,555 (85.94 %)	27,883 (0.10 %)	836 (0.00 %)
Ripe_Ctrl3	29,860,937	26,527,044 (88.84 %)	25,136,297 (84.18 %)	169,478 (0.57 %)	885 (0.00 %)
Ripe_Eg1	21,296,699	3,254,793 (15.28 %)	2,756,774 (12.94 %)	16,664,468 (78.25 %)	14,235,574 (66.84 %)
Ripe_Eg2	22,578,478	5,287,093 (23.42 %)	4,550,569 (20.15 %)	14,815,131 (65.62 %)	12,490,580 (55.32 %)
Ripe_Eg3	28,787,397	12,703,484 (44.13 %)	11,577,654 (40.22 %)	12,750,536 (44.29 %)	10,718,882 (37.23 %)
Ripe_Peg1	45,369,750	32,808,151 (72.31 %)	27,381,446 (60.35 %)	2,547,394 (5.61 %)	22,842 (0.05 %)
Ripe_Peg2	55,880,939	45,269,916 (81.01 %)	42,976,225 (76.91 %)	2,315,554 (4.14 %)	1,698,079 (3.04 %)
Ripe_Peg3	47,239,407	40,062,424 (84.81 %)	38,243,440 (80.96 %)	118,269 (0.25 %)	23,815 (0.05 %)
Bc1	22,223,388	76,740 (0.35 %)	21,423 (0.01 %)	20,072,229 (90.32 %)	14,108,503 (63.48 %)
Bc2	21,289,297	47,738 (0.22 %)	28,559 (0.13 %)	19,256,732 (90.45 %)	16,603,159 (77.99 %)
Bc3	22,254,222	50,719 (0.23 %)	17,798 (0.08 %)	20,086,452 (90.25 %)	16,522,732 (74.24 %)

Supplemental Table S3.8. List of genes used to validate the RNA-Seq expression values by q-PCR assay. Gene identification, gene description, and fold change from RNA-seq and qPCR are provided. HG, har- green berry; Trt, B. Cinerea inoculated; Ctrl, mocj inoculated; Peg, pre-egression; Eg, egression.

Gene ID	RNAseq (log2 fold change)				qPCR (log2 fold chnage)			
	HG (Trt vs Ctrl)	Ripe (Peg vs ctrl)	Ripe (Eg vs Ctrl)	Ripe (Eg vs peg)	HG (Trt vs Ctrl)	Ripe (Peg vs ctrl)	Ripe (Eg vs Ctrl)	Ripe (Eg vs peg)
VIT_01s0010g02020	0.03	7.60	10.83	3.23	0.06	8.36	10.49	2.14
VIT_01s0146g00480	0.80	4.84	7.36	2.52	1.38	4.05	5.91	1.86
VIT_02s0025g01670	0.56	-2.26	-3.51	-1.25	0.12	-2.16	-2.77	-0.61
VIT_03s0038g03130	-3.29	0.04	0.02	-0.02	-2.35	-0.71	-0.40	0.31
VIT_04s0023g03230	-0.03	-3.05	-4.92	-1.87	0.16	-2.68	-3.70	-1.02
VIT_05s0094g00360	1.84	3.38	5.12	1.75	1.41	2.98	4.27	1.29
VIT_07s0005g03340	2.22	2.37	4.52	2.16	1.12	1.94	3.48	1.53
VIT_08s0058g00690	1.61	2.17	3.69	1.52	1.23	1.42	2.69	1.27
VIT_08s0058g00790	3.23	2.78	2.55	-0.23	1.52	2.18	2.23	0.04
VIT_11s0052g01110	2.69	5.02	6.12	1.10	1.42	4.15	4.73	0.58
VIT_12s0059g01250	-0.10	-3.70	-2.68	1.02	-0.09	-2.62	-1.47	1.15
VIT_13s0074g00390	-0.44	-5.48	-4.76	0.72	-0.29	-6.58	-5.86	0.72
VIT_14s0066g01150	1.05	2.85	5.02	2.17	0.60	2.28	3.76	1.48
VIT_14s0171g00180	-0.45	-2.75	-3.05	-0.30	-0.44	-2.40	-3.13	-0.74
VIT_17s0000g09770	-2.00	3.83	3.04	-0.79	-1.56	1.78	1.55	-0.23
VIT_18s0001g14790	0.30	-6.42	-6.29	0.14	0.27	-4.32	-5.53	-1.21
VIT_19s0014g01780	-1.25	-2.44	-3.18	-0.74	-0.70	-2.20	-2.46	-0.26
VIT_19s0093g00320	0.03	3.82	9.04	5.21	0.07	4.02	7.79	3.78

Supplemental Table S3.10. Gene ontology terms enriched in the differentially expressed grapevine genes upon quiescent B. cinerea infection on hard-green berry, 4 wpi. Enriched GO terms are presented. BP, biological process; MF, molecular function; CC, cellular component; wpi, week post inoculation.

GO term	Ontology	Description	Number in input list	Number in reference list	p-value	FDR
GO:0006950	BP	response to stress	68	1715	2.50E-05	4.10E-04
GO:0009856	BP	pollination	28	203	6.00E-14	3.20E-12
GO:0006464	BP	protein modification process	97	2097	1.00E-09	2.70E-08
GO:0000003	BP	reproduction	32	439	2.00E-08	4.80E-07
GO:0019748	BP	secondary metabolic process	28	374	8.10E-08	1.70E-06
GO:0006350	BP	transcription	74	1857	1.10E-05	1.90E-04
GO:0009056	BP	catabolic process	44	1084	0.00031	4.20E-03
GO:0030246	MF	carbohydrate binding	39	403	1.50E-13	1.00E-11
GO:0004871	MF	signal transducer activity	77	1475	2.40E-10	4.00E-09
GO:0016301	MF	kinase activity	100	2132	3.00E-10	4.00E-09
GO:0016740	MF	transferase activity	170	4541	2.00E-08	1.90E-07
GO:0003700	MF	transcription factor activity	35	551	1.40E-07	1.10E-06
GO:0030528	MF	transcription regulator activity	39	858	7.10E-05	5.30E-04
GO:0005576	CC	extracellular region	45	887	1.50E-06	1.40E-04

Supplemental Table S3.11. Concentration of polyphenolic secondary metabolites in hard-green berry, mock inoculated (Ctrl) or with quiescent *B. cinerea* (Trt) at 4 wpi. The amount is given in µg/g fresh weight. p-value < 0.05, using unpaired heteroscedastic Student's t test, is highlighted. LOD, limit of detection; wpi, week post inoculation; SE, standard error.

Classe	Secondary metabolites	LOD(µg/g)	Ctrl		Trt		p-value
			Mean	SE	Mean	SE	
benzoic acids	<i>p</i> -hydroxybenzoic acid	0.005	1.00	0.06	1.15	0.18	3.96E-01
	vanillic acid	0.0025	0.01	0.00	0.01	0.00	2.64E-01
	gallic acid	0.025	0.11	0.02	0.16	0.06	4.03E-01
phenylpropanoids	fraxin	0.0025	0.01	0.00	0.00	0.00	3.42E-01
	caftaric acid	0.0125	595.38	38.89	660.14	93.16	5.08E-01
	caffeic acid	0.02	0.15	0.02	0.12	0.02	4.52E-01
	fertaric acid	0.0025	7.85	0.73	18.44	4.15	2.50E-02
dihydrochalcones	<i>trans</i> -coutaric acid	0.025	260.24	16.25	272.70	31.48	7.19E-01
flavonoids	phlorizin	0.0025	1.40	0.25	1.40	0.12	9.95E-01
	luteolin	0.0025	0.01	0.00	0.04	0.02	1.30E-01
	luteolin-7-O-Glc	0.0025	0.22	0.01	0.40	0.08	3.30E-02
	naringenin	0.0025	0.01	0.00	0.08	0.01	1.00E-03
	catechin	0.025	17.75	1.23	26.06	3.88	5.90E-02
	epicatechin	0.025	4.40	0.44	9.33	1.19	3.00E-02
	epigallocatechin	1.25	2.18	0.52	1.64	0.39	4.44E-01
	gallocatechin	0.25	55.54	10.82	47.12	4.59	5.06E-01
	epigallocatechin gallate	0.25	0.23	0.05	0.47	0.17	2.79E-01
	epicatechin gallate	0.025	0.10	0.02	1.67	0.29	1.30E-02
	procyanidin B1	0.0125	67.98	4.47	136.63	28.81	1.00E-01
	procyanidin B2 + B4	0.125	2.52	0.49	3.74	0.64	1.79E-01
	procyanidin B3 (as B1)	0.0125	25.27	1.28	47.21	9.14	9.80E-02
	taxifolin	0.0025	6.54	0.95	13.40	3.46	1.52E-01
	myricetin	1.25	1.22	0.03	1.30	0.16	6.79E-01
	Quercetin-3-Rha	0.005	0.04	0.01	0.06	0.02	3.06E-01
	kaempferol-3-Glc	0.0025	0.02	0.01	0.08	0.03	1.62E-01
	quercetin-3-Glc+quercetin-3-Gal	0.0025	4.17	0.28	6.82	1.26	1.32E-01
	isorhamnetin-3-Glc	0.0025	0.09	0.01	0.14	0.02	7.10E-02
	kaempferol-3-rutinoside	0.005	0.03	0.00	0.07	0.02	1.89E-01
Quercetin-3-Glc-Ara	0.005	0.02	0.00	0.05	0.01	9.90E-02	
rutin	0.0025	1.50	0.22	2.40	0.47	1.56E-01	
isorhamnetin-3-rutinoside	0.005	n.d.		0.02	0.01		
Quercetin-3-glucuronide	0.0125	27.21	2.83	36.84	7.30	3.06E-01	
Kaempferol-3-glucuronide	0.005	0.13	0.03	0.24	0.04	7.50E-02	
stilbenoids	arbutin	0.005	0.13	0.01	0.90	0.19	2.70E-02
	<i>trans</i> -resveratrol	0.005	n.d.		1.52	0.47	
	<i>cis</i> -resveratrol	0.0025	n.d.		0.01	0.00	
	piceatannol	0.0025	0.01	0.00	0.19	0.08	1.18E-01
	<i>trans</i> -piceide	0.0125	0.97	0.09	10.08	1.83	1.60E-02
	<i>cis</i> -piceide	0.0025	0.34	0.05	1.70	0.40	4.20E-02
	astringin	0.005	0.14	0.03	1.55	0.26	1.20E-02
	isorhapontin	0.005	n.d.		0.21	0.06	
	<i>trans</i> - ϵ -viniferin	0.005	n.d.		9.86	2.16	
	<i>cis</i> + <i>trans</i> - o -viniferin	0.0125	n.d.		0.30	0.07	
	caffeic acid+catechin condensation	0.05	2.01	0.28	4.76	1.22	1.17E-01
	pallidol	0.005	n.d.		0.60	0.19	
	ampelopsin D+quadrangularin A	0.025	n.d.		2.78	0.81	
	α -viniferin	0.0125	n.d.		1.86	0.66	
E- <i>cis</i> -miyabenol	0.0125	n.d.		0.91	0.34		
Z-miyabenol C	0.05	n.d.		0.40	0.12		
isohopeaphenol	0.0125	n.d.		0.16	0.05		

Supplemental Table S3.14. Gene ontology terms enriched in the differentially expressed grapevine genes in ripe berry with pre-egressed and egressed *B. cinerea* at 12 wpi. Enriched GO terms are presented. BP, biological process; MF, molecular function; CC, cellular component; wpi, week post inoculation.

Stage	GO term	Ontology	Description	Number in input list	Number in reference list	p-value	FDR
Pre-egression	GO:0019748	BP	secondary metabolic process	102	374	3.80E-14	1.40E-11
	GO:0050896	BP	response to stimulus	341	2206	9.00E-05	5.50E-03
	GO:0006810	BP	transport	350	2301	0.00023	8.30E-03
	GO:0043412	BP	macromolecule modification	363	2098	1.70E-09	2.10E-07
	GO:0006464	BP	protein modification process	363	2097	1.60E-09	2.10E-07
	GO:0004871	MF	signal transducer activity	295	1475	6.20E-15	2.40E-13
	GO:0016740	MF	transferase activity	721	4541	2.10E-09	4.00E-08
	GO:0030246	MF	carbohydrate binding	81	403	1.70E-05	2.70E-04
	GO:0005215	MF	transporter activity	215	1292	2.30E-05	3.30E-04
	GO:0003824	MF	catalytic activity	1652	11955	0.00058	7.30E-03
	GO:0005886	CC	plasma membrane	323	1654	1.00E-14	1.80E-12
GO:0016020	CC	membrane	823	5038	1.80E-12	1.60E-10	
Egression	GO:0019748	BP	secondary metabolic process	135	374	4.30E-16	1.60E-13
	GO:0050896	BP	response to stimulus	486	2206	8.60E-06	1.40E-03
	GO:0006950	BP	response to stress	385	1715	1.20E-05	1.40E-03
	GO:0006810	BP	transport	492	2301	0.00013	6.20E-03
	GO:0009056	BP	catabolic process	253	1084	2.10E-05	1.90E-03
	GO:0005975	BP	carbohydrate metabolic process	241	1063	0.0002	8.20E-03
	GO:0003700	MF	transcription factor activity	128	548	0.00092	2.80E-02
	GO:0005886	CC	plasma membrane	421	1654	1.20E-12	2.40E-10
	GO:0016020	CC	membrane	1096	5038	5.00E-09	4.80E-07
	GO:0005737	CC	cytoplasm	961	4644	4.70E-05	3.00E-03
	GO:0005623	CC	cell	2320	11670	9.20E-05	4.40E-03
GO:0044464	CC	cell part	2300	11600	0.00015	5.80E-03	

Supplemental Table S3.3. Differentially expressed *V. vinifera* genes due to quiescent *B. cinerea* presence on hard-green berry. (Provided as excel file)

Supplemental Table S3.4. Differentially expressed *V. vinifera* genes due to pre-egressed and egressed *B. cinerea* during ripening. (Provided as excel file)

Supplemental Table S3.5. Differentially expressed *Botrytis cinerea* genes during egression on ripe berry as compared to PDB grown *B. cinerea*. (Provided as excel file)

Supplemental Table S3.6. *Botrytis cinerea* genes expressed in planta, in hard-green berry during quiescent infection. (Provided as excel file)

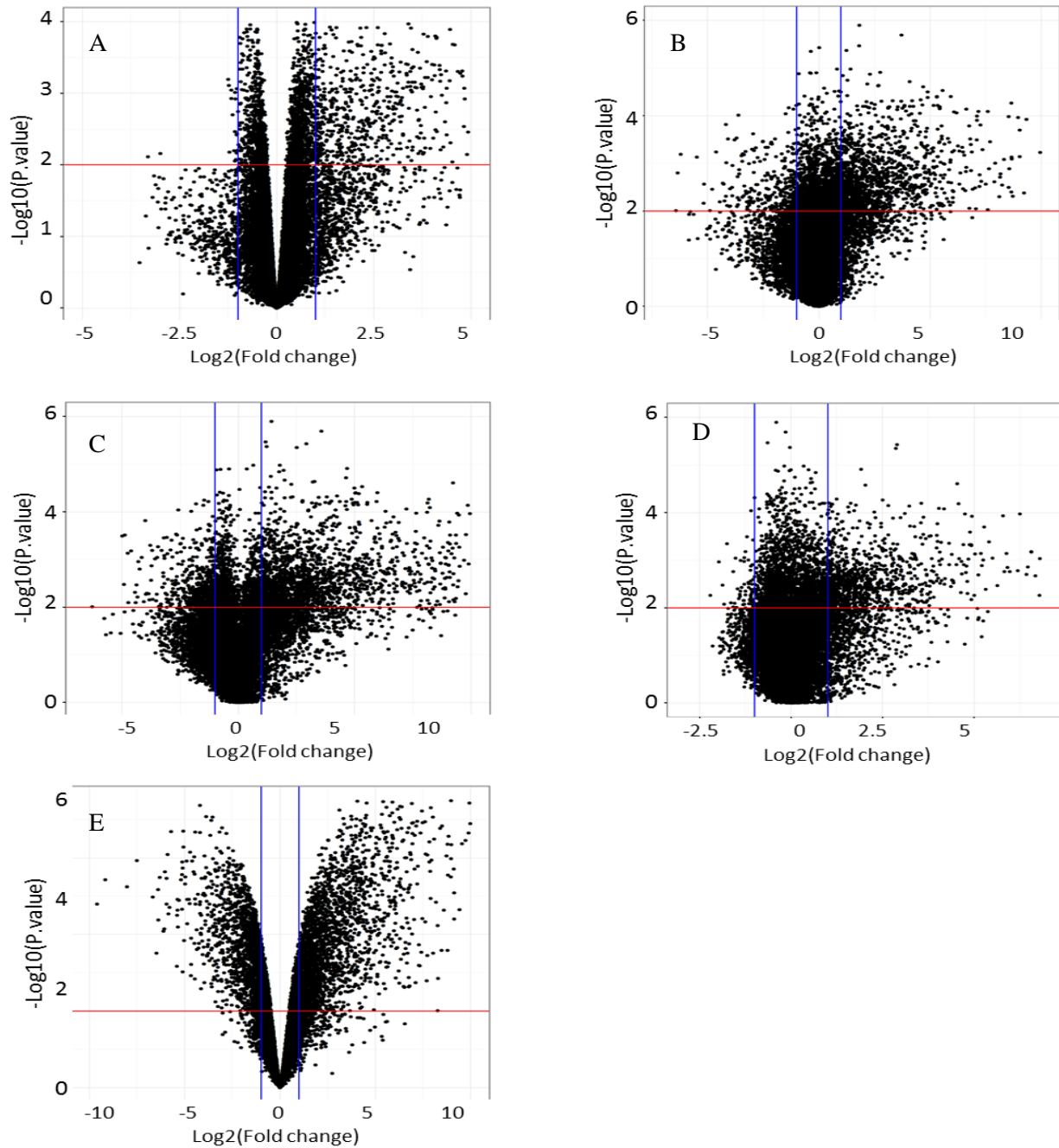
Supplemental Table S3.7. *Botrytis cinerea* genes expressed in planta, in ripe berry (pre-egressed). (Provided as excel file)

Supplemental Table S3.9. Gene ontology (GO) annotation of quiescent *B. cinerea* genes expressed in planta in hard-green berry stage. (Provided as excel file)

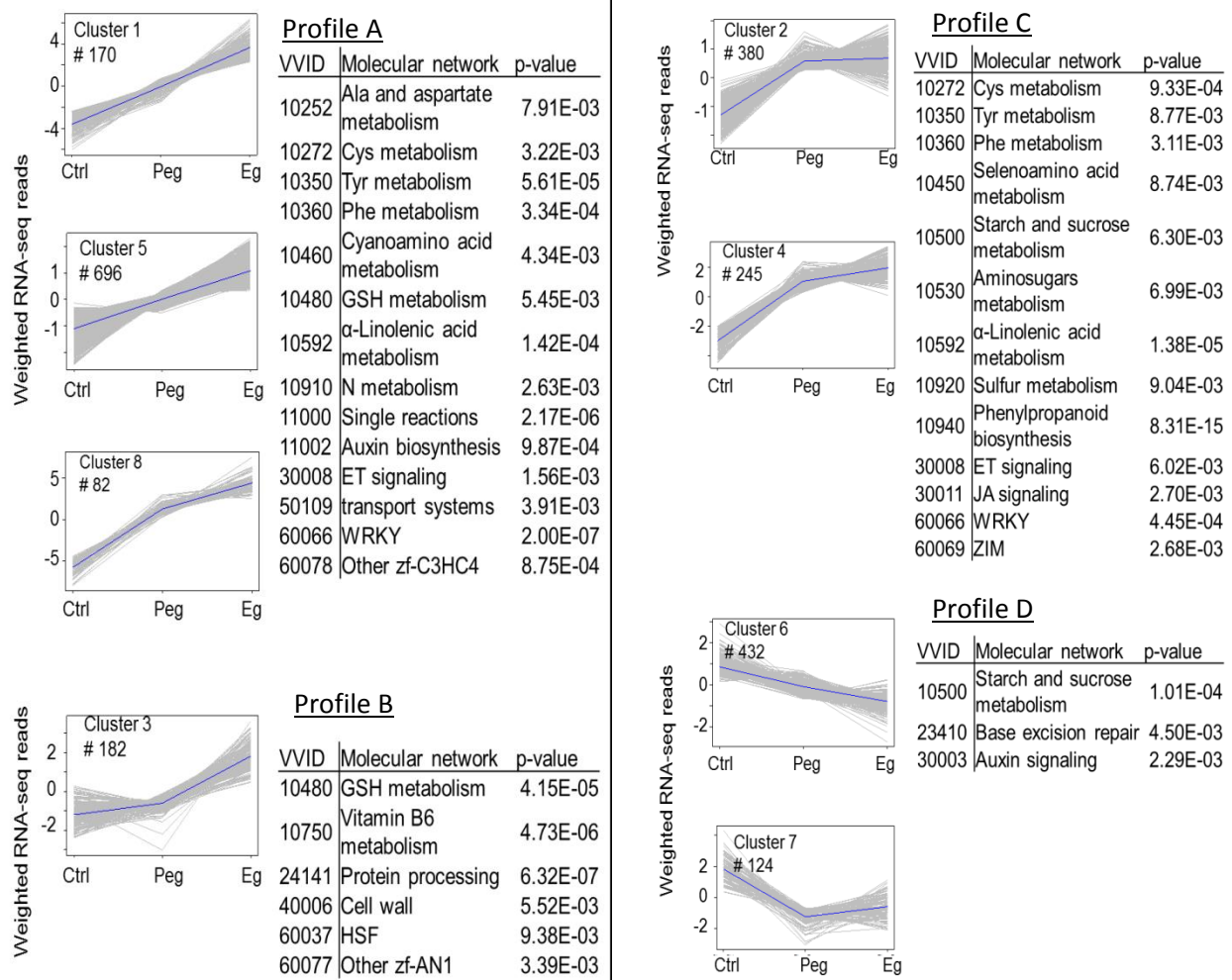
Supplemental Table S3.12. Gene ontology (GO) annotation of in-planta-expressed genes of pre-egressed *B. cinerea* in ripe berry. (Provided as excel file)

Supplemental Table S3.13. Gene ontology (GO) annotation of genes of egressed *B. cinerea* in ripe berry. (Provided as excel file)

3.8.2. Supplemental figures



Supplemental Figure S3.1. Volcano plots of grapevine and *B. cinerea* gene expression values. A, har-green berry, Trt vs Ctrl; B, Ripe berry, pre-egressed vs Ctrl; C, Ripe berry, egressed vs Ctrl; D, Ripe berry, egressed vs pre-egressed; and E, *B. cinerea*, egressed vs PDB cultures. Genes in the left top rectangle [$\log_{10}(P. \text{value}) > 2$ and $\log_2(\text{fold change}) < -1$] were selected as downregulated; whereas, genes in the right top rectangle were selected as upregulated [$\log_{10}(P. \text{value}) > 2$ and $\log_2(\text{fold change}) > 1$].



Supplemental Figure S3.2. Profiles of grapevine berry transcripts at ripe stage in response to pre-egressed and egressed *B. cinerea* inoculation. K-means clustering of grapevine genes based on the Euclidean distance of the weighted RNA-seq reads. Genes that showed at least twofold expression difference with p-value < 0.01 were considered, and clustered into 8 clusters. The clusters fall into 4 major profiles (A, B, C, and D). Molecular enrichment analysis based on VitisNet was provided for each group.

4. CONCLUDING REMARKS

The research reported in this thesis investigated the interaction between *B. cinerea* and grapevine inflorescences/berry at infection initiation, entry to quiescence, quiescence, and egression. Confocal microscopy, classical plating out method, and molecular analyses were used on samples inoculated with B05.10 conidia or mock at bloom (EL25/26 grapevine phenological stage).

The increased level of expression of *B. cinerea* virulence related genes involved in plant cell wall degradation, ROS accumulation, and phytotoxins biosynthesis, upon conidial contact with the flower surface, instigated defense responses in the grapevine tissues. The flowers, upon perceiving the threat, reprogrammed the transcriptions of genes: encoding different antimicrobial proteins, involved in ROS accumulation and secondary metabolites biosynthesis pathways, in phytoalexin production and cell wall reinforcement. These physical and chemical defense responses of the grapevine flowers were all together very efficient in blocking *B. cinerea* growth and inducing quiescence. Similar defense mechanisms were also deployed by the hard-green berries, 4 wpi, to keep the pathogen in quiescent state. From the disease management point of view, the quiescent infection is a very important one as the infecting pathogen remains undetected and causes the disease that impairs crop quantity, quality, and appearance when the conditions are right for re-initiating the infection. Depending on the pathogen and host condition, quiescent stage can last from few days to months. In this study, *B. cinerea* underwent 12 weeks of quiescence before it resumed its active growth at ripening.

During egression at ripe, almost all *Botrytis* virulence and growth related genes were expressed. Hence, the fungus was able to cause bunch rot despite the futile defense responses of the berries. From the results, it seems that the fungus perceived and exploited ripening associated physico-chemical changes and favorable external conditions to switch to an active state of growth from its long-lived quiescence state. In berries with egressed *Botrytis*, the expression level of a number of genes involved in cell wall self-disassembly were higher than in the control berries, suggesting that the egressed *Botrytis* exploited the ontogenically activated cell wall self-disassembly genes. Besides, it was also observed that the cell wall strengthening process, used as a physical barrier to block the pathogen from entering into the inner layers of the infected tissue, was not activated. Perhaps, since cell wall self-disassembly is a general physiological cue during fruit ripening, cell wall stiffening might not be used as defense response by ripening fruits.

In conclusion, according to the results obtained, the defense responses of the grapevine flowers and the hard-green berries were able to keep *B. cinerea* under quiescence. However, exploiting the ripening associated physico-chemical changes in the ripe berries, the fungus recovered an active metabolism and pathogenic activity and caused bunch rot at ripe.

ACKNOWLEDGMENTS

After spending four years at the Fondazione Edmund Mach (FEM), S. Michele, Italy, now is the time to write this note of thanks in the finishing moment of my stay, wrapping up all what I have done in the past 4 years. It has been a very nice period of learning for me, both scientifically and on personal level. I, therefore, would like to reflect on the people who have supported and helped me so much throughout my stay.

Firstly, I would like to express my sincere gratitude to my advisors Dr. Claudio Moser and Dr. Elena Baraldi for the continuous support of my Ph.D study, for their motivations, and encouragements. Their guidance helped me in all the time of research and writing of this thesis.

Secondly, I would like to thank collaborators Dr. Giulia Malacarne, Dr. Kristof Engelen, Dr. Michela Zottini, Dr. Paolo Sonogo, Dr. Stefania Pilati, and Dr. Urska Vrhovsek for their technical help and insightful comments. I, in particular, am grateful to Stefania. Stefania, you were always there whenever I needed your help. Your encouragements, suggestions and comments were incalculable. Thank you!

I thank my fellow lab mates Dr. Lisa Giacomelli and Dr. Carmen Leida for the discussions we have had, Daniele and Susanna for lending your hands. I would like to extend my thanks to Domenico Masuero for polyphenol analysis and Umberto Salvagnin for the nice grapevine pictures in my thesis.

Furthermore, this PhD thesis was only possible due to the financial support of the FEM, S. Michele, Trentino, Italy. I highly appreciated that I was also able to attend symposia.

I also want to thank Prof. Dr. Paul Tudzynski, Dr. Ulrike Siegmund and Dr. Julia Schumacher, from Westf. Wilhelms University of Muenster, for help with microscopy and for providing the GFP labelled B05.10 strain of *B. cinerea*.

Moreover, my wholehearted thanks go to old friends and friends I met here at FEM for your encouragements and all good times we have had together.

Last, I want to say a very big thank you to my family, who were and are very patient with me and supported and encouraged me.